

Master Thesis

Corrosion Monitoring Concept for Oil Wells



Supervised by:

Univ.-Prof. Dipl.-Ing. Dr.mont. Herbert Hofstätter
Ao. Univ.-Prof. Dipl.-Ing. Dr.mont. Gregor Mori

AFFIDAVIT

I declare in lieu of oath, that I wrote this thesis and performed the associated research myself, using only literature cited in this volume.

Place, date

Signature

Acknowledgement

First of all I would like to thank the head of my home- department “Petroleum Production and Processing”, Univ.-Prof. Dipl.-Ing. Dr.mont. Herbert Hofstätter, for his support and time- not only in the last months- but more for the last academic years at my alma mater in Leoben. Besides his support concerning this thesis and the academic guidance, he helped me finding valuable internships and always tried to create a personal connection to students by joining field trips and other events.

I also would like to express my sincerest thanks to the head of “CD- laboratory” and “Corrosion Department” of University of Leoben, Ao. Univ.-Prof. Dipl.-Ing. Dr.mont. Gregor Mori, for the academic and personal guidance he provided. During passed months, he pushed me far beyond my expected limits and believed in me also within harder times. With his support, I had chance to get a small insight to the fascinating world of material science. Professor Mori supported me additionally in fulfilling my experiments necessary for this work at his department, where I experienced a friendly and familial environment. In this situation I also would like to thank DI Tanja Wernig, Hubert Falk, DI Luca Moderer, DI Clemens Vichytil, Christoph Holzer and Andreas Umgeher for letting me join their community so easily.

To achieve optimum experimental results, DI Thomas Vogl contributed his expertise, experience and sacrificed a lot of working- time to help me. Thank you for your efforts!

Furthermore I would like to thank the austrian Oil Company that contributed corresponding data and financial support. I had the chance to collaborate with both the Production and Corrosion Department and would like to thank representatives of both departments for sharing experience, skills and time.

Above all, I am grateful for my mothers' unconditional support throughout the last 24 years and her help whenever things did not run that well. Words can not describe how much I appreciate your guidance and motherly love.

My girlfriend Christina was always there for me. Thank you for your strength, care and love in good as well as in bad times.

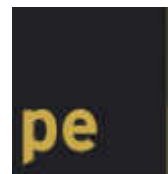


Table of Contents

1	Introduction	1
2	Theory of CO₂ Corrosion.....	2
2.1	Basic Reactions	2
2.2	Effect of Key Parameters on CO ₂ Corrosion.....	3
2.2.1	Fluid Characteristics, Contents and Watercut	3
2.2.2	CO ₂ and H ₂ S Partial Pressures.....	6
2.2.3	Fluid Velocity	10
2.2.4	Temperature.....	12
2.2.5	Inhibitors	13
2.3	CO ₂ Corrosion Models.....	17
2.3.1	De Waard- Milliams- Smith	17
2.3.2	NORSOK	21
3	Field Data	25
3.1	Fluid Characteristics and Watercut.....	25
3.2	Fluid Velocity	29
3.3	CO ₂ and H ₂ S Partial Pressure.....	32
3.4	Temperature.....	42
3.5	Inhibitor Performance.....	45
4	Experimental	53
4.1	Materials	53
4.2	Autoclave Testing.....	54
4.3	Evaluation.....	55
5	Experimental Results.....	56
5.1	Repeatability.....	56
5.2	Partial Pressure CO ₂	56
5.3	Temperature.....	57
5.4	Inhibitor Performance.....	58
6	Discussion.....	61
6.1	Watercut	61
6.2	Fluid Velocity	61
6.3	CO ₂ and H ₂ S Partial Pressure	61
6.4	Temperature.....	62
6.5	Inhibitor Performance.....	62
7	Conclusions	64
8	Recommendations & Future Work.....	65
8.1	Measurement Concept	65
8.1.1	Start.....	65
8.1.2	Frequency	65
8.1.3	Documentation.....	66

8.2	Future Work.....	67
8.2.1	FS2 Analysis	67
8.2.2	FS1 and FS2 Performance connected to Sediments.....	67
8.2.3	Proving protective Layers on Measurement Coupons in Wells	67
8.2.4	Implementation and Verification of Measurement Concept	67
9	Appendix	68
9.1	Background Data	68
9.2	Spreadsheets	85
	Data 1 st Installation	85
	Data 2 nd Installation	89
	Data 3 rd Installation.....	94
	Data Downhole Measurement and Deviations.....	98
	Data Watercuts, Chloride Content, Velocities, Tubing Sizes.....	102
	Data Watercuts CO ₂ & H ₂ S Contents, Surface (Partial-) Pressures, Pump setting Depth, Casing Pressure.....	107
	Data Watercuts Partial Pressures Downhole, P _{CO2} /P _{H2S} Ratio, Temperature.....	111
	List Green Inhibitors Inhibitor Doses, Corrosion Rates and Watercut.....	116
	List Green Inhibitors Content CO ₂ & H ₂ S, Velocity, Partial Pressure CO ₂	116
	List Green Inhibitors Partial Pressure H ₂ S, Chloride Content, additional Info	117
10	Literature.....	118

List of Figures

Figure 1 – Example of Buildup of dissolved Iron Concentration on pH and Corrosion Rate at 20 °C, 100 bar System Pressure and 1 % CO ₂ at 1 m/s	5
Figure 2 – Corrosion Rates of Steel St52 at 90 °C as a Function Partial Pressures of CO ₂ for flow rates of 20 m/s and differing pH	7
Figure 3 – Example of Effect of H ₂ S Concentration at 100 bar, 50 °C, 1 % CO ₂ , 1 m/s, supersaturated in FeCO ₃	9
Figure 4 – Comparative Corrosiveness of 3 common Gases in water solutions (25 °C, 5-7 days exposure, 2-5 g/l NaCl, HCO ₃ alkalinity <50 mg/l- computed from several data sources).....	10
Figure 5 – Baker Diagram showing Flow Behaviour depending on Gas and Liquid Velocity (D= 1", 3% NaCl Brine, CO ₂ Partial Pressure =150 psg, Temperature= 160°F or 71 °C).....	11
Figure 6 – Corrosion Rate of X65 Steel as a function of temperature (408 hours with Partial Pressure CO ₂ of 0.8 MPa and 1 m/s).....	12
Figure 7 – Corrosion Rate of A516 Steel in 450 psi of CO ₂ at different temperatures and Concentrations of H ₂ S.....	13
Figure 8 – Illustration of a 10 ppm Threshold Concentration in the Performance Curve of a Corrosion Inhibitor;5 liter Flow Loop, Forties Brine, 50 °C, 1 bar CO ₂	14
Figure 9 – Schematic of Adsorption of an Inhibitor	16
Figure 10 – Numbered Downhole and “Surface 1. Installation” Watercuts versus corresponding Corrosion Rates	27
Figure 11 – “Surface 1. Installation” Corrosion Rates versus Watercut and Wellhead Velocity ..	28
Figure 12 – Downhole Corrosion Rates versus Watercut and Wellhead Velocity	29
Figure 13 – “Surface 1. Installation” Corrosion Rate versus Wellhead Velocity.....	31
Figure 14 – Downhole Corrosion Rate versus Tubing Velocity	32
Figure 15 – “Surface 1. Installation” Corrosion Rates versus CO ₂ Partial Pressures for Watercuts > 80 % and Velocities > 0.15 m/s	33
Figure 16 – Downhole Corrosion Rates versus CO ₂ Partial Pressures Watercuts > 80 % and Velocities > 0.11 m/s	33
Figure 17 – “Surface 1. Installation” Corrosion Rates with Respect to Partial Pressures CO ₂ and H ₂ S for Watercuts > 80 % and Velocities > 0.15 m/s.....	35
Figure 18 – Downhole Corrosion Rates with Respect to Partial Pressures CO ₂ and H ₂ S for Watercuts > 80 % and Velocities > 0.11 m/s	35
Figure 19 – “Surface 1. Installation” Corrosion Rates versus numbered Partial Pressures of H ₂ S for Watercuts > 80% and Velocities > 0.15 m/s	36

Figure 20 – Downhole Corrosion Rates versus numbered Partial Pressures of H ₂ S for Watercuts > 80% and Velocities > 0.11 m/s	36
Figure 21 – Partial Pressure CO ₂ and H ₂ S Ratio versus “Surface1. Installation” Corrosion Rates connected to corresponding Well Number for Watercuts > 80 % and Velocities > 0.15 m/s after Pots	37
Figure 22 – Partial Pressure CO ₂ and H ₂ S Ratio versus Downhole Corrosion Rates connected to corresponding Well Number for Watercuts > 80 % and Velocities > 0.15 m/s after Pots	38
Figure 23 – “Surface 1. Installation” Corrosion Rate versus Wellhead Velocity without H ₂ S Wells.....	39
Figure 24 – Downhole Corrosion Rate versus Tubing Velocity without H ₂ S Wells	40
Figure 25 – Downhole Corrosion Rate versus Partial Pressure CO ₂ without H ₂ S Wells for Watercuts > 80 % and Velocities > 0.11 m/s	41
Figure 26 – “Surface 1. Installation” Corrosion Rate versus Partial Pressure CO ₂ without H ₂ S Wells for Watercuts > 80 % and Velocities > 0.11 m/s	41
Figure 27 – Numbered Downhole Corrosion Rates with Respect to Temperature at Coupon setting Depth for Watercuts > 80 % and Velocities >0.11 m/s.....	43
Figure 28 – Downhole Temperatures versus Downhole Corrosion Rates for Watercuts > 80 % and Velocities > 0.11 m/s.....	44
Figure 29 – Downhole Corrosion Rate versus Downhole Temperature without H ₂ S for Watercuts > 80 % and Velocities > 0.11 m/s	45
Figure 30 – Inhibitor FS1 versus Surface Corrosion Rates of 1 st Installation- Coupons for Watercuts > 80 % and Velocities > 0.15 m/s	46
Figure 31 – FS1 versus Surface Corrosion Rates of 2 nd Installation- Coupons for Watercuts > 80 % and Velocities > 0.15 m/s	48
Figure 32 – FS1 versus Surface Corrosion Rates of 3 rd Installation- Coupons for Watercuts > 80 % and Velocities > 0.15 m/s	48
Figure 33 – Inhibitor FS1 versus Corrosion Rates of “List Green Inhibitors”	49
Figure 34 – Inhibitor FS2 versus Corrosion Rates of “List Green Inhibitors”	50
Figure 35 – Inhibitors FS1 and FS2 versus corresponding Corrosion Rates of “List Green Inhibitors”	51
Figure 36 – Partial Pressure CO ₂ Distribution with Variations in Temperature from Autoclave Experiments.....	57
Figure 37 – Temperature Distribution with Variations in Partial Pressure CO ₂ from Autoclave Experiments.....	57
Figure 38 – Inhibitor FS1 Performance with Variations in Partial Pressures at Roomtemperature.....	58
Figure 39 – FS1 Performance with Variations in Partial Pressures at 80 °C	59

Figure 40 – FS1 Performance with Variations in Partial Pressures at 120 °C	59
Figure 41 – Comparison FS1 to FS2 with Variations in Inhibitor Doses of FS1	60

List of Tables

Table 1 – pH Verification via NORSOK.....	26
Table 2 – Lower Limits of “Surface 1. Installation” and Downhole Velocity.....	30
Table 3 – Corrosion Rate Curriculum of highest “Surface 1. Installation” Corrosion Rates	47
Table 4 – Deviations of Concentrations between FS1 and FS2 Inhibitors of FS1 Wells exceeding Corrosion Limit'	52
Table 5 – Comparison of Inhibitors FS1 and FS2 via alternative Parameters'	52
Table 6 – L80 Steel Composition'	53
Table 7 – L80 Steel mechanical Properties'	53
Table 8 – Testing Conditions for Autoclave Experiments.....	54

Abstract

This “Master of Science” thesis deals with the creation of a corrosion monitoring concept of oil wells. In the end, the reader should have a deeper understanding regarding important parameters affecting corrosion, parameters to be measured in terms of corrosion surveillance and the connected prevention of metal deterioration. At the beginning, a theoretical background is provided to create an overview on corrosion issues. As a second step, a field data analysis of oil wells in Austria is being performed, where critical parameters are screened and checked for validity. Field data investigations do not show a good match according to literature and so reliable outputs, like an optimum dose of inhibitors to be injected downhole, can not be published by means of field data investigations only. That is why autoclave experiments, with respect to selected field data parameters, have been performed and results, indicating clear trends towards critical questions, are being published at the experimental section in this work. At the end of this work, guidelines for a measurement concept are recommended to achieve a reliable feedback by means of routine measurements

This project has been carried out in close cooperation between an austrian oil company and University of Leoben. Departments of petroleum production and corrosion of both institutions have been involved. The employed software was Microsoft Excel 2010 and Origin 8.5. Valuable input came from several industry experts, while further information was taken from books, papers and journals. All used sources were stated using ISO 690 convention for citation, in order to honour the authors and to make sure that continuative research can start from this work’s final stage of knowledge.

1 Introduction

Corrosion is a dominant problem in the oil and gas industry. About 10 % of the price for crude oil serves for maintenance costs due to corrosion and approximately 4 % of the gross national product is lost in industrial countries due to corrosion processes.¹⁹ As may be expected, controlling corrosion is a target very difficult to be reached and set-ups, granting 100 % reliability, have not been found so far.

Of course also oil companies in Austria are familiar with corrosion problems. In fields of Austria, with over 50 years of oil and gas production history, watercuts of approximately 90 % are being faced. Basically, inhibitors are injected to keep the corrosion rate below the threshold-limit of 0.05 mm/a. The corrosion rates are being measured via coupons placed either downhole, or at surface installations, where fluid streams are in contact with coupons' surface.

As a matter of fact, bigger variations concerning corrosion rate measurement-outputs and actual tubing replacements have been experienced in the past. Wells, with corrosion rates lower than 0.05 mm/a, still show larger traces of corrosion on tubing walls than expected. Those corrosion rates are to be analysed intensively, in order to understand backgrounds and the reason for deviations of corrosion measurements and actual corrosion failures. Secondly, inhibition doses have been adjusted independently in the past, because no guideline was created regarding measurement and inhibitor concentration. Focus is set on an optimum concentration of inhibitors, whereas the corrosion measurement-methods and inhibitor doses injected so far have to be verified and controlled for correct application. To achieve a level of comparison between field data and laboratory experience, several autoclave experiments will be done. In connection to the correct inhibitor dose, optimum coupons measurement-adjustments regarding location, duration and frequency need to be evaluated to maintain control and overview on field's corrosion status.

Before analyses of field data is conducted, a theoretical backup of corrosion principles and influences is presented.

This thesis should provide a major guideline in corrosion management, to achieve a reduction of corrosion problems and failures.

2 Theory of CO₂ Corrosion

One of the most common corrosion types in oil and gas production is Carbon Dioxide (CO₂) corrosion.^{1,2} In order to understand CO₂ corrosion, basic equations and important side effects of this corrosion process have to be demonstrated. As a matter of fact, this process is a function of many influences in production environments³.

2.1 Basic Reactions

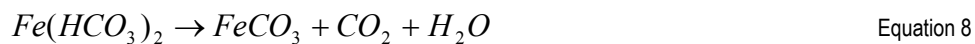
Generally CO₂ dissolves in water and results in carbonic acid, a weak acid compared to mineral acids but still able to deteriorate the surface condition of carbon steel.



Four equations, following up, summarize the corrosion process and demonstrate three cathodic and one anodic reaction.¹



In connection to Fe²⁺ ions the following reaction products are precipitating:



As a consequence of reactions illustrated above, produced iron carbonate (FeCO₃) can be important in protection of metal surfaces and preventing advanced corrosion.⁴

2.2 Effect of Key Parameters on CO₂ Corrosion

In the following subchapter, relevant parameters regarding oilfield corrosion are being elaborated. Other parameters affecting CO₂ corrosion have not been considered.

2.2.1 Fluid Characteristics, Contents and Watercut

Oil

Crude oils are not corrosive at typical oil and gas production temperatures and can provide a barrier for water and prevent corrosion processes on the metal surface because of that.^{3, 5, 14}

Basically, hydrocarbons can, because of their complex composition, be classified with respect to their geochemical history.⁶ Types are based on their maturity and Kerogen type, which is defined as the organic fraction within the sedimentary rock. By determination of the amount of aromatics and paraffins and their geochemical history, three types⁶ of Kerogen can be defined.

Kerogen I: Crude oils derived from algal matter, contain mainly paraffinic chains and is poor in aromatics

Kerogen II: Consists of both paraffinic and aromatic structures from marine organic substrates

Kerogen III: Mostly aromatic chains derived from terrestrial plants

It has to be mentioned that crude oil, which contains organic acids, supports corrosion via decrease of pH- value.^{7, 8, 9} Nevertheless, influences of organic acids are not presented in this work.

Wettability

Generally oil is not considered to be corrosive^{3, 5, 14}; corrosion only takes place if water wets metal surface. According to Kermani², there are two concepts of water wetting relevant to corrosion modelling, one in connection to electrochemistry and surface physics, the other one related to CO₂ corrosion, that are to be mentioned shortly in this section.

“Electrochemistry and surface physics wetting” concept relates to simple contact of liquid to metal surface. This concept delivers high support in modeling of water wetting. CO₂ corrosion related concept is based on liquid soaked porous films holding water, even if temporarily media in contact with the film has no carrying traces of water. Behavior of corrosion processes within that concept can be different regarding scales of protective layers and can occur in connection to shut down periods of wells or slug flow velocities. This is the reason why watercuts’ impacts on corrosion rates should be analyzed in connection with the flow velocity and the two associated concepts of water wetting.²

In order to model wetting phases of particular fluids, De Waard and Smith postulated wettability relations to oil, water and steel with help of interfacial tension ($\gamma_{\text{liquid-steel}}$), where a lower value indicates better wetting. As a matter of fact, $\gamma_{\text{oil-steel}}$ varies with different crude oils, which is not expected to be the case at $\gamma_{\text{water-steel}}$.³

$$\gamma_{\text{water-oil}} = \gamma_{\text{oil-steel}} - \gamma_{\text{water-steel}} \quad \text{Equation 9}$$

Equation 9 implies, under consideration of improved water wetting characteristics of iron carbonate films on steel surfaces³, interfacial tension between oil and steel to be bigger. This assumption seems reasonable, since generally water tends to wet metal surfaces more easily. Depending on crude oil gravity, different amounts of water can be carried before separation into two phases. That means lighter oils are less effective in forming water- oil emulsions, increasing water wetting tendencies and thus the corrosion potential.³ Additional information is being found in chapter “2.3.1 Corrosion Models- De Waard- Williams- Smith”.

Watercut

Water is the basis of every corrosion process, even though pure water does not show corrosive tendencies up to boiling temperatures.¹⁰ With addition of corrosive gases like oxygen, CO₂ or H₂S, corrosion is able to attack metal surfaces.^{10, 19, 21} Whereas oxygen influence is considered to be excludable in oil reservoirs and its upstream installations², CO₂ is able to create an acid and consequently attacks subsurface installations like demonstrated within Equation 1 and its theoretical background, presented below in “2.2.2 CO₂ partial pressure” section.

The watercut (WC) simply describes the percentage [%] of water that is being produced in an oil and gas production flow stream. That is why corrosion basically is a function of water content in “local crude oil/ produced water” mixtures for constant environmental conditions.¹¹ Produced waters are strongly linked to the corresponding oil and its tendency to form water- oil emulsions. This leads to a threshold- watercut, where corrosion commences. Investigations of Carew et al.^{11, 12} showed a threshold watercut of 30 to 40 % within their experiments with different crude oils, where no significant corrosion processes were evident. Below this value water is completely dispersed in oil, above, water is wetting metal surfaces. Higher this volume, both localized as well as uniform corrosion was found. Results additionally showed sharper slopes concerning corrosion rates at watercuts of 50 to 70 % than within 70 % to 100 %, ¹² indicating a level, where water is fully covering the metal surface. This leads to an increased electrochemical activity at the steel surface, making corrosion rates rise.

pH and Fe²⁺ Content

To refresh one’s memory, pH, ranges from 1 to 14, whereas 7 stands for neutral state. It describes the concentration of dissolved hydronium ions in solutions. The higher the pH, the lower is its H₃O⁺ concentration;

$$pH = -\log(H^+) \quad \text{Equation 10}$$

Major impacts on corrosion rates of oil wells that produce water to a certain extent, are linked to the pH value.^{13, 17, 18} Equation 5 describes theoretically the anodic dissolution rate, when no additional solid reaction is formed, with its ability to proceed intermediates that involve hydroxyl ions (OH⁻) and thus decreasing its rate with decreasing pH.¹³ As a matter of fact, this effect is expected rarely in practice because of control of cathodic reaction, illustrated under deaerated conditions by Equation 4. A higher pH affects primarily the cathodic reaction, making the reduction of H⁺ ions slower and so the anodic dissolution of iron as well.²⁵ The increase in rate of cathodic reaction with decreasing pH more than offsets pH dependence of the intermediate reaction of anodic Equation 5. The net effect is that corrosion rates increase with decreasing pH.¹³ In H₂S – CO₂ mixed environments in-situ pH is based²¹ on

- HCO₃⁻ via Equation 1
- HS⁻ via Equation 13

Calculations for pH evaluations in CO₂ corrosion prediction models are principally based on measured bicarbonate concentrations, CO₂ solubilities and carbonic acid dissociation constants.³

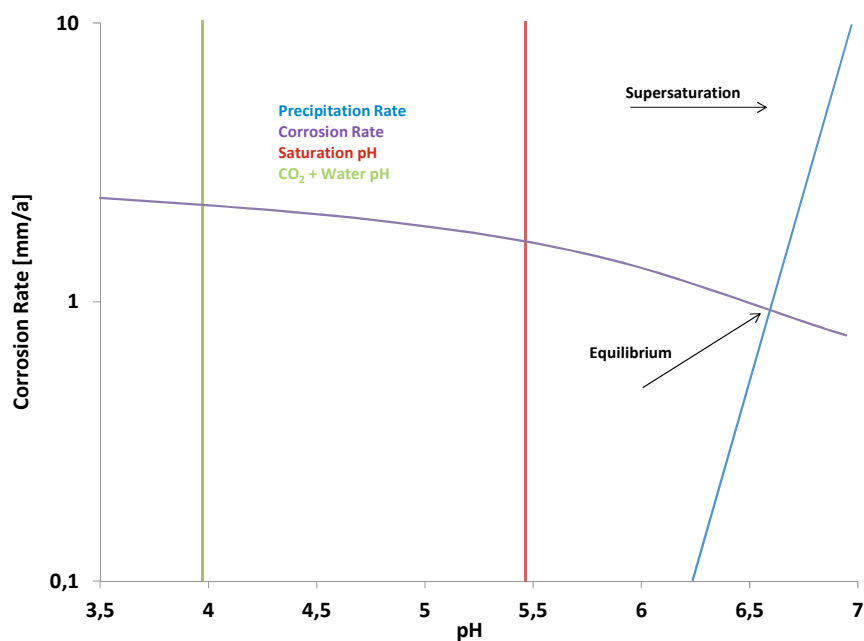


Figure 1 – Example of Buildup of dissolved Iron Concentration on pH and Corrosion Rate at 20 °C, 100 bar System Pressure and 1 % CO₂ at 1 m/s¹⁴

The increase of corrosion rates with decreasing pH is also shown in connection to Fe²⁺ concentrations in solutions affecting the already mentioned protective FeCO₃ films. Iron contents are depending on anodic reaction mechanisms¹⁵ and solubility varies with CO₂ concentrations, temperature, pH and concentration of other ions.² Equation 8 describes the creation of supersaturation, where the concentration of Fe²⁺ is higher than the solubility limit of FeCO₃, increasing the pH and reducing corrosion rates.^{4, 16} Figure 1 illustrates an example,

where a solution with variations in Fe^{2+} saturations is being plotted. It can be seen that corrosion rates decrease with Fe^{2+} saturation (and pH increase).¹⁴ In natural environments, fluids very often are saturated or even supersaturated with iron carbonate explaining the high iron carbonate scale frequency.¹⁴

2.2.2 CO₂ and H₂S Partial Pressures

CO₂

It is a widely used simplification that systems' total pressure is the sum of corresponding partial pressures of ideal gases. Still assuming ideal conditions, partial pressures are calculated by

$$x_i = \frac{P_i}{P} = \frac{n_i}{n} \quad \text{Equation 11}$$

where P_i is the partial pressure, x_i mole fraction and n_i the amount of moles of an individual gas. P and n are total values of corresponding parameters.

CO₂ partial pressures are in direct relationship to pH and its calculations, explained by Equation 1. De Waard¹⁷ postulated via Equation 12, Henry's law and knowing that concentration of carbonic acid is proportional to CO₂ partial pressure

$$pH = -\frac{1}{2} \cdot \log(P_{CO_2}) + const \quad \text{Equation 12}$$

where P_{CO_2} describes the CO₂ partial pressure and the constant implies the dissociation constant (K) and Henry's constant, both depending on temperature.

In literature, often partial pressures are related to corrosion rates^{2, 17} via their impacts on pH and the connected changes of corrosion rates.

Describing non-ideal gases in connection to partial pressures of CO₂ is an issue. That is why very often CO₂ fugacity is added for exact calculations and investigations on corrosion rate impacts.^{3, 18} Even more problematic is the relation of non-ideal gas phase at high rate gas wells to the water phase, where an activity coefficient should be introduced for homogeneity. Due to weak availability of activity coefficients for water phases out of Pressure – Volume – Temperature (PVT) data, predictions of corrosion behaviour very often are limited to fugacities.²

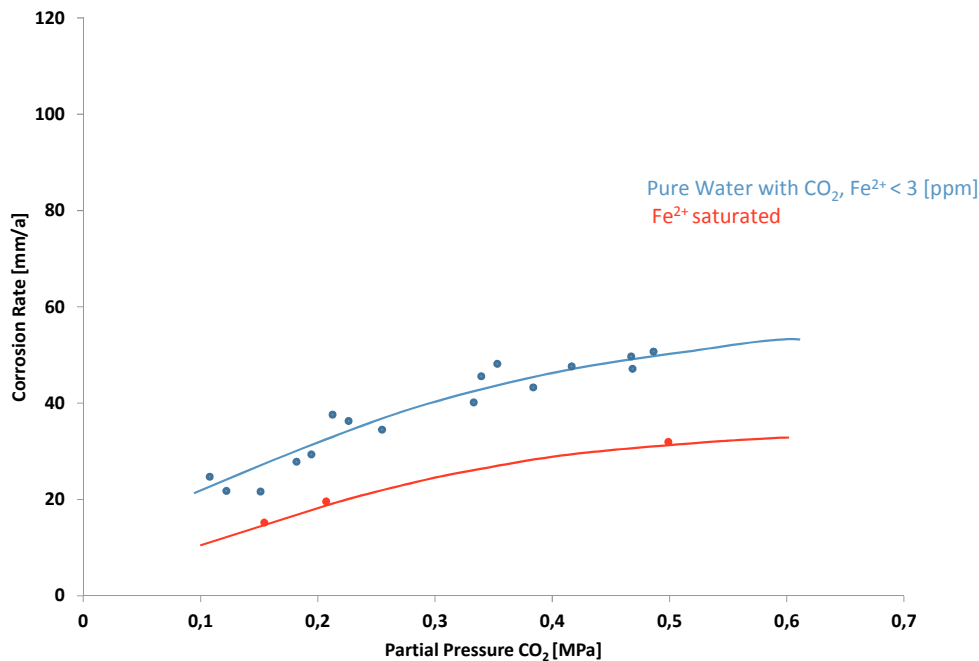


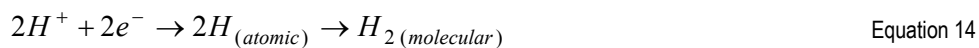
Figure 2 – Corrosion Rates of Steel St52 at 90 °C as a Function Partial Pressures of CO₂ for flow rates of 20 m/s and differing pH¹⁶

Figure 2 demonstrates the influence of CO₂ partial pressure on steel. As can be seen, experiments with Fe²⁺ saturated electrolytes show once more lower corrosion rates at 90 °C, compared to the ones that are connected to fluids with low amounts of iron ions. In Literature, often slopes of the partial pressure curves are decreasing with increasing partial pressure of CO₂.^{16, 19}

H₂S

Dihydrogen Sulphide (H₂S) containing wells, also known as “sour” wells, have increased steadily in recent years, as by production of only “sweet” reservoirs (not containing H₂S) demand can not be met nowadays.²⁰

Basically H₂S corrosion follows reactions, depending on parameters fluid chemistry, organic acids, flow velocity and presence of elemental sulphur.²¹



The anion HS⁻ splits further up to H⁺ and S²⁻. S²⁻ results via Fe²⁺ in FeS, a commonly found corrosion product. Those iron sulfide scales act under certain conditions highly protective against corrosion.²¹ In mixed CO₂ and H₂S environments, corrosion causes are not easier to be found. Ignoring the metal cracking effects of H₂S sour services, low levels of hydrogen sulfide can influence corrosion in different ways. H₂S either supports CO₂ corrosion by accelerating anodic dissolution- reaction of Equation 5 through sulfide adsorption, or it decreases “sweet” corrosion of CO₂ by formation of an iron sulfide layer^{20, 21, 22, 23, 24}, that, contrary to insulating effects of iron carbonate layers, exhibit electronic conductivity.²⁵ Due to the fact that H₂S relation

to CO₂ corrosion is not fully understood, available equations or models for corrosion prediction must be handled with care. However, Pots et al.²⁶ postulated in 2002 via CO₂ and H₂S ratios three different domains for corrosion management:

- $P_{CO_2} / P_{H_2S} < 20$
 - Corrosion dominated by H₂S
 - FeS as the main corrosion product
- $20 < P_{CO_2} / P_{H_2S} < 500$
 - Mixed by CO₂/ H₂S corrosion dominance
 - A mixture of FeS and FeCO₃ as the main corrosion products
- $P_{CO_2} / P_{H_2S} > 500$
 - CO₂ corrosion dominates
 - FeCO₃ as the main corrosion product

Details are found at Background Data 1 and Background Data 2 in Appendix section.

Other experimental flow- loop investigations²¹ on low H₂S partial pressures showed same tendencies. Via H₂S partial pressures of $1.5 \cdot 10^{-3}$, $1.5 \cdot 10^{-2}$ and $1.5 \cdot 10^{-1}$ psi, (0.0001, 0.001 and 0.01 bar) with H₂S concentrations of 100, 1000 and 10000 ppm in gas phase, tests were carried out on X65 steel at 30, 50 and 75 °C in presence of 14.7 psi (1 bar) CO₂. Environmental details are illustrated in Background Data 1. Out of those tests low corrosion rates in connection to low H₂S concentrations can be concluded.²¹ Results indicate that low levels of H₂S, defined to be below limits of SSC occurrence of 0.05 psi, can reduce CO₂ corrosion by a factor of 3 to 4.²¹

Brown et al.²¹ concluded that small amounts of H₂S (10 ppm) can reduce CO₂ corrosion rates, without presence of protective iron carbonate and sulphide layers. Protective adherent films were formed at 60 °C with 25 ppm H₂S at pressures of 114.6 psi (7.9 bar) and a pH of 6.

In cases where FeS breakdown occurs the corrosion rate can be an order of magnitude higher than the corresponding rate for pure CO₂. This high corrosion rate in the presence of H₂S is a result of drop in the pH due to the reduction of the dissolved iron ions that occurs with FeS precipitation and galvanic couple formed between the steel and corrosion scale.¹⁴ This phenomenon is called “Pitting” and its probability of occurrence increases with increasing H₂S partial pressure, like Figure 3 demonstrates.^{2, 14, 19, 21, 22}

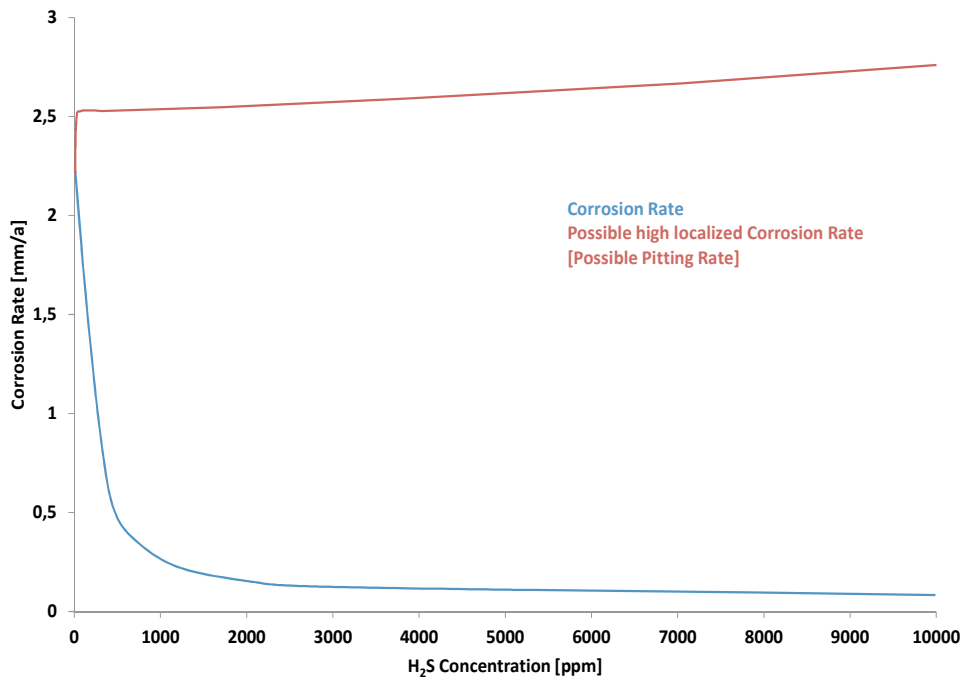


Figure 3 – Example of Effect of H₂S Concentration at 100 bar, 50 °C, 1 % CO₂, 1 m/s, supersaturated in FeCO₃¹⁴

It has to be kept in mind, that reactions published so far are strongly connected to anaerobic conditions. Especially speaking about iron carbonates, stability of scales is affected and reduced significantly when oxygen is present.¹ Like already mentioned, presence of oxygen is unlikely in oil reservoirs and its upstream installations², but the small chance, that a finite amount of oxygen migrates into installations, exists.¹

Oxygen contamination is recognized as a main difficulty studying corrosion influences in laboratory experiments.²⁷

A simple comparison of dominant gases in hydrocarbon production, CO₂ and H₂S, and oxygen is shown by Jones²¹ in Figure 4. This plot is based on data gained by exposing clean carbon steel samples to water solutions containing various conditions of each gas at 25 °C. Of course, this plot is not considering synergistic effects of corresponding gas mixtures and is for example material selection not applicable. Nevertheless, it gives an idea about corrosion tendency as well as aggression concerning metal deterioration of those three gases. As can be seen, oxygen is due to its ability to mutate Fe²⁺ ions into ferric ions of Fe³⁺ and its ability to accelerate cathodic reactions^{1,27} the most aggressive gas regarding corrosion.

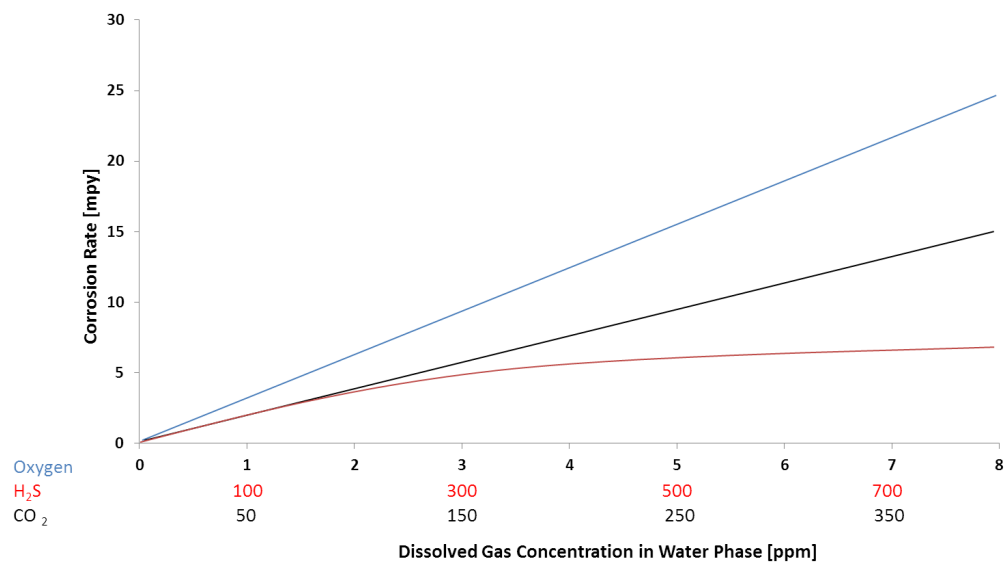


Figure 4 – Comparative Corrosiveness of 3 common Gases in water solutions (25 °C, 5-7 days exposure, 2-5 g/l NaCl, HCO₃ alkalinity <50 mg/l- computed from several data sources)²¹

2.2.3 Fluid Velocity

The effect of velocities on corrosion tendency is not fully understood today as well.² However, it is not only the fluid content that needs to be verified in corrosion predictive modelling; flow regimes have to be analyzed as well, even though they are difficult being determined. Key factors can be presented with oil- water ratios, emulsion tendencies and stabilities, as well as with gas- oil ratios (GOR).² For many crude oils, watercuts, higher than 30 %, lead to water wetting tendency and thus to potential corrosion risk.^{2, 11, 12} Also with increasing GORs, continuous water wetting by condensed water can be expected.²

Figure 5 below illustrates main flow regimes possible in two phase flow. One major problem dealing with velocities is the property of removal of protective layers.^{16, 28, 29} In flow loop experiments of Nesic et al.²⁸ protective films formed, generally were resistive to severe flow conditions. At lower temperatures, within pH values of 5.1 and 6.8, precipitation of iron carbonate films were not permanently the case even if FeCO₃ concentration exceeded the saturation limit; at higher pH values only the very thin Fe₃C film was strengthened as the only protective layer. Fe₃C films did not show any protective tendencies in those experiments and contribute to even higher corrosion rates contrary to FeCO₃ films, formed with increasing temperatures more easily. It was found that slug flow, with high fluctuating wall forces, causes higher damage to these films compared to single phase flow. In most cases, highest corrosion rates were found in vicinity of flow disturbance. Similar results with coupons exposed to flow streams are gained by Heuer.²⁹ Again, evident changes in protective film thickness are noticed changing from full pipe flow to slug flow. Additionally, with slug flow, streaked corrosion films

became less common and were replaced by rougher films, allowing the enhanced transport of reacting materials to the metal surface. Furthermore, flow impacts can change basic temperature influences on corrosion processes; in slug flow conditions, thinner corrosion films and no FeCO_3 crystals are found on metal surfaces and films remained constant over temperature variations between 40 °C to 80 °C. Showing no maximum within that ranges of temperatures contrary to full pipe flow, evidence suggested flow impacts on temperature influences, in that case.

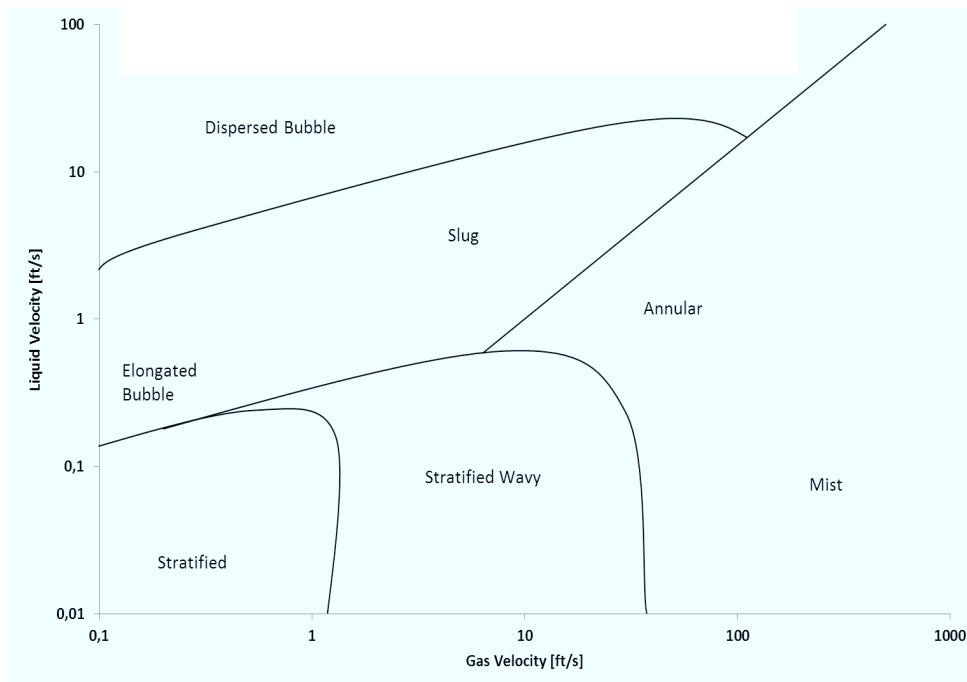


Figure 5 – Baker Diagram showing Flow Behaviour depending on Gas and Liquid Velocity ($D= 1''$, 3% NaCl Brine, CO_2 Partial Pressure =150 psg, Temperature= 160 °F or 71 °C)¹⁹

For corrosion rate prediction, the common primary parameter for velocity consideration is the wall shear stress between liquid and pipe walls.¹⁸ But not only slug flow, causing maximum wall shear stress, is considered to be a crucial velocity parameter. The removal of oil films or damage of FeCO_3 films, covering metal surfaces protecting against corrosive influences, can be removed by higher velocities of conventional full pipe flow as well.^{11, 28, 29} Of course the oil-removal tendency is governed by the velocity itself and the watercut. The higher the watercut, the thinner is the oil film on metals and the less resistant it is against turbulent velocities.^{11, 12}

Even more problems occur if velocity is connected to transport of particles. No industry guidelines concerning that topic have been published.² Often used API RP- 14E² is as well not considering particulates as such and refers to the formula:

$$v_e = \frac{C}{\sqrt{\rho_m}} \quad \text{Equation 15}$$

where v_e is the mixed velocity, ρ_m the mixed fluid density and C is supposed to be a material constant.

2.2.4 Temperature

Temperature is one important parameter talking about iron carbonate films. At temperatures below 60 °C solubility of FeCO_3 is of higher dimensions and protective layers are not formed unless pH is increased compared to reference pH of 60 °C. In lower temperature ranges, to approximately 60- 80 °C (depending on pH), corrosion rate is proportional to temperature increase, since diffusion and reaction speeds are being stimulated, until temperature values higher than 80 °C make the precipitation of iron carbonate possible, resulting in a reduction of corrosion rates.^{1, 2, 25, 46} Figure 6 below gives an example where iron carbonate precipitates cause a corrosion rate reduction with a temperature of approximately 80 °C.³⁰

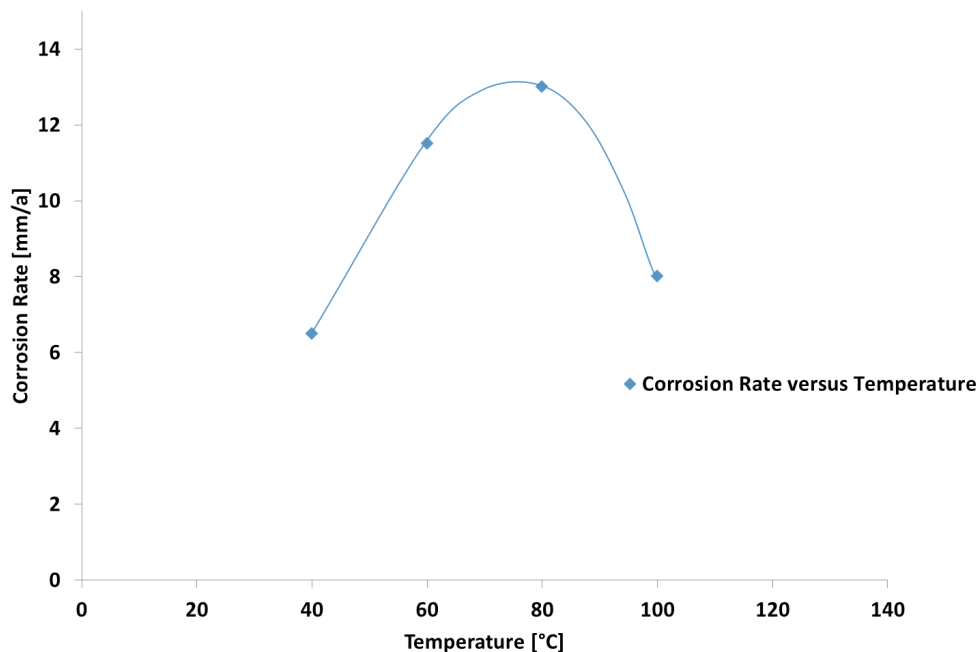


Figure 6 – Corrosion Rate of X65 Steel as a function of temperature (408 hours with Partial Pressure CO_2 of 0.8 MPa and 1 m/s)³⁰

Summarizing, precipitation of iron carbonate is not only influenced by temperature, but also by pH and CO_2 partial pressure, since CO_2 is being transformed to carbonic acid, which is the primary source for carbonates and thus the basis for protective layers (Equation 2 & 3). At pH values of for example 6.5, carbonate films can be formed at room temperature.²⁵

In combination with hydrogen sulfide, corrosion behavior with respect to temperature can be found differently, as Valdes et al.³¹ concluded. In Autoclave Weight Loss Experiments within temperatures of 50, 100 and 150 °C and CO_2 pressures of 450 psi with additions of 10, 20, 30 and 40 ppm of H_2S , the corresponding corrosion rates were examined. The test solution was 5 % NaCl during 96- 120 hours test procedures. Results indicate an acceleration of corrosion rates in presence of very low amounts of H_2S at temperatures lower than 50 °C.

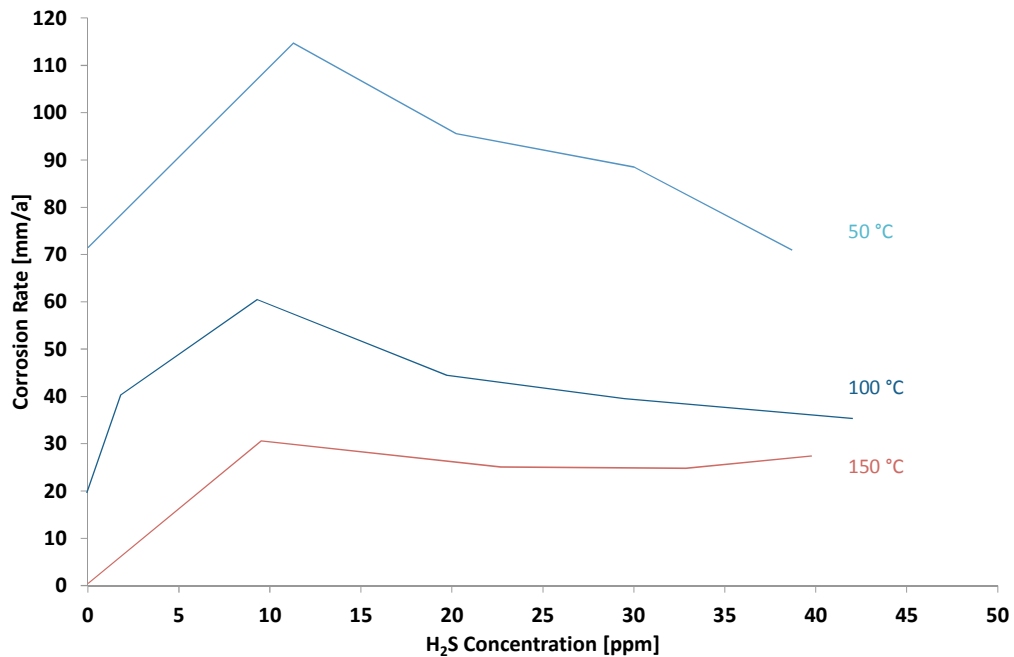


Figure 7 – Corrosion Rate of A516 Steel in 450 psi of CO₂ at different temperatures and Concentrations of H₂S³¹

As can be seen in Figure 7, as temperatures increase the corrosion rate as well as the influence of H₂S decrease. Here, a critical value of approximately 10 ppm can be obtained, before protective layers are formed and corrosion rate are reduced.³¹ Temperature has major impacts on H₂S solubility and stability of corrosion products.³¹

2.2.5 Inhibitors

In the oil and gas industry, chemicals, usually on an amine basis, are used to reduce corrosion rates. With concentrations in dimensions of [ppm] levels, fine layers are formed on metal surfaces, inhibiting electric conductivity.¹⁹

For a general overview, the following types³² of inhibitors can be classified:

- Amides and imidazolines
- Salts of nitrogenous molecules with carboxylic acids (fatty acids, naphthenic acids)
- Nitrogen Quaternaries
- Polyoxylated Amines
- Nitrogen heterocyclics

Application in the Fields

Laboratory screening should be performed in order to find best inhibitors for corresponding reservoirs and their corrosive environments.

In daily operations, continuous inhibition is preferred to batch inhibition procedures, since permanent availability of corrosion restricting amines on surfaces of steels is being realized.³³ Direct downhole injection via annulus has the great advantage of protection of lower casing parts as well as tubing surfaces.³³

Batch inhibitor treatment is carried out by squeezing inhibitors into formation, with respect to reservoir compatibility of the chemicals with the formation, to produce the inhibitor with the expected reservoir fluids.³³

Inhibitor Performance

Very often inhibitor concentrations are plotted versus the corresponding corrosion rates in order to see the overall performance of the inhibitor.^{34, 35, 38, 45} Below an example is given, where out of flow loop experiments, a threshold value for that particular case of 10 ppm was concluded.⁴⁵

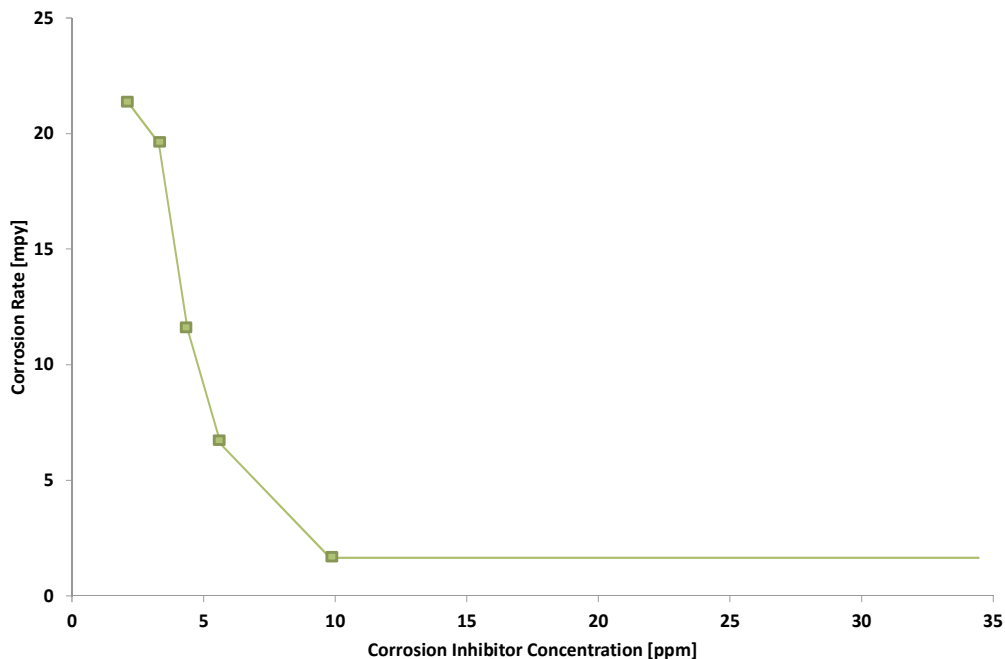


Figure 8 – Illustration of a 10 ppm Threshold Concentration in the Performance Curve of a Corrosion Inhibitor; 5 liter Flow Loop, Forties Brine, 50 °C, 1 bar CO₂⁴⁵

Inhibitor performance is based on three elements³⁶ describing main procedures of chemical inhibition. Additionally influences of sand and flow are being mentioned.

Partitioning

Corrosion Inhibitors partition between oil and water phases according to their partition coefficient; it describes the relative concentrations of the inhibitor in the water phase, C_w [ppm], to the relative concentration in the oil phase, C_o [ppm], assuming the solutions to be dilute. It is assumed that corrosion inhibitors are not affecting the miscibility of the two fluids and that molecular state of the corrosion inhibitor is unchanged between the two phases.³⁶

$$P_{wo} = \frac{C_w}{C_o} \quad \text{Equation 16}$$

The amount of inhibitor partitioning into the aqueous phase is strongly related to the volume fraction of oil in the system.³⁸

To realize the complexity of the partitioning effect, laboratory tests of Josten³⁷ et al. with an inhibitor in connection to watercuts are given as an example:

It was found that partitioning between oil and water varied by several orders of magnitude depending on the watercut (or volume fraction of oil). In the lower watercut region (< 20 %), the inhibitor preferentially partitioned into the water phase ($P_{wo} = 17$), whereas with decreased contents of oil (< 20 %) the partitioning coefficient was evaluated to be around 0.5. This trend was seen at ambient and elevated temperatures, as well with differing concentrations. Partitioning does not follow any concepts of solubility³⁷ within that example. In the petroleum industry, very often one single partitioning coefficient is assumed for calculations, which has to be treated with a lot of caution, like investigations³⁷ have shown. Josten recommended further investigations on the corrosion inhibitor to determine whether this case is unusual or not, but still underlining that various inhibitors are known showing that tendency.

However, the partition coefficient depends, besides the watercut, on the relative contribution of the molecules' hydrophilic and hydrophobic properties and the tendency of formation of microemulsions, as a consequence.³⁸ Additionally, temperature, brine salinity, pH and nature of the oil phase are influential. Inhibitor partitioning coefficients are needed very often to fully understand inhibitor performance.³⁹ For many products, like inhibitors that are being faced in this work later on, this information is not available.

Dissociation

Before the corrosion inhibitor can be adsorbed on a surface it has to be dissociated in the aqueous phase.³⁶ The dissociation process is assumed from a non- ionic to an ionic state, whereas the ionized form is able adsorb on the pipe wall and creates a surface film, inhibiting electron flow of the corrosion process. The dissociation constant:

$$K_d = \frac{[C_w^{+/-}]^2}{C_w} \quad \text{Equation 17}$$

Adsorption

Like already mentioned, corrosion inhibition mechanisms are assumed as a protective layer, created by adsorption on the metal surface.^{19, 36} Because of that, the inhibitor can occupy a certain area or volume on the surface valued via the surface coverage (θ). Langmuir's isotherm connects the adsorption to the desorption phenomena within the inhibition process and reflects only mono- atomic adsorption onto surface, showing adequate results:

$$\theta = \frac{K_L \cdot C_w^{+/-}}{[1 + K_L \cdot C_w^{+/-}]} \quad \text{Equation 18}$$

where K_L is supposed to be the Langmuir's Constant, $C_w^{+/-}$ the ionic concentration.³⁶

The higher θ is, the higher is the rate of adsorption.³⁶ Increasing the efficiency of the corrosion inhibitor surface coverage has to be maximized and dissociation has to be in equilibrium with the adhesion process. Corrosion inhibitors that preferentially partition into the oil phase, decrease corrosion inhibitor concentration in the water phase and thus corrosion rates are increased.³⁶ That is why generally water soluble inhibitors should be preferred to oil soluble inhibitors.

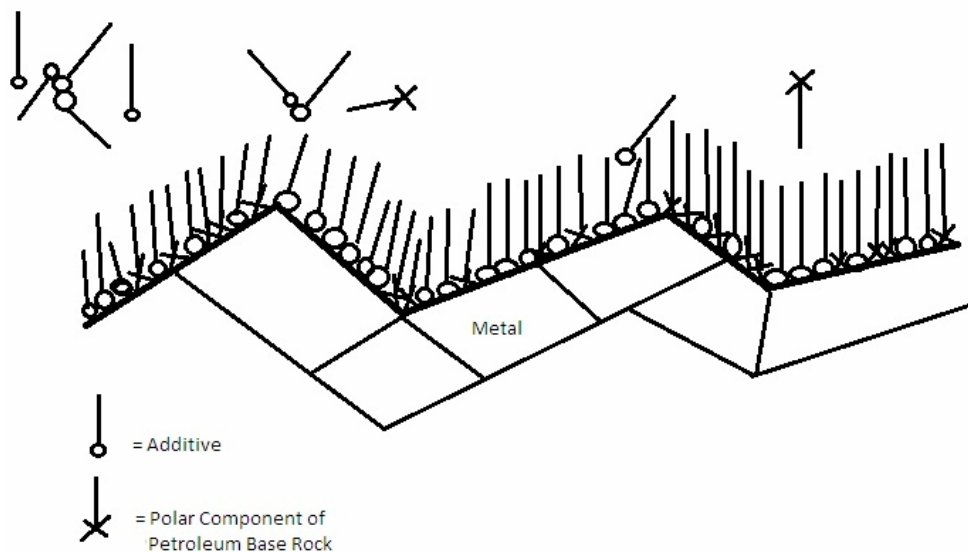


Figure 9 – Schematic of Adsorption of an Inhibitor¹⁹

The formation of a fine inhibitor- layer on the metal surface, which prevents the electrons from passing through it, is shown in Figure 9.

Flow Influences

Basically, critical flow intensities can cause a limitation of corrosion inhibitor efficiencies and thus be a reason for flow induced localized corrosion. A number of studies performed in the past did not show up any significant inhibition deterioration of state-of-the-art inhibitors up to flow velocities of 9- 20 m/s or 1400 Pa wall shear stress.^{40, 41, 42} Secondary flow effects, like high gas liquid interfaces resulting in foam conditions or liquid- liquid interfaces can cause adsorption loss.^{40, 43, 45} Figure 5 shows different flow regimes possible in a pipe. During slug flow, gas bubbles can be entrained into the liquid hitting the bottom of the pipe during horizontal flow and collapse, removing an inhibitive film.^{40, 43, 45}

It is to be mentioned, that produced sediments like clay, sands or various types of carbonates can influence inhibitor performances negatively by adsorption or erosion of the inhibitor's fluid films.^{44, 45}

2.3 CO₂ Corrosion Models

Controlling corrosion means full understanding of corrosion processes and predicting future performance of corrosive cases as a consequence. In order to have future outlooks, numerous models on CO₂ corrosion are published and three of them, that are considered to be most important, are presented in following subchapters. All equations and variables are presented and prepared for application in oil fields. Points, especially relevant for pipeline engineering e.g., like presence of glycol, were excluded in corresponding models.

2.3.1 De Waard- Milliams- Smith

De Waard- Milliams

In 1975 C. De Waard and D. E. Milliams published one of the most famous and still applicable CO₂ corrosion models so far. With help of weight loss, polarization resistance measurements, relations of carbonic acids and CO₂ partial pressures corrosion rates can be predicted. The gained values are considered to be worst case scenarios (especially at temperatures higher than 40 °C, since FeCO₃ precipitation was not considered).¹⁷

In the same year De Waard and Milliams published an alternate form containing the critical parameters in "The first International Conference on Internal and External Protection of Pipes", emphasized on wet natural gas.⁴⁶ Generally corrosion rates do not differ significantly and also assume worst case scenario corrosion rates⁴⁶, but are applicable more easily. Additional factors are introduced, including protective scales decreasing corrosion.

$$\log(V_{nomo}) = 5.8 - \frac{1710}{T} + 0.67 \cdot \log(f_{CO_2}) \quad \text{Equation 19}$$

This equation shows the relations of the “nomogram corrosion rate” (V_{nomo}) to temperature and fugacities (or partial pressures), which can be elaborated with straight lines as well in relevant nomograms illustrated in Background Data 5. Here, fugacities instead of partial pressures, applied in the first publication of 1975, are chosen for more reliable investigations, since with increasing pressure non-ideal behaviour of gases play a bigger role. Like above, pressures and temperatures are valid as [bar] and [Kelvin].⁴⁶

$$f_{CO_2} = a \cdot P_{CO_2} \quad \text{Equation 20}$$

A chart providing basic fugacity constants (a) is provided in Background Data 6, valid for the binary CO₂-CH₄ system.

Formation of protective films is also being included by an additional scaling factor (F_{Scale}) gained by division of observed corrosion rates with nomogram corrosion rates at temperatures above 60 °C and finding best fit to 1/T and $\log(f_{CO_2})$ by multidimensional regression analysis.

$$\log(F_{\text{scale}}) = 2400 \cdot \left(\frac{1}{T} - \frac{1}{T_{\text{Scale}}} \right) \quad \text{Equation 21}$$

$T > T_{\text{scale}}$, otherwise F_{scale} is chosen as maximum (=1).⁴⁶ T_{Scale} [Kelvin] is defined as the temperature with maximum corrosion rates possible.

$$T_{\text{Scale}} = \frac{2400}{6.7 + 0.6 \cdot \log(f_{CO_2})} \quad \text{Equation 22}$$

In order to include pH and Fe²⁺ content, the pH factor is introduced. First of all, pH is defined as a result of CO₂ and water only. During experiments with constant volumes of water at constant pressures of CO₂, the Fe²⁺ concentration will increase while the H⁺ concentrations decrease until solution saturation. That precipitation of FeCO₃ and Fe₃O₄ does not necessarily mean formation of protective films, meaning corrosion still can take place in a saturated solution.⁴⁶

$$pH = 3.71 + 0.00417 \cdot T_{\text{Celsius}} - 0.5 \cdot \log(f_{CO_2}) \quad \text{Equation 23}$$

This equation, with T_{Celsius} as temperature [°C] and f_{CO_2} again as fugacity of CO₂, is also available as a nomogram in Background Data 7. Indeed, the pH factor is governed by the actual and saturated pH values of the solution.

$$\log(F_{pH}) = 0.32 \cdot (pH_{\text{sat}} - pH_{\text{act}}) \quad \text{Equation 24}$$

for $pH_{\text{sat}} > pH_{\text{act}}$. When actual pH values are greater than the saturated values due to alkaline substances, the following equation is recommended:

$$\log(F_{pH}) = -0.32 \cdot (pH_{\text{act}} - pH_{\text{sat}})^{1.6} \quad \text{Equation 25}$$

It has to be understood, that application of both, pH and scale factors is not valid. The corrosion rate of scale covered steel is more likely to be under pH and Fe^{++} concentration control, resulting from a local saturation of $FeCO_3$ and Fe_3O_4 at corresponding surfaces. Because of that, F_{pH} is set to 1 if $F_{scale} < 1$.⁴⁶

Calculations regarding the saturated pH additionally have to be treated with caution. Equation 19 refers to steady state corrosion rate readings with necessary Fe^{2+} concentrations needed for $FeCO_3$ and Fe_3O_4 saturations in 10 % NaCl.⁴⁶ The results can be approximated by

$$pH_{sat} = 1.36 + \frac{1307}{T_{Celsius} + 273} - 0.17 \cdot \log(f_{CO_2}) \quad \text{Equation 26}$$

which is connected to Fe_3O_4 . Equation 27 on the other hand, is for $FeCO_3$. The smaller the pH_{sat} value, the more stable and earlier the corresponding corrosion product is being formed.⁴⁶ Investigations of Dunlop et al. confirm Fe_3O_4 to be the primary corrosion product compared to $FeCO_3$.⁴⁶

$$pH_{sat} = 5.4 - 0.66 \cdot \log(f_{CO_2}) \quad \text{Equation 27}$$

Application of pH factors is valid within a temperature range of 20- 80 °C.

Talking about hydrocarbon inhibiting effect, oil factors with respect to water content and crude velocity are also presented within this model. After Lotz et al.⁴⁶ at least 30 % of water can be accommodated before creating a water wetting state, making $F_{oil} = 0$ at $WC < 30$ % and crude velocities > 1 m/s. If velocities are lower than 1 m/s in horizontal flow lines, separation of oil and water can take place and dispersion of water is not the case. If those two laws are violated, F_{oil} is assumed to be 1. In that situation it is important to know, that those threshold values were elaborated for pipeline flow conditions.

The effect of an inhibitor decreasing the corrosion rates can be included by a simple multiplication of corrosion rates with an inhibitor efficiency factor.

However, a major issue concerning De Waard Milliams relationship is the absence of velocity in calculations, making this model of limiting application in oilfields.¹³

De Waard- Smith

L. Smith and C. De Waard published another model^{3, 14} especially for oil field application. Here, a special focus was set on the already mentioned wettability (Equation 9). A semi empirical model with bases of reaction kinetics V_r and rate of mass transport, divided into carbonic acid and acetic acids can be presented. Below, the model for SI units is elaborated.

$$\frac{1}{V_{Cor}} = \frac{1}{V_r} + \frac{1}{V_{m_{H_2CO_3}} + V_{m_{HAc}}} \quad \text{Equation 28}$$

Every term is treated separately below

$$\log(V_r) = 4.84 - \frac{1119}{T_{\text{Celsius}} + 273} + 0.58 \cdot \log(f_{\text{CO}_2}) - 0.34 \cdot (pH_{\text{actual}} - pH_{\text{CO}_2}) \quad \text{Equation 29}$$

pH_{actual} and pH_{CO_2} are the actual pH and the pH of pure water at given partial pressure CO_2 , respectively.

The calculations were based on measured bicarbonate concentrations, CO_2 solubilities, carbonic acid dissociation constants and on best fit equations for their temperature dependence.³ So, if the actual pH is increased by supersaturation of Fe^{2+} e.g., corrosion rate is lowered. In those calculations, pH_{CO_2} is chosen as a reference pH value.

Again, fugacities can be calculated via Equation 20³, but also with the following update¹⁴:

$$\log(f_{\text{CO}_2}) = \log(P_{\text{CO}_2}) + \left(0.0031 - \frac{1.4}{T + 273}\right) \cdot P \quad \text{Equation 30}$$

Like already mentioned, the mass transfer rate [mm/a] is split up and below the following equations are found. Of course, if acetic acids are not present in the system, the term can be neglected.

$$V_{m_{\text{H}_2\text{CO}_3}} = 2.8 \cdot \frac{u_L^{0.8}}{D^{0.2}} \cdot f_{\text{CO}_2} \quad \text{Equation 31}$$

$$V_{m_{\text{HAc}}} = k_m \cdot [\text{HAc}]_{\text{undiss}} \quad \text{Equation 32}$$

k_m is the mass transfer rate of HAc, containing of diffusion coefficient D_{HAc} of HAc in water, the kinematic viscosity ν [m^2/s] and already presented variables velocity [m/s] and inner diameter [m]. $[\text{HAc}]_{\text{undiss}}$ refers to the bulk concentration of undissociated HAc [mol/l], K to dissociation constant [mol/l] and H^+ the concentration of hydrogen ions [mol/l]. D is connected to pipe inner tubing diameter [m] and u_L to liquid flow velocity [m/s].¹⁴

$$[\text{HAc}]_{\text{undiss}} = \frac{[\text{HAc}]_{\text{total}}}{1 + \frac{K_{\text{diss}}}{\text{H}^+}}$$

$$k_m = \frac{D_{\text{HAc}}^{0.7}}{\nu^{0.5}} \cdot \frac{u_L^{0.8}}{D^{0.2}} \quad \text{Equations 33}$$

Compared to de Waard- Milliams models, de Waard- Smith is emphasizing on inhibiting factors of oil, flow velocity and FeS film formation. Besides the scaling factor, also other factors are published additionally.

$$\log(F_{Scale}) = \frac{2400}{T_{Celsius} + 273} - 0.6 \cdot \log(f_{CO_2}) - 6.7 \quad \text{Equation 34}$$

Also the influence of crude oils concerning wetting of steel in relation to watercuts and oil gravity has been investigated more closely via data analysis of two fields with oil gravities of 49 °API and 38 °API. With definition of W_{break} , implying how much water can be dispersed before separation into water and water-in-crude-oil emulsions and including W_{break} into the oil factor equation, makes the factor valid for multiple oil gravities, which are presented within Background Data 15.³ As can be seen, lighter oils have lower water entrainment tendencies than heavier ones.

$$W_{break} = -0.0166 \cdot API + 0.83 \quad \text{For } 50 > \text{°API} > 20 \quad \text{Equation 35}$$

$$F_{oil} = 0.059 \cdot \frac{W}{W_{break}} \cdot U_{liq} + \frac{1.1 \cdot 10^{-4}}{W_{break}^2} \cdot \frac{\alpha}{90} + 0.059 \cdot \frac{W}{W_{break}} \cdot U_{liq} \cdot \frac{\alpha}{90} \quad \text{Equation 36}$$

where α is the angle of deviation [degrees°] from vertical and W is supposed to be the Watercut measured at wellhead.

Theoretically, a watercut of 74 % is the maximum possible to be carried in an emulsion, after Ostwald. Since the corrosion inhibiting effects of oil is expected to be very low in that situation, the oil factor is conservatively assumed to be 1 with Watercuts >80 %.³

To account the presence of iron sulphide films, a factor with respect to partial pressures of H_2S and CO_2 is introduced. It has to be mentioned, that scaling factors, both concerning $FeCO_3$ and FeS films, are in a speculative relation to reality. Both layers can reduce corrosion rates significantly but creation is primarily not guaranteed or can suffer breakdown with time.

$$F_{H_2S} = \frac{1}{1 + 1800 \cdot \frac{P_{H_2S}}{P_{CO_2}}} \quad \text{Equation 37}$$

For calculations, a “Partial Pressure CO_2 / Partial Pressure H_2S ” ratio of 200 would decrease the corrosion rate by 90 %. The standard deviation of corrosion rate prediction increases with 5 % to overall 30 % compared to lean CO_2 corrosion forecasting.

2.3.2 NORSOK

This model is based on empirical investigations for carbon steel corrosion in water containing CO_2 at different temperatures, pHs, CO_2 fugacities and wall shear stresses (S) via flow loop installations. Temperature ranges from 5 °C to 160 °C. It does not include H_2S impacts.

$$CR_t = K_t \cdot f_{CO_2}^{0.62} \cdot \left(\frac{S}{19} \right)^{0.146 + 0.0324 \cdot \log(f_{CO_2})} \cdot f(pH)_t \quad \text{Equation 38}$$

K_t is found via linear extrapolation between the calculated corrosion rate above and below the desired temperature (Background Data 8). The function of pH is illustrated in Background Data 10. All input parameter ranges and requirements for oil well upstream calculations are attached in the appendix section starting from Background Data 8 to Background Data 14. The pH calculations are based on Equation 1 to Equation 5 reactions, as well as sodium bicarbonate and sodium chloride to be only present salts in solutions.¹⁸

$$K_H = \frac{C_{CO_2}}{P_{CO_2}} \quad \text{for} \quad CO_{2(g)} \rightarrow CO_{2(aq)}$$

$$K_0 = \frac{C_{H_2CO_3}}{C_{CO_2}} \quad \text{for} \quad \text{Equation 1}$$

$$K_1 = \frac{C_{HCO_3^-} \cdot C_{H^+}}{C_{H_2CO_3}} \quad \text{for} \quad \text{Equation 2}$$

$$K_2 = \frac{C_{CO_3^{2-}} \cdot C_{H^+}}{C_{HCO_3^-}} \quad \text{for} \quad \text{Equation 3}$$

$$K_W = C_{H^+} \cdot C_{OH^-} \quad \text{for} \quad H_2O \rightarrow H^+ + OH^- \quad \text{Equations 39}$$

Above, the routine calculation of pH is based on equations presented on the right hand side and results in chemical equilibrium constants (K), respectively.¹⁸

Combining constants from above with the assumption of electro neutrality, the following equation¹⁸ for formation waters' H^+ concentration can be gained:

$$C_{H^+}^3 + C_{0,Bicarb} \cdot C_{H^+}^2 - (K_H \cdot K_0 \cdot K_1 \cdot P_{CO_2} + K_W) \cdot C_{H^+} - 2 \cdot K_H \cdot K_0 \cdot K_1 \cdot K_2 \cdot P_{CO_2} = 0$$

$$\text{Equation 40}$$

This equation is to be solved by using Newton's method.¹⁸ $C_{0,Bicarb}$ equals the initial concentration of bicarbonate, C_{H^+} the concentration of hydrogen ions in the system.

Fugacities are calculated via same principle performed in Equation 20.

Wall shear stresses S [Pa] are also an important parameter for corrosion rate prediction including flow velocity in calculations. As can be seen in Background Data tables, many parameters like watercuts, oil- gas- water viscosities or compressibility are inserted. It has to be kept in mind, that within that model, only average shear stresses are assumed and calculated. If for example obstacles are influencing flow streams, fluctuations of shear stresses could be

obtained, where peak shear stresses might exceed the average limit in higher dimensions and, because of that, even higher corrosion rates are faced than those calculated by the model.¹⁸

The mean wall shear stress at medium or high velocities for liquids:

$$S = 0,5 \cdot \rho_m \cdot f_{friction} \cdot u_m^2 \quad \text{Equation 41}$$

where

$$f_{friction} = 0,001375 \cdot \left[1 + \left(20000 \cdot \frac{k}{D} + 10^6 \cdot \frac{\mu_m}{\rho_m \cdot u_m \cdot D} \right)^{0,33} \right] \quad \text{Equation 42}$$

with ρ_m , u_m describing the mixed density [kg/m³] and velocity [m/s], k for the pipe roughness [m] and D for the pipe inner diameter [mm]. μ stands for viscosities [Pas], Q for flowrates [Sm³/day] for liquids and [MSm³/day] for gas and the subindices L, G, O and W account for liquid, gas, oil and water. Remaining equations for proper application of the model are found below.

$$\begin{aligned} \rho_m &= \rho_L \cdot \lambda \cdot \rho_G \cdot (1 - \lambda) \\ \rho_L &= \varphi \cdot \rho_w + \rho_o \cdot (1 - \lambda) \\ \rho_G &= 2,7 \cdot 14,5 \cdot 16,018 \cdot P \cdot \text{spec. gravity} / Z \cdot (460 + T_f) \\ u_m &= u_L^S + u_G^S \\ \mu_m &= \mu_L \cdot \lambda \cdot \mu_G \cdot (1 - \lambda) \\ \lambda &= \frac{Q_L}{Q_L + Q_G} \end{aligned} \quad \text{Equations 43}$$

Z for the compressibility of gas, s for superficial and variables P and T_f stand for total system pressure [bar] and temperature [°F].

Also flow effects are determined empirically, which does not allow determining any critical velocities via NORSOK.⁴⁷

The viscosity of the water wet region, that means above the inversion point of dispersed flow, the viscosity of any dispersion is given as¹⁸:

$$\mu_L = \mu_w \cdot \left(1 + \frac{\frac{1-\phi}{B_w}}{1,187 - \frac{1-\phi}{B_w}} \right)^{2,5} \quad \text{Equation 44}$$

where B_w :

$$B_w = \frac{1 - \phi_c}{1,187 \cdot \left(1 - \left(\frac{R_\mu}{\mu_{rel/\max}} \right)^{0,4} \right)} \quad \text{Equation 45}$$

If corresponding data for upper equations are not available, medium viscosity of oil/water dispersion is being used. For 60 °C, a maximum relative viscosity to oil, $\mu_{rel/ max}$, of 7.06 is assumed at watercuts, ϕ , of 0.5 with water viscosities of 0.00046 Pas and R_{μ} , μ_w/μ_o , equal to 0.42.¹⁸

For 20 °C to 150 °C:

$$\mu_w = 1,002 \cdot \left(10^{\frac{(1,3272 \cdot (20 - T_c) - 0,001053 \cdot (T_c - 29)^2)}{T + 105}} \right) \cdot 10^{-3} \quad \text{Equation 46}$$

Units can be converted with support of conversion tables in the Appendix, which is to be found at "10 Literature".

Concluding from literature the following parameters result in trends given below:

- Increase of Partial Pressure CO₂, which decreases pH, raises corrosion rates.
- Increase of Partial Pressure H₂S reduces corrosion rates (to a certain extent). The "partial pressure CO₂" to "partial pressure H₂S" ratio is of importance in terms of protective FeS film dropout.
- Increase of Flow Velocity is considered to increase corrosion rates.
- At temperatures of 80°C a corrosion peak is experienced, so exceeding that temperature value, protective FeCO₃ films are formed reducing corrosion rate.
- Correct inhibitor injection and application result in corrosion rate reduction.

3 Field Data

Data is provided by an oil company (O.C.), in order to have a clear picture on the corrosion situation of austrian oilfields. Coupons have been installed on surface within a three phases measurement cycle, where three coupons were installed one after another at wellhead region for 69 days each (average). After each phase, adjustments concerning inhibition could have been set. Pictures to understand coupons installation are provided within Background Data 17 and Background Data 18. Downhole investigations have been performed as well prior to surface measurements, where coupons have been installed below the sucker rod pumps inside the tailpipe (Background Data 18). Of course downhole coupons were exposed to corrosive environments for a longer period of time (888 days average), since workover and thus undesired production stop is required to extract the samples.

For evaluation of influential parameters (except inhibitor performance), only uninhibited wells were chosen as reference. The first installed coupons of surface measurements include the greatest amount of uninhibited wells as well as the shortest time gap between downhole and surface measurements.

3.1 Fluid Characteristics and Watercut

pH and Fe^{2+}

pH values measured in austrian oilfields range from 6.5 minimum to 7, according to the oil company's laboratory experiments.⁴⁸ Still it has to be kept in mind, that those pH values of water- samples are being measured under atmospheric laboratory conditions, where influences of pressures are decreased dramatically. That is why, for example at dealing with FeCO_3 and its precipitation temperature, the correct assumption of pH is an issue.

Like already mentioned in the theoretical part, with pH values of 6.5, FeCO_3 is able to precipitate at room temperature already.²⁵ Downhole measurement tools are often applied to measure the pH of formation waters downhole under relevant conditions in the oil and gas industry.^{49, 50} To include the partial pressure CO_2 in pH analysis, two corrosion prediction models are used. Calculating the pH values, based on representative surface- and downhole oilfield data, by means of NORSOK, the following values can be gained:

Table 1 – pH Verification via NORSOK¹⁸

Parameter	Surface Condition	Downhole Condition
Temperature [°C]	20	40
Pressure [bar]	8	30
Partial Pressure CO ₂ [bar]	0.1	4
Bicarbonate [ppm]	0	0
Ionic Strength [g/l]	50	50
pH	4.3	3.5

Formulas are to be found in the NORSOK sector. As shown in the table above, bicarbonates are not considered and ionic strength values were set to the NORSOK default value for formation waters and constant.

Calculating the pH via de Waard- Milliams approach (Equation 23), implying a diffusion factor of 1, a partial pressure of CO₂ of 0.1 bar and a temperature estimate of 20 °C, a result of approximately 4.3 can be gained as well. Further investigations can be done easily by means of Background Data 7- nomogram and Background Data 9, which shows graphically the distribution and the influence of partial pressure CO₂ and bicarbonates. This shows that laboratory pH measurement results can not be used within this work, whereas it has to be understood, that those pH calculations are approximations and have to be treated with caution as well, since a number of parameters (H₂S, chlorides, acetic acids etc.) were not considered. Formation waters are considered to be Fe²⁺ saturated.¹⁴

Watercut

The percentage of water produced in oil and gas production is represented by the watercut. Water supports corrosion by serving as an electrolyte and creating acids in combination with corrosive gases.^{1, 2, 10, 19, 21}

Below uninhibited wells' surface and downhole corrosion rates are plotted with respect to its watercuts and are sorted after decreasing surface watercuts. In this situation it is important to know, that oilfields of Austria are faced with an average watercut of approximately 90 %. Considering that value, inhibiting support of oil- water emulsions can not be expected after Smith.^{3, 14} Below 80 % of water content in the fluid stream, an inhibitive factor for the oil phase, is applied within that corrosion prediction model (Chapter "2.3.1 De Waard- Milliams- Smith").³ As can be seen, higher amounts of wells show watercuts below 80 %, which of course needs to be analyzed more deeply, because of the strong deviation from the fields' average. Since there are bigger time gaps between some surface and downhole measurements, the watercuts are being presented separately.

Figure 10 shows low corrosion rates at wells with watercuts lower than 80 %. Especially by following the surface watercut decrease, the impact of the oil can be seen.

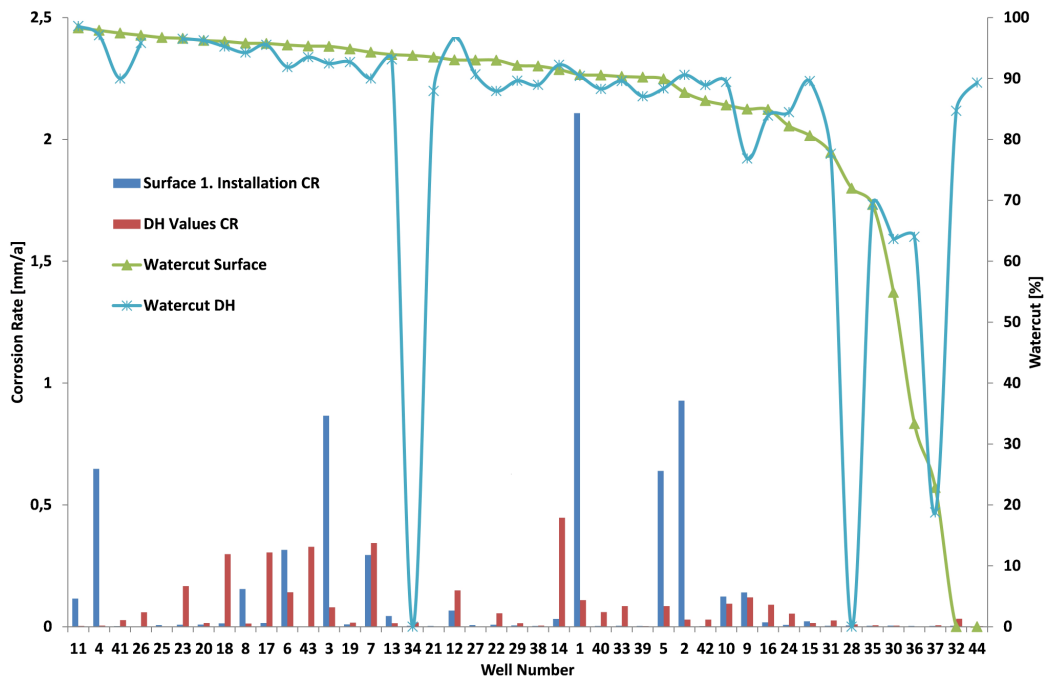


Figure 10 – Numbered Downhole and “Surface 1. Installation” Watercuts versus corresponding Corrosion Rates⁵¹

But still there are low corrosion rates at higher watercuts that can not be explained by inhibiting effects of oil (Number 19, e.g.). This is why other parameters are expected to influence measurements and their results.

Like already mentioned, low watercuts like illustrated in Figure 10 are not distinctive for fields in that region. That is why the corresponding velocity is being screened and a correlation between the watercut can be found. The reason for the low water content is the connected low velocity. During measurement interval, pump and flow velocity as a consequence, were being reduced for some reason not to be identified anymore. With increasing velocity, a higher amount of water is being sucked into the borehole and creating a higher watercut because of that. On the other hand, with a lower velocity, oil can accumulate and separate downhole more easily and decrease watercut and corrosion rate.

Figure 11 as well as Figure 12 show clearly the dependence of the watercut on velocity already described above. Here it can be seen that watercut increases with velocity. With the lower limit of approximately 0.1 m/s, a threshold value of velocity could be found additionally to the watercut limit of 80 %. Details regarding velocity calculations and closer description of the velocity distribution and its corrosive limits are elaborated in the next subchapter “3.2 Velocity”.

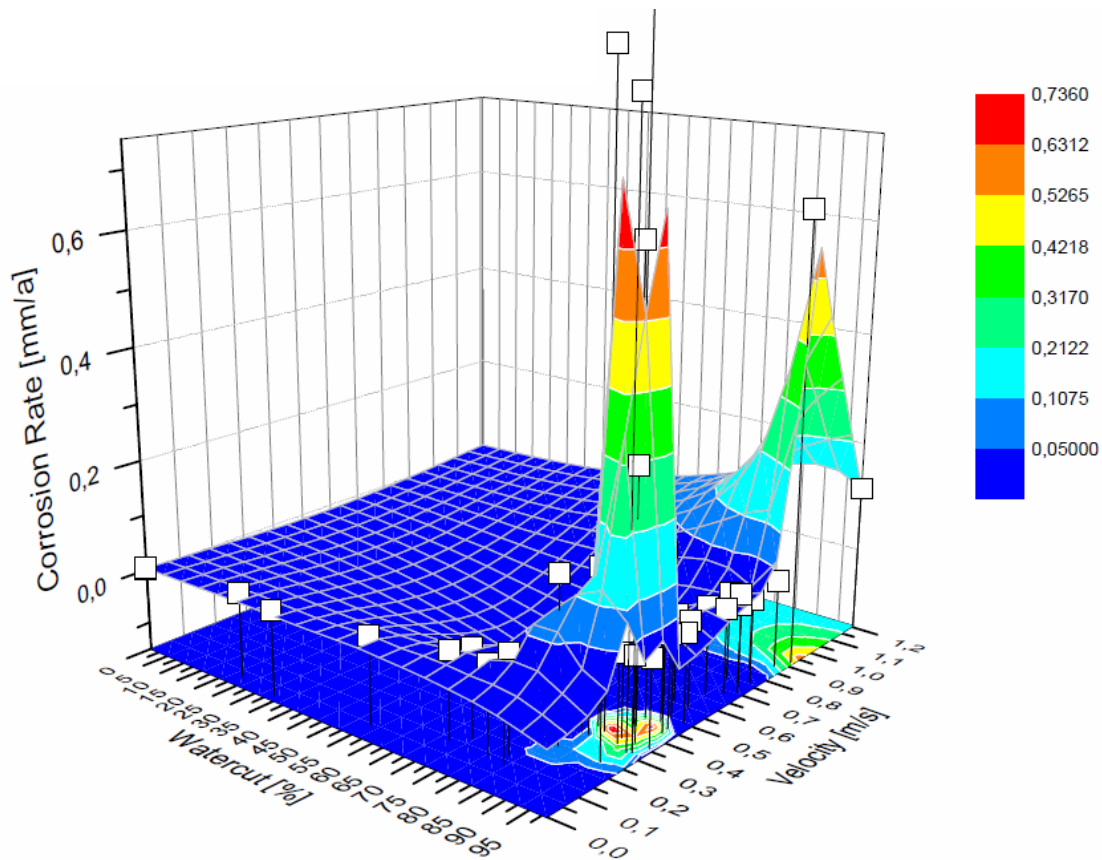


Figure 11 – “Surface 1. Installation” Corrosion Rates versus Watercut and Wellhead Velocity⁶⁶

The 3D diagrams are created with Origin® 8.5; in order to fit an appropriate surface on the data points, the “Kriging” correlation was selected. The “Kriging” correlation uses a weighted average interpolation, minimizing the variance of a certain point with help of the weighted average of surrounding points. The weighted average is evaluated via the correlation structure connected to the corresponding area of the original data points.⁵² A 20 x 20 matrix, with a radius of investigation of 2, a minimum- maximum point window from 10 to 100 and a smoothing grade of 1 was created. Smoothing the plane simply creates a better picture for the reader. Whereas 0 does not influence the diagram and its plane, a too high smoothing grade can lead to a misleading output. The investigation radius defines the number of data points next to the newly created data point, chosen as calculation basis.⁵² As can be seen, the z- values of the plane are calculated via x- and y axis’ values. To see the real background distribution, “raw” data points, marked as white squares, from the plotted measurement are included in 3D diagrams. To have a more precise look on relevant issues, highest corrosion rates can not be seen sometimes in the plots. Figure 10 can be used for total corrosion rate inspection and connecting relevant corrosion data to the well number and so to the full data background of every well in the Appendix Section. A major problem with “Kriging” correlations can be seen at Figure 11 and Figure 12 for the first time. If the number of data points of one sector is low, high values create extraordinarily high peaks. This could lead to a misinterpretation of tendencies and would be even more dangerous if “raw” data was not inserted in 3D figures. There is one

value exceeding 0.05 mm/a at Figure 12 at a watercut of 76 % creating such a peak (Corrosion rate 0.12 mm/a), whereas all other measurements stay below the threshold- limit of 0.05 mm/a. Nevertheless create those 3D plots a good overview about interaction of parameters and are applied whenever necessary throughout this work.

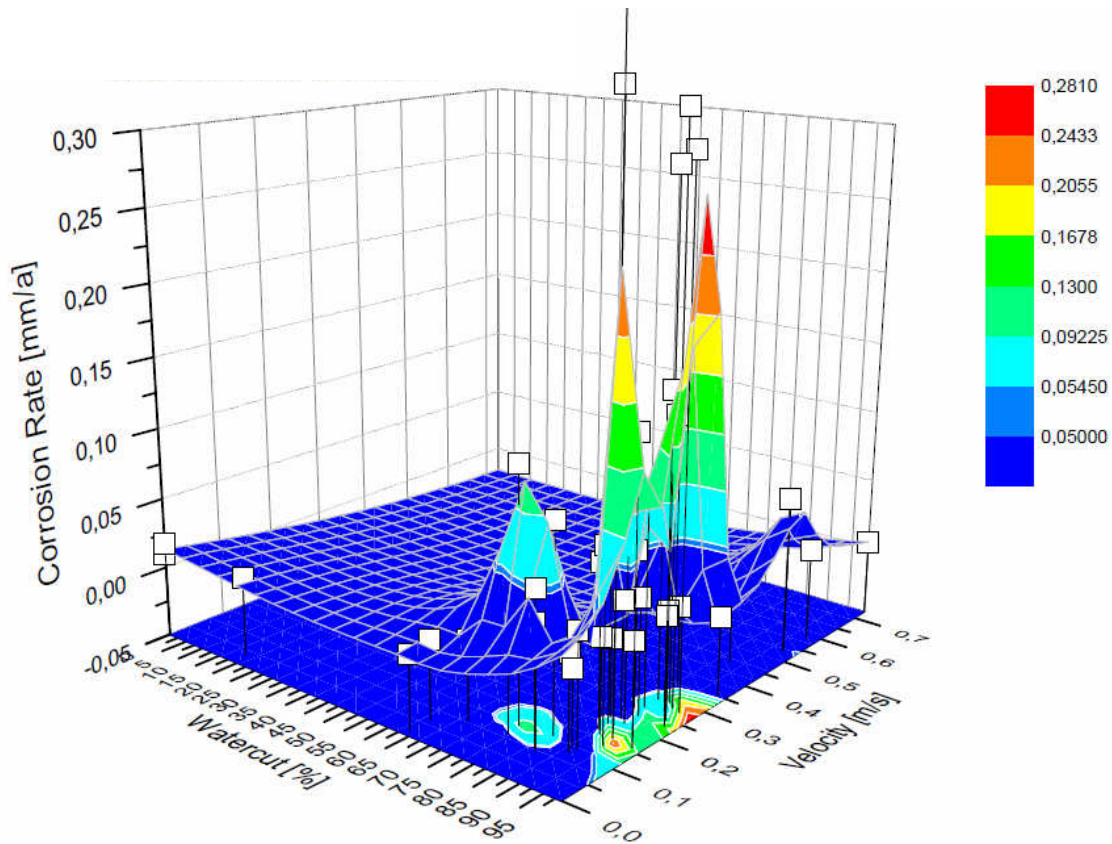


Figure 12 – Downhole Corrosion Rates versus Watercut and Wellhead Velocity⁶⁶

Lower watercuts could be explained via low velocities and disappear as soon as velocity exceeds a velocity lower limit. In order to “lift” the measurements to a comparable stage, watercut limits are applied in further steps to make sure that other external forces and influences on corrosion are identified more clearly.

3.2 Fluid Velocity

Velocity calculations are based on the average flowrates produced within the measurement time interval and the diameter of the pipe, where the coupons have been installed and liquid streams were able to interact with coupons’ metal surfaces. The production of gas and multiphase flows as a consequence was not considered in analysis.

$$v = \frac{2 \cdot Q}{\left(\frac{D^2 \pi}{4}\right) \cdot 24 \cdot 3600}$$

Equation 47

where Q stands for the flowrate in [m³/day], D for the inner diameter of the coupon location [m], 24 and 3600 conversion factors to achieve a velocity in [m/s]. The factor 2 accounts for the creation of upstream velocity only at the upstroke of the sucker rod pump.

Generally it has to be understood, that only with upstroke movement of the sucker rod pumps, fluid is passing by the coupons. For this calculation, a uniform constant flow with the corresponding upstroke fluid velocity is assumed as an approximation.

As already mentioned in previous chapters, velocity can contribute highest support for corrosion and metal deterioration. High fluid velocity streams, independent of particle or solid content, is able to remove protective layers, like FeCO₃, FeC or conventional oil films, increasing corrosion processes.^{10, 11, 28, 29} With increasing velocity, higher wall shear stresses are created and impacts of liquid streams on metal surfaces are higher.¹⁸ Generally, there should be a threshold velocity. Below that limit, no impacts of velocity on metal structures can be determined or they are of lower importance.

Figure 13 and Figure 14 sketch the velocity distribution illustrated in Figure 11 and Figure 12 in a more precise manner to have a better overview on the distribution. As can be seen, “Surface 1. Installation” velocities are higher to a certain degree, explained by the smaller (inner-) exposure diameter of 2”, compared to the possible downhole tubing diameters of 2 7/8” and 3.5” (Inner Diameters of 2.441” and 2.992”). Like already described, for calculations the inner diameters of tubings were chosen. Additionally a velocity lower limit of both, surface and downhole, can be gained and applied to future investigations to make the operation with most relevant data possible.

Table 2 – Lower Limits of “Surface 1. Installation” and Downhole Velocity⁵¹

Measurement Type	Velocity Limit [m/s]
Surface 1. Installation	>0.15
Downhole	>0.11

Calculation of Reynolds numbers with respect to threshold velocity limits:

$$N_{Re} = \frac{\rho v D}{\mu}$$

Equation 48

by inserting the inner diameter of the largest tubing with 2.992” or 0.076 m (of 3.5” tubing), the velocity of 0.11 m/s, the dynamic viscosity (μ) and density (ρ) of water, a Reynolds number of 8360 can be obtained.

In full pipe flow, turbulent flow occurs with $N_{Re} > 4000$.⁵³ Practically spoken, even conservatively calculated, flow is considered to be turbulent, which is critical to conservation of protective layers.^{10, 11, 28, 29}

Most low velocity values deal with low watercuts (Figure 14). In one example, with well number 24,(Background Data 20) the low velocity of approximately 0.07 m/s includes a higher watercut of 84 %. But that value is not being considered regarding the velocity limit and assumed to be controlled, since the surface value of the first coupon installed are far below the limit and comparable velocities do not show corrosive tendencies.

Secondly, with increasing velocities, a large number of low corrosion rates in surface (Figure 13) as well as in downhole measurements (Figure 14) is found. This decrease in corrosion rates under advanced velocity was already visualized within 3D- plots of Figure 11 and Figure 12. Those low values could be explained by certain flow anomalies created with increasing flow velocities, which can not be proven reasonably in this situation. With progressing investigations on corresponding data within this work, explanations need to be found in order to understand those velocity distributions.

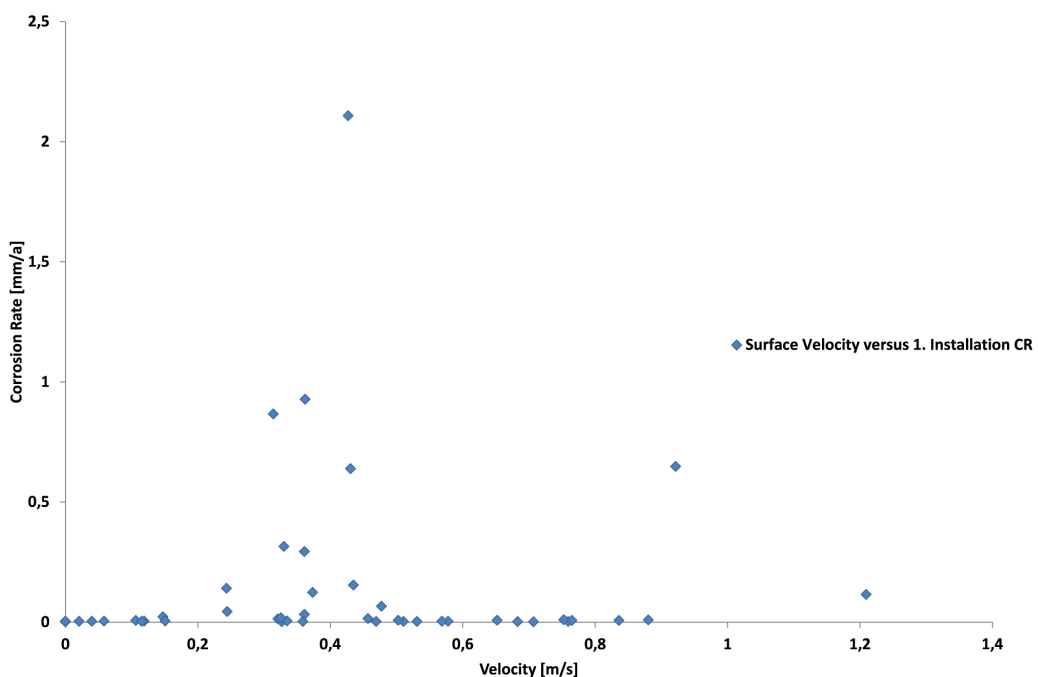


Figure 13 – “Surface 1. Installation” Corrosion Rate versus Wellhead Velocity⁵¹

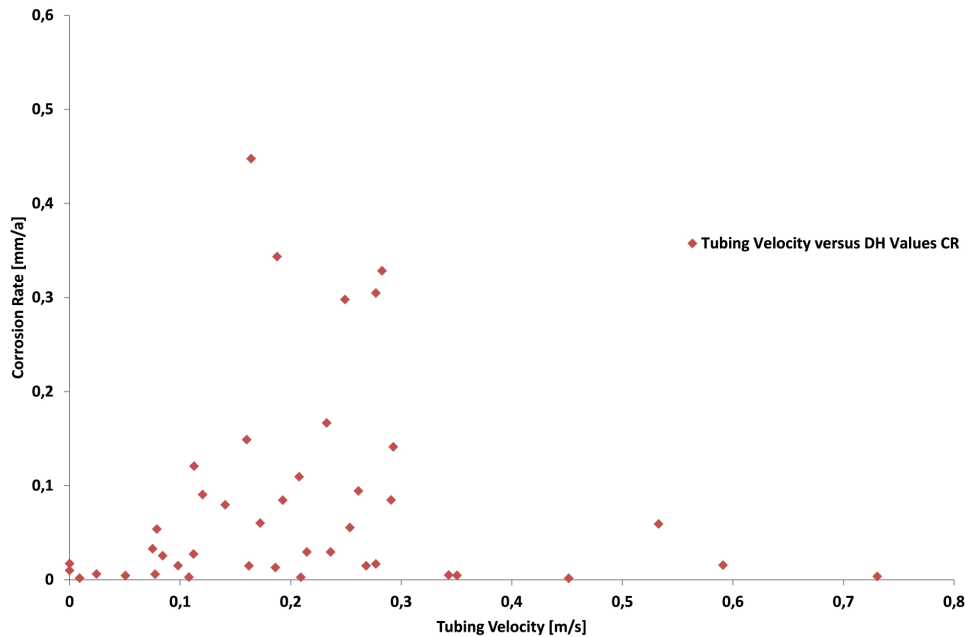


Figure 14 – Downhole Corrosion Rate versus Tubing Velocity⁵¹

To connect the sketched data from above to corresponding well names and other data, alternative illustrations, sorted after decreasing velocities are attached within Background Data 19 and Background Data 20. The term “Tubing Velocity” accounts for the velocity in the tailpipe, the lowest part of the tubing string, where the coupons are installed internally.

The threshold values of the velocities as well as concerning the watercut are used in future parts of this work to create an equal level for interpretations.

3.3 CO₂ and H₂S Partial Pressure

Oxygen is not present in the system and can be excluded.⁵⁴

Partial pressures (Equation 11) are calculated on the basis of coupons position. Downhole partial pressures are calculated via dynamic fluid levels of the corresponding sucker rod pump. The hydrostatic column of this fluid level to the tailpipe entrance, where the coupons are located, was chosen as system’s total pressure.

$$P_{\text{Downhole}} = \rho \cdot g \cdot h_{\text{Fluid_Annulus}} + P_{\text{Casing}} \quad \text{Equation 49}$$

Surface partial pressures are based on wellhead pressures chosen to be the total system pressure in that situation.

CO₂ partial pressures dominate corrosion processes over creation of carbonic acid and reduction of pH because of that. With decrease of pH, the reduction of H⁺ ions is accelerated

and so the whole corrosion process.¹³ Basically, the corrosion rate in CO₂ corrosion processes can be considered as proportional to the CO₂ partial pressure.^{19,21}

In Figure 15 and Figure 16, input gained from literature can not be strengthened. As a matter of fact, in both surface and downhole measurements, there is a high amount of measurements resulting in low corrosion rates at relatively high partial pressures of CO₂. Partial Pressure CO₂ and the corresponding corrosion rates are not to be correlated in a proper manner within those data points and so no outcome of these can be published.

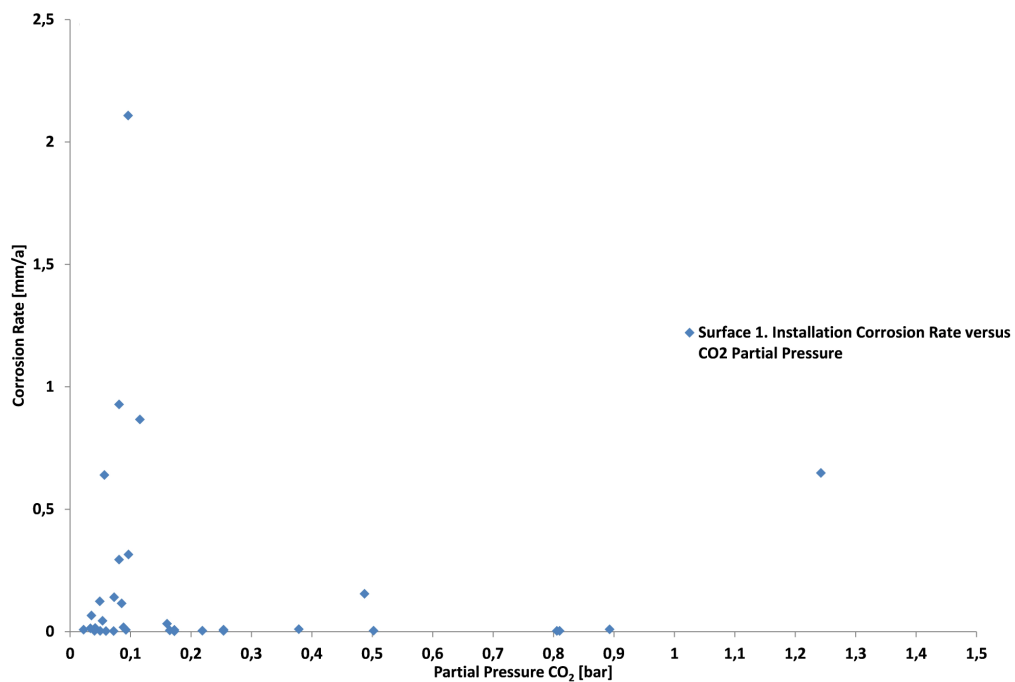


Figure 15 – “Surface 1. Installation” Corrosion Rates versus CO₂ Partial Pressures for Watercuts > 80 % and Velocities > 0.15 m/s⁵¹

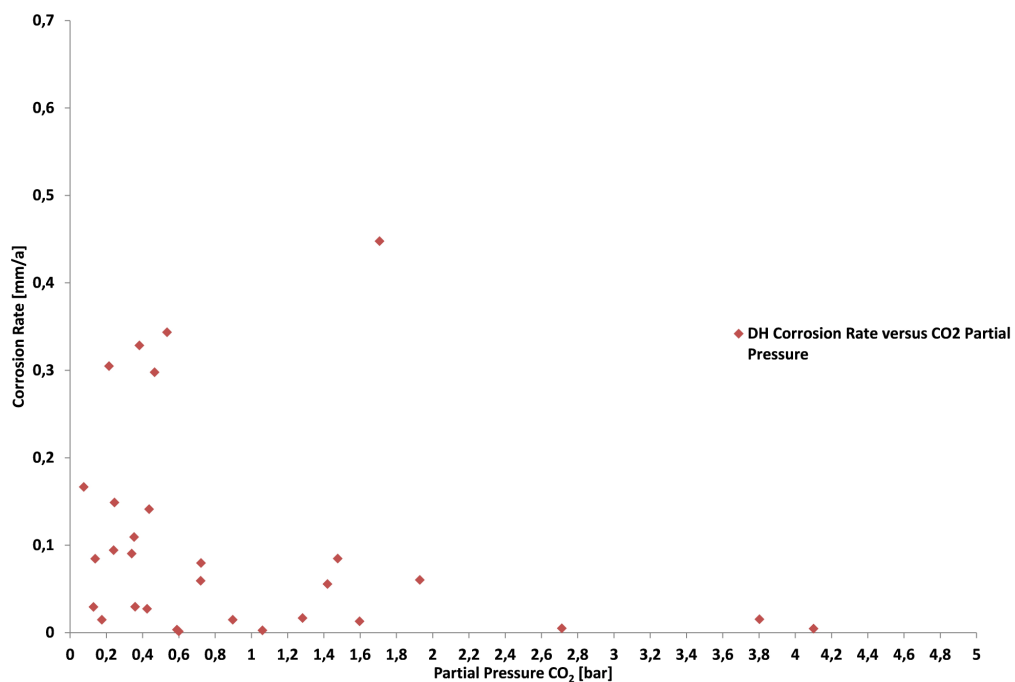


Figure 16 – Downhole Corrosion Rates versus CO₂ Partial Pressures Watercuts > 80 % and Velocities > 0.11 m/s⁵¹

Of course downhole pressures are, due to the dynamic fluid column, higher compared to the wellhead pressured samples on surface. To have again the possibility to compare freely various wells in the Appendix and also to have an alternative view on the data, Background Data 21 and Background Data 22 are provided.

For those partial pressure- investigations, velocity and watercut restraints, presented in previous sectors, were applied to filter low corrosion rates caused by those parameters.

To find an explanation for the low corrosion rates and the corresponding distribution, other parameters have to be screened. Focussing on protective films, which possibly could lead to a reduction of coupons' corrosion rate, FeS is the first that is considered. Screening the H₂S contents in affected wells, using the same system pressures, new outputs are possible to be found.

Iron sulphide layers can be created also in lower temperature regions and can accumulate at the metal surface in a dynamic or in a static system.²¹

Below, figures on page 35 show H₂S partial pressures in connection to CO₂ partial pressures versus corrosion rates. Again, "Surface 1. Installation" and Downhole values are split into two diagrams; for a better picture on the impact of H₂S partial pressures, 3D diagrams with help of "Kriging" correlations and same adjustments like in watercut investigations, are applied. As can be seen in Figure 17 and Figure 18, corrosion rates decrease with increasing partial pressure of H₂S. This is not only valid for downhole values; also for "Surface 1. Installation" measurements, where partial pressures are lower, it can be accounted. In the past, flow loop investigations proved the creation of protective iron sulphide films with pressures lower than 0.0001 bar partial pressure H₂S.²¹

Again, the weaknesses of the "Kriging" Correlation can be seen. Especially Figure 17 creates a peak due to one single data point at approximately 1.2 bar CO₂ pressure. That can be explained by a lack of data in the radius of investigation of the correlation. Changing the radius is also not changing that problem, since data points are not distributed equally and may result in a misleading picture at regions, where higher amounts of data is present.

Looking on the provided data and considering Figure 19 and Figure 20, where the necessary numbered H₂S wells are presented, the formation of protective films could be expected. Still, there are wells not showing low corrosion rates in connection to its hydrogen sulphide partial pressures. Well number 4, 8 and 11 from "Surface Measurements" or for example 18, 43 and 16 at downhole measurements show raised corrosion rates.

Nevertheless, those charts show in average much higher corrosion rates on the right hand side, where no partial pressure of H₂S is registered, compared to the ones where H₂S was measured.

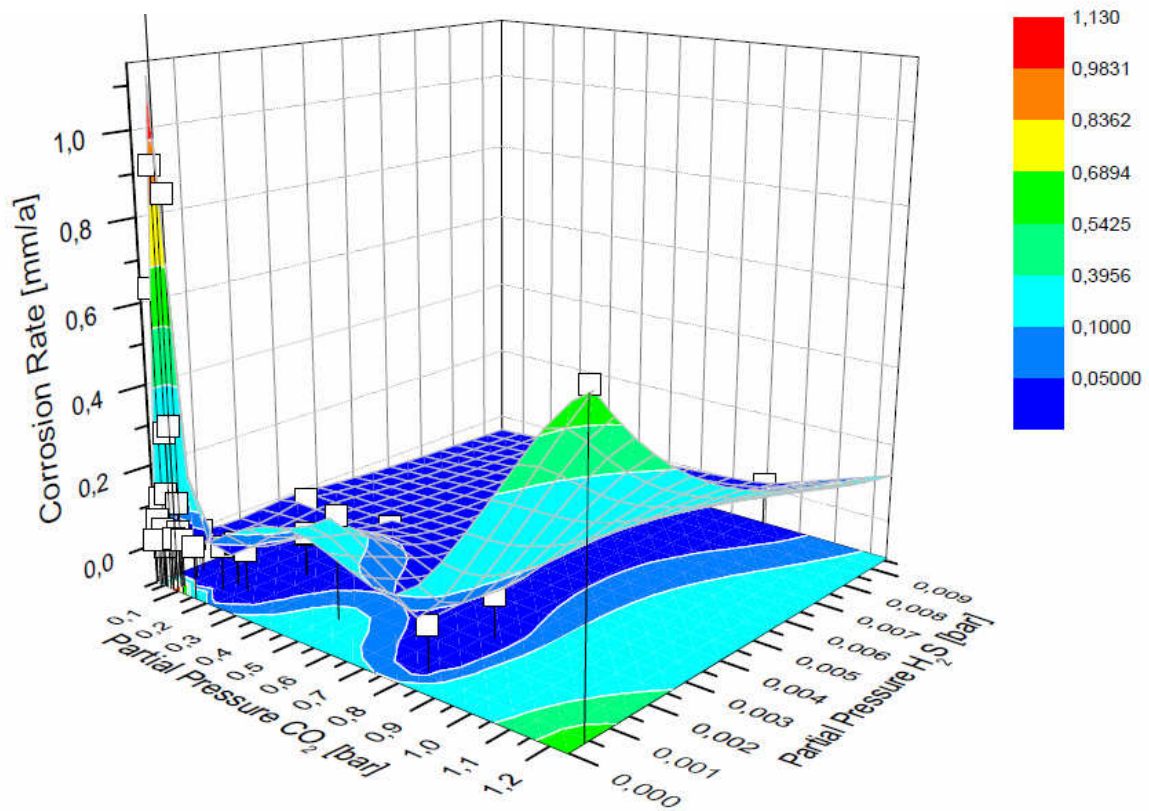


Figure 17 – “Surface 1. Installation” Corrosion Rates with Respect to Partial Pressures CO₂ and H₂S for Watercuts > 80 % and Velocities > 0.15 m/s⁵¹

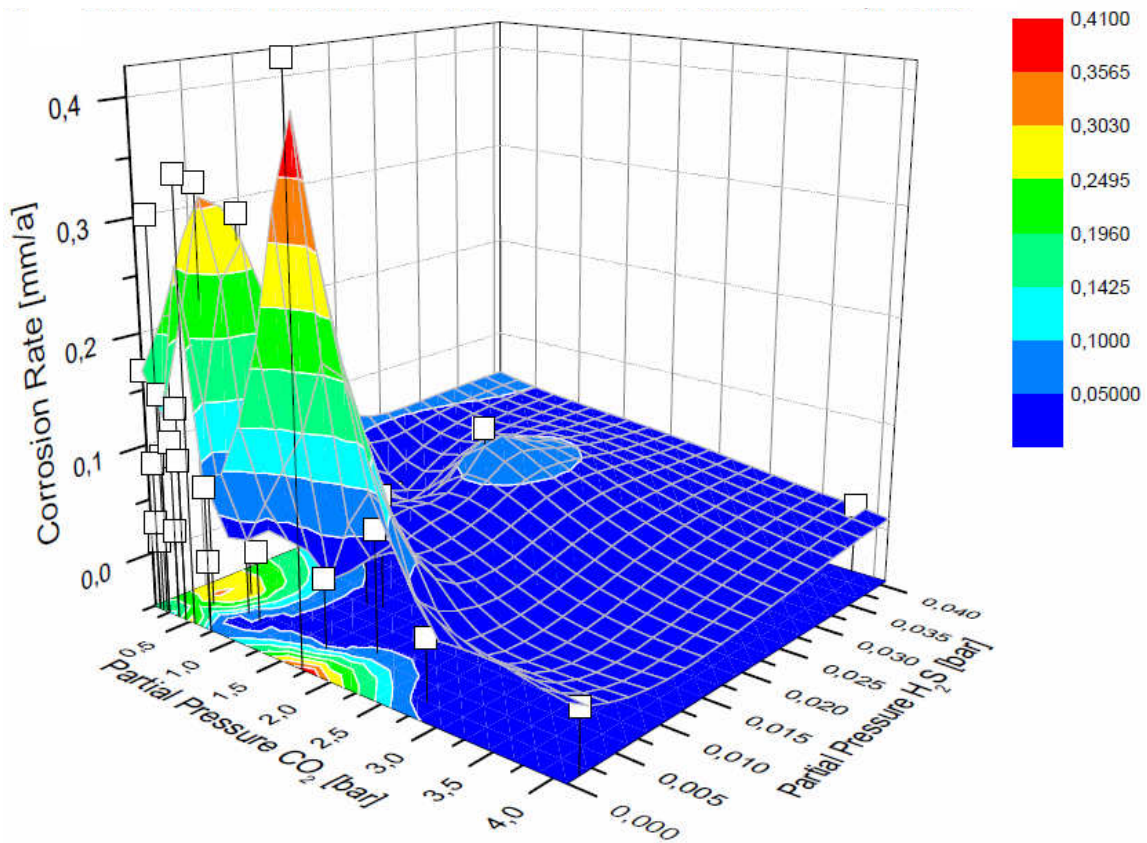


Figure 18 – Downhole Corrosion Rates with Respect to Partial Pressures CO₂ and H₂S for Watercuts > 80 % and Velocities > 0.11 m/s⁵¹

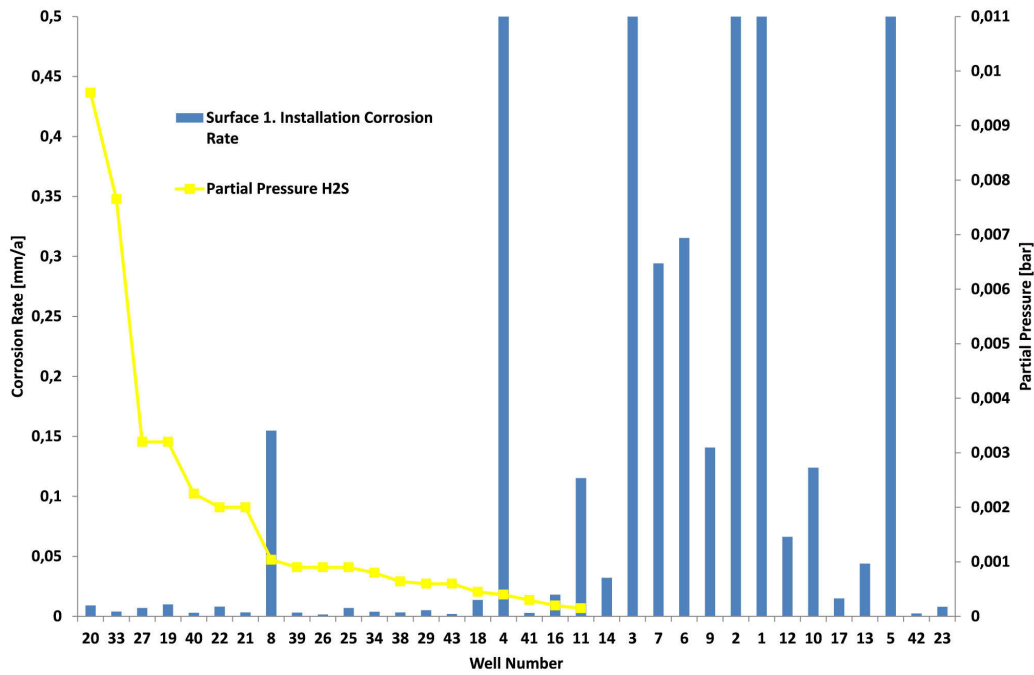


Figure 19 – “Surface 1. Installation” Corrosion Rates versus numbered Partial Pressures of H₂S for Watercuts > 80% and Velocities > 0.15 m/s⁵¹

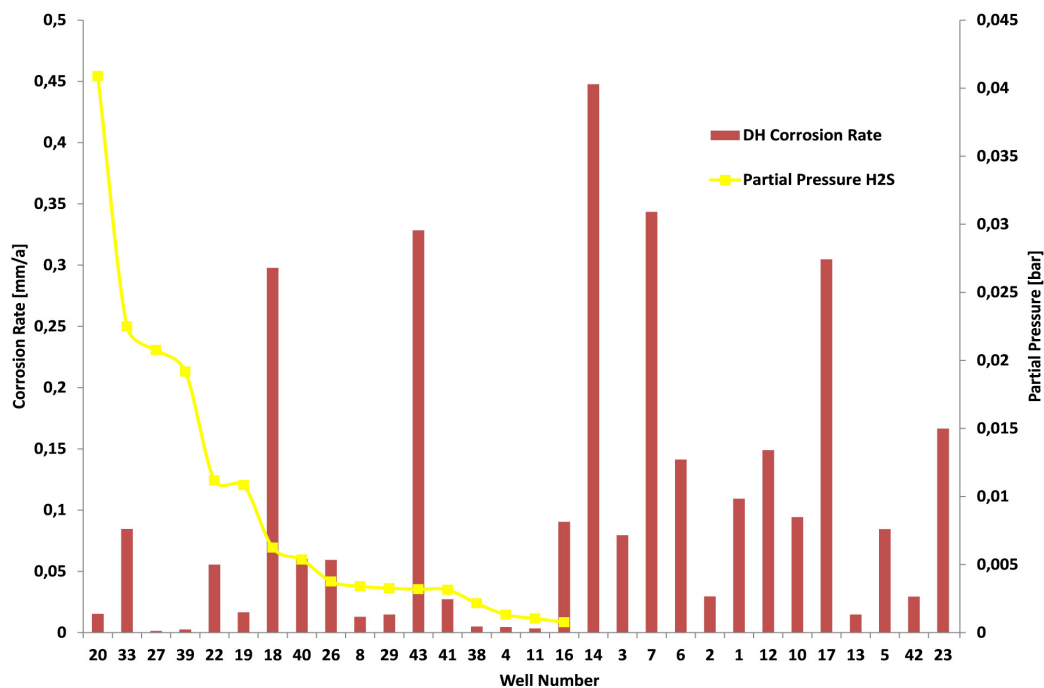


Figure 20 – Downhole Corrosion Rates versus numbered Partial Pressures of H₂S for Watercuts > 80% and Velocities > 0.11 m/s⁵¹

To have an additional view on the data, a diagram based on Pots²⁶ et al. theory, concerning the partial pressure ratios of CO₂ and H₂S is created. (Figure 21, Figure 22). Basically, between 20 and 500 (P_{CO_2} / P_{H_2S}) a mixed corrosion process of CO₂ and H₂S takes place. That means, besides FeCO₃, also iron sulphide (FeS) is able to precipitate. As can be seen in relevant figures, most H₂S wells screened are located in the mixed corrosion region. Above 500, the formation of iron sulphide films is unlikely and CO₂ corrosion could attack freely. As seen in

previous charts, a possible sulphide layer created, would not be that efficient downhole compared to “Surface 1. Installation”.

In downhole measurements, again 18, 43 and 16 do not fit to other results. This could be explained by a possible removal of iron sulphide film and localized corrosion or also called “Pitting” tendency of the material. The pitting probability increases with increasing H_2S partial pressure.¹⁴ Also in surface analysis, the corrosion rates of coupons exposed to the corrosive fluid stream can not be connected 100 % to the formation of FeS layers. Of course the pressure ratios are the same surface and downhole, since there is no variation of CO_2 and H_2S contents. But still, the surface and downhole conditions are differing in temperature and fluid velocity (only parameters mentioned, that are considered in this work).

Especially temperature influence is important talking about $FeCO_3$ precipitation and its formation as a protective layer. Compared to FeS films, temperatures as well as pH are more critical in $FeCO_3$ precipitation.^{21, 25, 26, 31, 55} In the subchapter “3.4 Temperature” discussion of temperature-influence on $FeCO_3$ scales is emphasized.

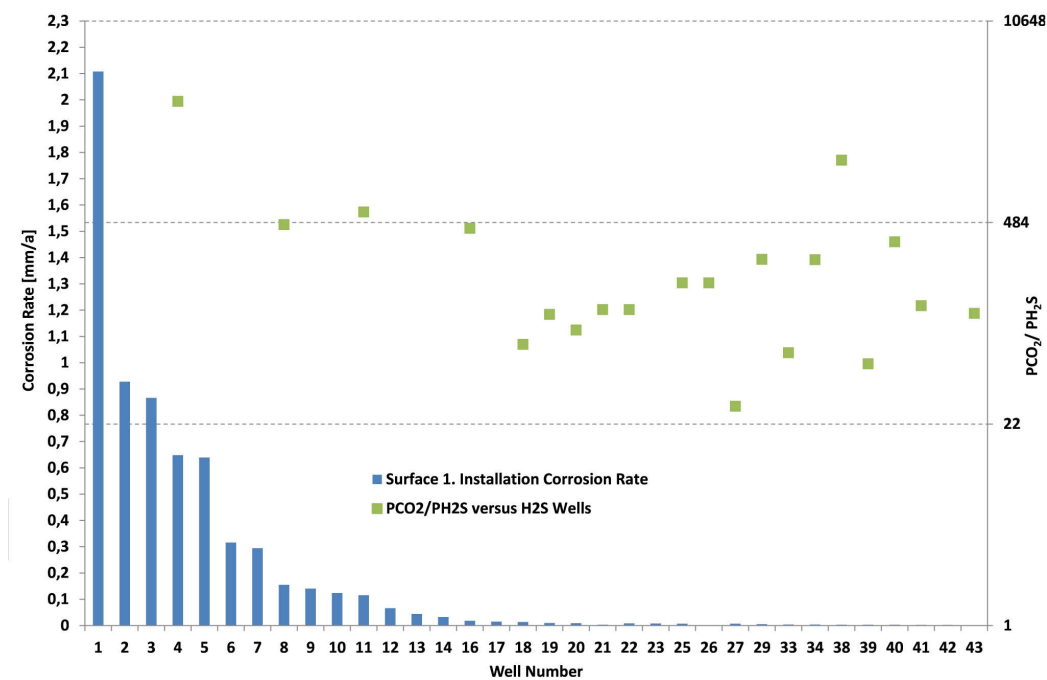


Figure 21 –Partial Pressure CO_2 and H_2S Ratio versus “Surface1. Installation” Corrosion Rates connected to corresponding Well Number for Watercuts > 80 % and Velocities > 0.15 m/s after Pots⁵¹

All wells were included in Figure 21 and Figure 22 to keep track which wells contain H_2S . Only corrosion rates (and pressure ratios), measured at H_2S wells, are illustrated.

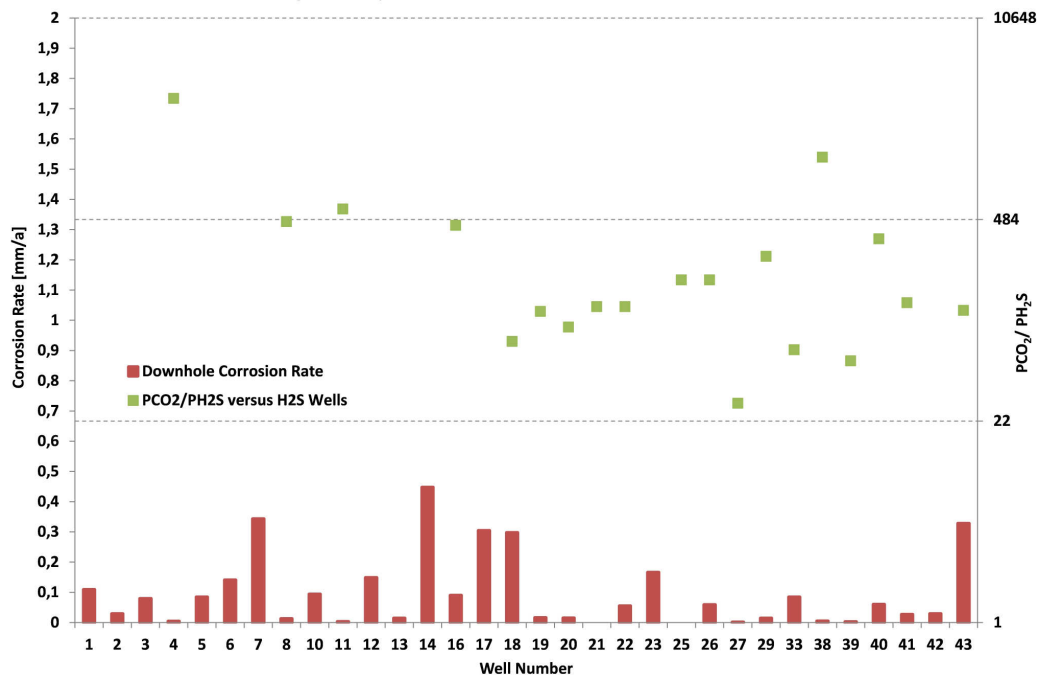


Figure 22 – Partial Pressure CO₂ and H₂S Ratio versus Downhole Corrosion Rates connected to corresponding Well Number for Watercuts > 80 % and Velocities > 0.15 m/s after Pots⁵¹

Parameters without H₂S Wells

To obtain relevant well numbers and deeper information from Appendix the reader is advised to consult previous figures with numbers, containing H₂S wells, or look up the numbered distributions without H₂S wells in the Background Data section. In this subchapter same figures like published before with the main parameters, except temperature, which is presented separately, are shown without the possibly influential H₂S measurements. Since all H₂S partial pressures are theoretically able to form protective films²¹, all H₂S containing wells have been excluded to have an alternative perspective on respective parameters.

Velocity

Velocity was the first parameter, where no generic output was proposed in previous investigations. Very low corrosion rates with increasing velocity could not be explained. Low corrosion rates may to be reasoned by FeS layers on installed coupons, preventing impacts of velocities and its shear stresses.

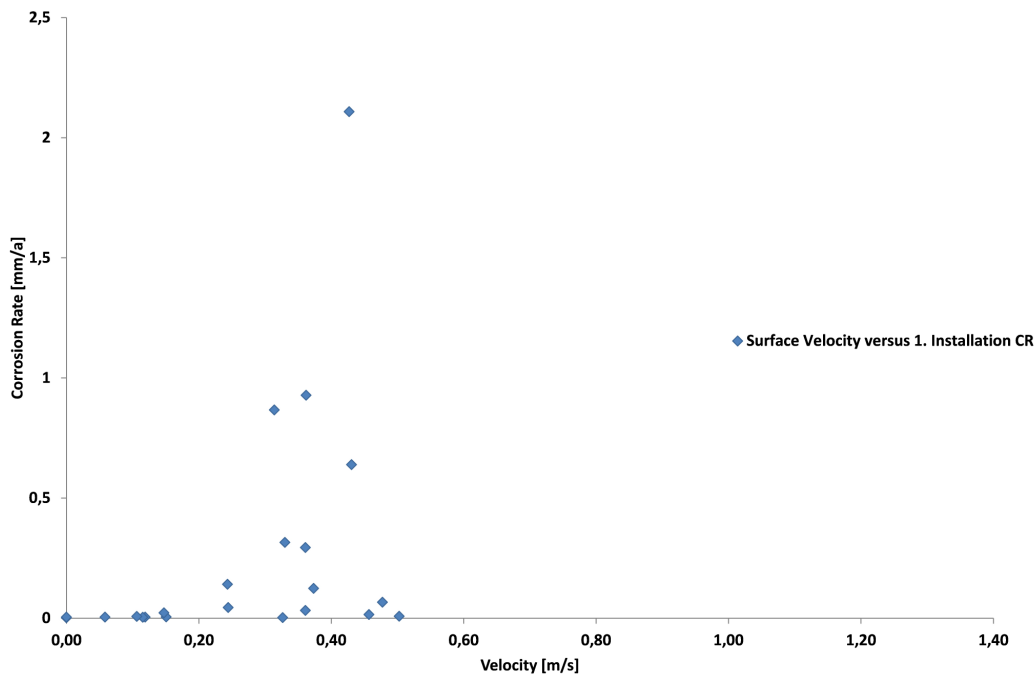


Figure 23 – “Surface 1. Installation” Corrosion Rate versus Wellhead Velocity without H₂S Wells⁵¹

The modified velocity distributions, Figure 23 as well as Figure 24 show a weak correlation related to the literature output. Here, the velocity constraints were not considered, since the figure needs to demonstrate an overall picture on velocities. Nevertheless it can be seen in both figures, that high amounts of low corrosion rates, compared to Figure 13 and Figure 14, have disappeared by extraction of H₂S wells. That makes the influence of velocity according to literature more obvious and shows weakly, that with increasing velocity the corrosion rate increases.

It still has to be kept in mind that also a small amount of high corrosion rates are lost in the H₂S data extraction process. Once more, those corrosion rates could be referred to pitting.^{2, 14, 19, 21, 22} But still there are low corrosion rates in advanced velocity regions. In surface installations, well measurement numbers 23, 12, 17, 14 and 42 and downhole well measurement numbers 13, 2 and 42 (from highest to lowest velocities; Background Data 23 and Background Data 24) are below the corrosion limit.

The main issue with FeS layers is the possibility to prove it in that situation. Since relevant coupons are not available for visual inspection, the provided velocity output can not be verified regarding a protective sulphide layer, even though partial pressures, faced in the oil fields of Austria, are experienced to create FeS precipitation according to cited literature.^{2, 14, 19, 21}

So, the extraction of H₂S wells and the resulting trend of downhole and surface velocity to the corrosion rates is speculative and can only be seen as a strong indicator.

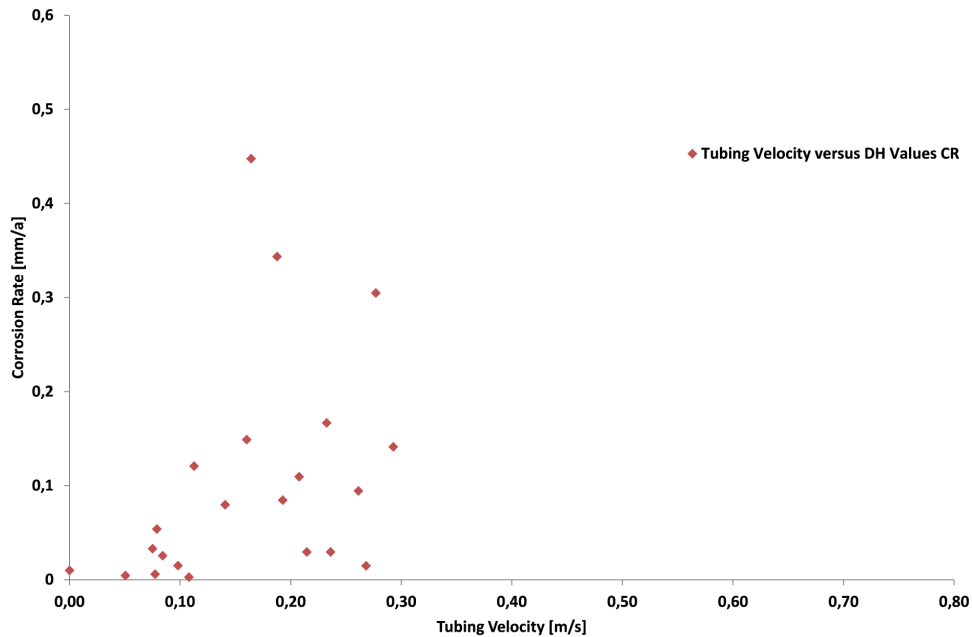


Figure 24 – Downhole Corrosion Rate versus Tubing Velocity without H₂S Wells⁵¹

CO₂ Partial Pressure

The same procedure performed with velocities has been applied also to surface and downhole partial pressures to demonstrate that parameter without H₂S influence.

Comparing critical well numbers 23, 12 and 17 (Figure 23), with the surface partial pressures of CO₂, it can be concluded that those values have the lowest partial pressure CO₂ values of all H₂S free uninhibited wells with watercuts higher than 80 % and wellhead velocities higher than 0.15 m/s (Background Data 25). Well number 42 ranges in average partial pressure region and 14 even is calculated as a maximum.

Screening the partial pressure distribution of “Surface 1. Installation” and Downhole measurements, again, like in the modified velocity distribution, only a weak proportional relation to corrosion rate can be seen. (Figure 25 and Figure 26)

Downhole well number 13, 42 and 2 are, with progressing partial pressure, below the critical corrosion rate limit of 0.05 mm/a. Explaining other wells with comparable partial pressures of CO₂ (compared to well 13, 42 and 2) and still equipped with higher corrosion rates than number 13, 42 and 2 via higher velocities, is not possible. As can be seen in Background Data 24 and Background Data 26, this is not the case. Numbers 13 and 42 are linked to low tubing velocities, but well number 23 or 5 have comparable values and still show higher corrosion rates.

To summarize, not all anomalies of modified partial pressures and velocity plots can be explained via corresponding velocity or partial pressure distributions.

It has to be underlined, that Figure 25 as well as Figure 26 show increased corrosion rates with increased partial pressures by application of a linear interpolation trendline, but from an

engineering point of view, the trendline could be seen as parallel to the y- axis. That is why the “partial pressure CO₂ to corrosion rate”- correlation is considered to be very weak.

The reader is free to control or deepen investigations via Background Data 23 to Background Data 26 and corresponding data sheets in the Appendix section.

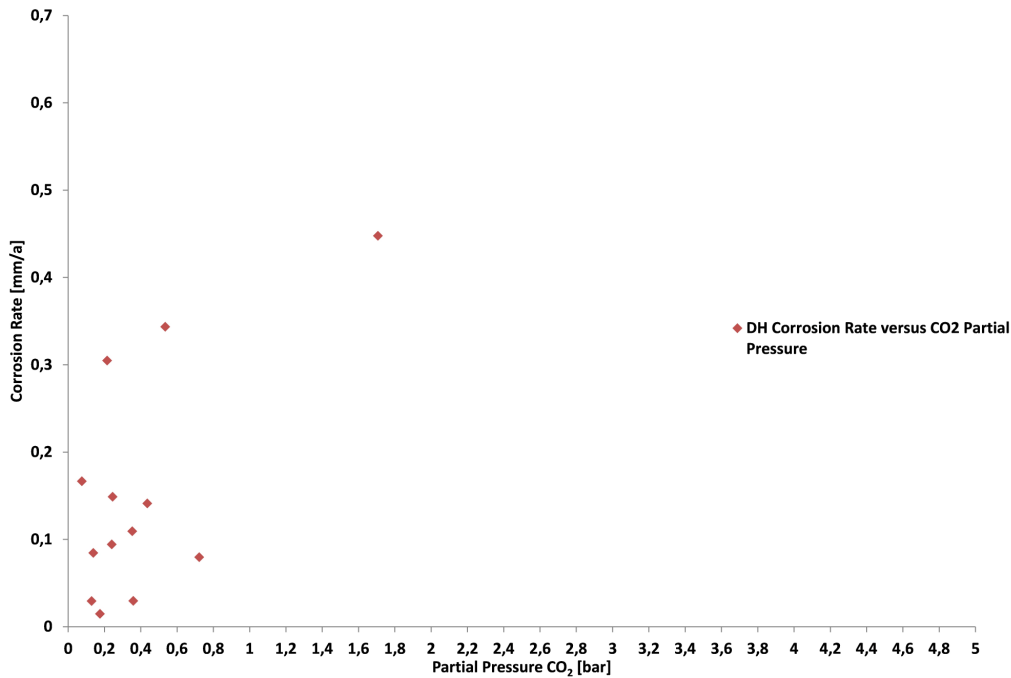


Figure 25 – Downhole Corrosion Rate versus Partial Pressure CO₂ without H₂S Wells for Watercuts > 80 % and Velocities > 0.11 m/s⁵¹

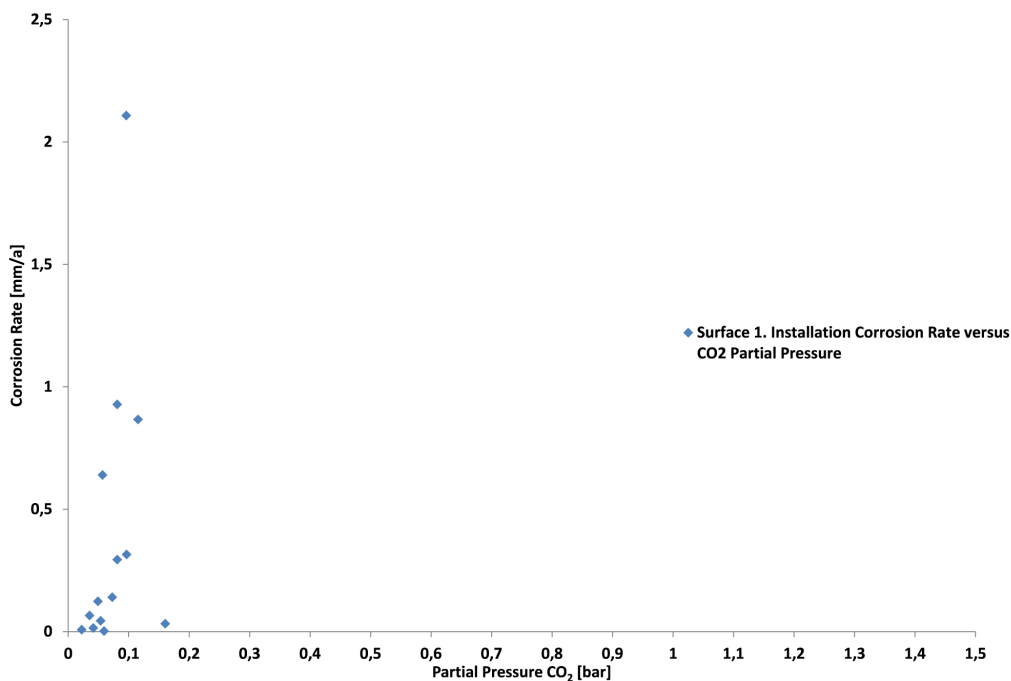


Figure 26 – “Surface 1. Installation” Corrosion Rate versus Partial Pressure CO₂ without H₂S Wells for Watercuts > 80 % and Velocities > 0.11 m/s⁵¹

Contrary to previous investigations, the application of 3D diagrams was decided not to be meaningful, since the number of data points is too small.

For definition of a minimum CO₂ partial pressure, Figure 26 is most important, since lower pressures are being faced. Downhole as well as surface measurements show a corrosion rate increase at very low CO₂ partial pressures. Considering the low partial pressures and the first violation of corrosion- limits with approximately 0.05 bar partial pressure CO₂ in Figure 26, a lower limit is not to be found in this situation, since only one data point exists lower than 0.05 bar. Estimation of an independent downhole value is not performed, due to the equal problem. Downhole, the lowest partial pressure- value immediately violates threshold corrosion- rate.

3.4 Temperature

Temperature is another very important parameter influencing corrosion. Its main role is referred to the dependency of FeCO₃ to precipitate and being able to form protective layers to reduce corrosion with increasing temperature.^{21, 25, 28}

The pH was calculated to approximately 4.3 previously.

Focussing once more on Figure 21, high surface corrosion rates of well numbers 4, 8 and 11 in the lean CO₂ corrosion process after Pots are visualized. FeCO₃ dropout and the formation of a protective layer is unlikely under surface conditions and temperatures of 20 °C, facing a pH value of approximately 4.3.^{21, 25, 28} The lack of a protective FeCO₃ layer could be an explanation for the high corrosion rates in Figure 21.

Of course FeCO₃ layers are, like FeS layers, not to be proven in that situation without the analysis of the coupons' surfaces.

Since surface temperature is assumed to be constant, only downhole values are plotted versus temperature. To have a more detailed look on the gained data, threshold values of watercut and downhole velocity are applied, decreasing the number of wells to be investigated. It has to be mentioned, that temperature values are calculated by means of "3.3 °C/100 m" gradient.

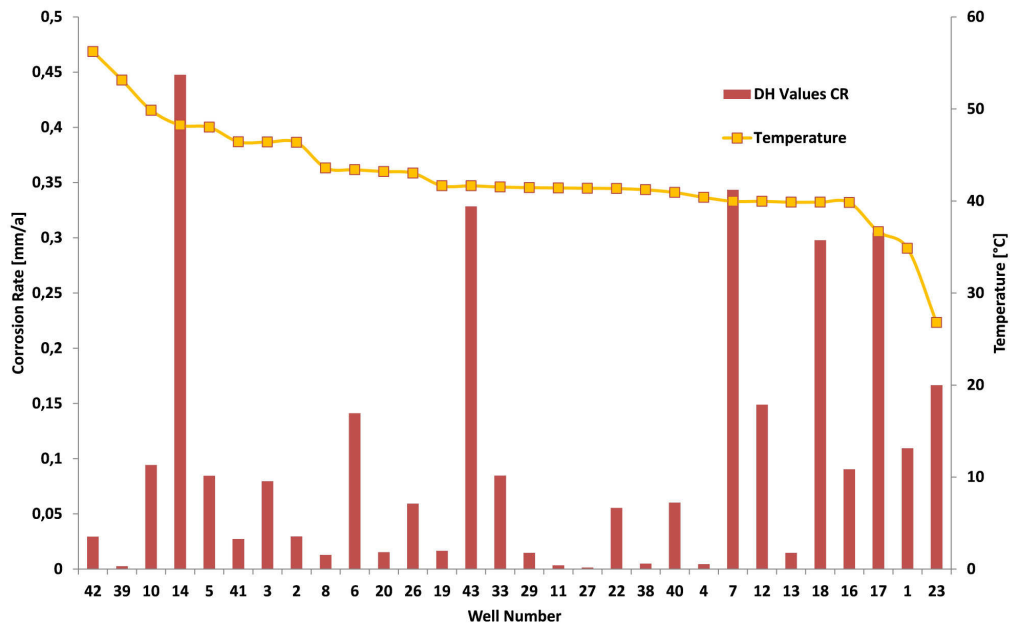


Figure 27 – Numbered Downhole Corrosion Rates with Respect to Temperature at Coupon setting Depth for Watercuts > 80 % and Velocities > 0.11 m/s⁵¹

Figure 27 makes the distribution of downhole- temperature related to corrosion rates visible. The majority of those values range below 45 °C and nor on this chart, neither in Figure 28, where trends usually can be seen more easily, a correlation according to literature investigations could be found. Also downhole, pH is, besides temperature, an important parameter talking about FeCO₃ precipitation. In both relevant figures corrosion rate variation is very high not allowing any conclusions. Basically, the corrosion rates are expected to increase to a certain threshold temperature, where the corrosion rate finally decreases due to the formation of protective iron carbonate films.²¹ Additionally, there is the possibility of FeS layers of H₂S wells, which are precipitating out of solutions more easily compared to FeCO₃, misleading the interpretation of both plots. Extraction of H₂S wells was performed because of that one more time.

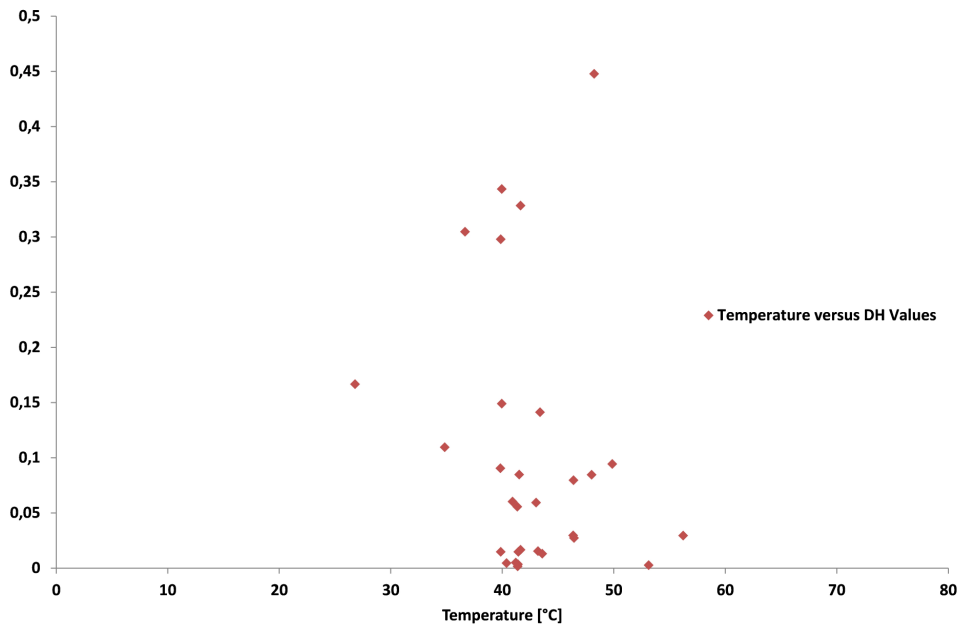


Figure 28 – Downhole Temperatures versus Downhole Corrosion Rates for Watercuts > 80 % and Velocities > 0.11 m/s⁵¹

Temperature without H₂S Wells

Figure 29 shows the distribution of temperature without H₂S influence. Wells below corrosion-limit are again the same demonstrated in figures before, 42, 2 and 13, whereas 42 is exposed to highest and 13 to lowest temperature of those three measurements.

As a matter of fact, trends of temperature influence according to literature can not be seen. Again, low corrosion rates of 42, 13 and 2, that could not be explained by lower tubing velocities compared to others, can also not be reasoned by the impact of temperature.

Furthermore, due to the removal of H₂S containing wells, a grand amount of low corrosion rates disappeared, but a redesigned distribution, supporting temperature impacts, is not created because of that. Indeed it is possible, that temperature influences can not be concluded due to the low deviation of temperatures.

If the iron- sulphide- precipitates- thesis is true, iron sulphide precipitations are independent of temperature ranges from approximately 40 °C to 55 °C as a consequence.

A graph equipped with well numbers is found at Background Data 27.

Temperature as well as partial pressure distributions are influenced by lots of factors downhole as well as on surface not to be included in data analysis within this work. That is why especially partial pressure CO₂ and temperature correlations do not show a sufficient match to literature publications and may create a misleading picture of dominance of those factors.

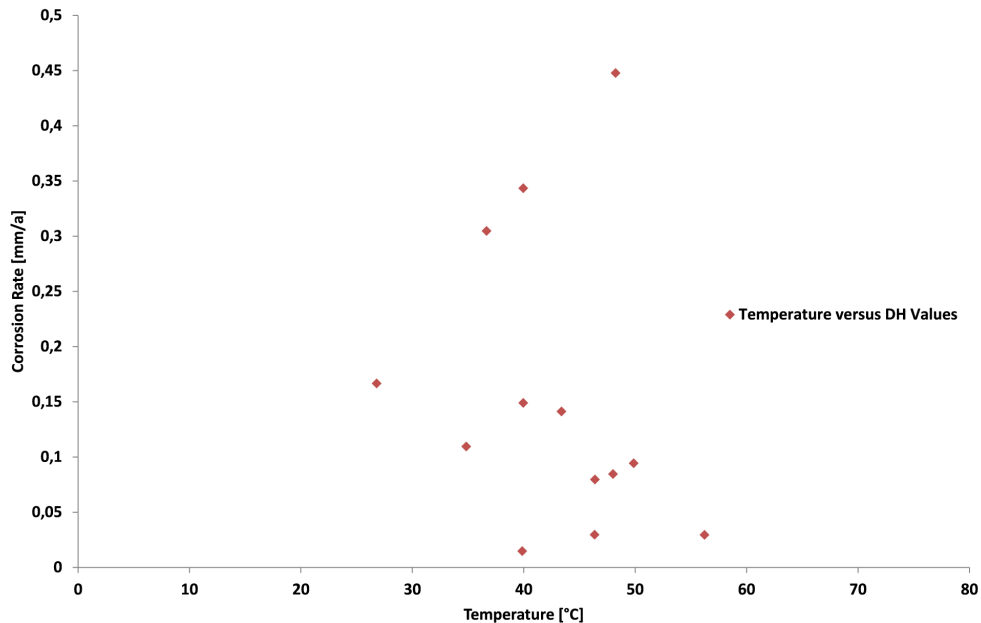


Figure 29 – Downhole Corrosion Rate versus Downhole Temperature without H₂S for Watercuts > 80 % and Velocities > 0.11 m/s⁵¹

3.5 Inhibitor Performance

For evaluation of inhibitor performances in austrian oilfields, only surface coupons measurements are available. Basically, two types of inhibitor are injected continuously via the annulus into the borehole. FS1 and the newly acquired FS2 have shown within several laboratory experiments and field analyses their positive effects regarding metal conservation and corrosion prevention. Nevertheless, a general guideline in inhibitor application as well as optimum doses was not elaborated by responsables. To screen the inhibitor performance, corrosion rates versus the respective inhibitor dose, injected during coupons exposure, was plotted. Inhibitor concentrations [ppm] are based on the brutto production of treated wells. The assumption that water soluble inhibitors, like FS1 and FS2, remain only in the water phase is not valid, obviously.^{36, 37} Deeper investigations on partitioning of both inhibitors are not possible, since partitioning coefficients are unknown. Influences of low watercuts and low velocities are excluded to achieve an optimum picture of the inhibitor efficiency. Compositions and trade-names of inhibitors are illustrated within Background Data 28.

FS1 Evaluation

FS1 was screened via conventional coupons surface measurements, whereas a separation of data sets between “1- 3 installation” (measurements by O.C.’s corrosion department) and an alternative screening, called “List green Inhibitors”⁵⁷, where 17 wells were measured, has been performed. That separation makes an exact comparison of FS2 and FS1 corrosion rates in future parts of this work possible. “List green Inhibitors” was not supportive in prior parameter evaluations, since uninhibited measurements have not been performed within this report.

Surface Installation 1- 3

Looking at FS1- inhibitor performance chart of first installed coupons, a corrosion rate decrease related to the inhibitor dose increase can be seen. Highest corrosion rates are already inhibited with approximately 30 ppm, showing a high deviation between the corrosion rates.

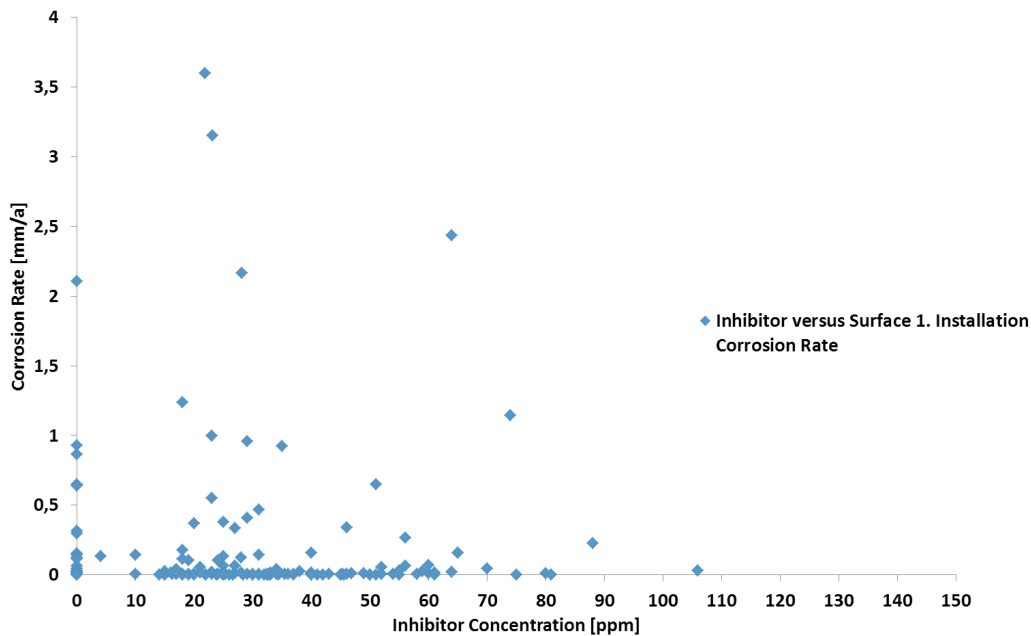


Figure 30 – Inhibitor FS1 versus Surface Corrosion Rates of 1st Installation- Coupons for Watercuts > 80 % and Velocities > 0.15 m/s ⁵⁶

Especially to be mentioned are very low corrosion rates, even though no inhibition was applied within the measurement time interval. This leads to the assumption, that there are wells that have no corrosive tendency.

The average of all corrosion rates decrease with further installation measurements, illustrated within Figure 31 and Figure 32, where the final maximum corrosion rate of the third installation is approximately 1.2 mm/a. Possible environmental differences, like acidizing stimulations, which often are responsible for elevated corrosion rates, between those measurements could not be found. “Surface Installation” figures indicate again the problems of corresponding field measurements. Various influential parameters are creating high deviations of corrosion rates not to be explained 100 % within this work. This can be reasoned once more by the lack of measurement coupons and the maturity of the data itself, respectively.

Below in Table 3, 7 example- corrosion rates are presented, where a high deviation of the corrosion rates is illustrated.

Table 3 –Corrosion Rate Curriculum of highest "Surface 1. Installation" Corrosion Rates⁵⁶

Inhibitor	Corr. Rate	Inhibitor	Corr. Rate	Inhibitor	Corr. Rate
1.Installation	1.Installation	2.Installation	2.Installation	3.Installation	3.Installation
[ppm]	[mm/a]	[ppm]	[mm/a]	[ppm]	[mm/a]
21.8	3.6	21.8	0.6	26.5	0.004
23.1	3.2	36	0.003	38	0.002
64	2.4	66	0.2	67	0.4
28.1	2.2	28.1	0.4	37.9	0.02
0	2.1	15	0.2	7	0.02
18	1.2	90	0.8	100	0.2
74	1.1	35	0.9	37	0.1

Corrosion rate points 3.6, 2.2 and 2.4 mm/a change at second phase to corrosion rates of 0.6 mm/a, 0.4 and 0.2 mm/a with no change of inhibitor dose at points 3.6 and 2.2- and a low raise of inhibition of 2 ppm at point 2.4. The fourth point chosen to be a presented additionally is 3.2 mm/a, where after a raise of inhibitor concentration of 13 ppm corrosion rate decreases to 0.003 mm/a in second evaluation process.

To keep in mind, all surface coupons measurements have been performed chronologically for 69 days average. After each coupons measurement, the following coupon was installed immediately for the same amount of time.

Indeed it has to be understood, that with progressing measurements and after the first results have been gained, more and more wells needed to be inhibited in order to decrease their corrosion rates. That leads to elevated corrosion rates in connection to higher inhibitor doses, since often the optimum amount was not injected, only decreasing the corrosion rates to a certain degree. Practically spoken, if for example corrosion rates already inhibited with 20 ppm of FS1 is exceeding 0.05 mm/a and after injection of 80 ppm still exceed that limit (but with a lower corrosion rate), inhibition performance plots could give a wrong impression.

Exactly this is the reason, why at first installed measurements the optimum dose of inhibition is, read off at Figure 30, roughly at 80 ± 20 ppm, 90 ± 10 ppm at Figure 31 and 100 ± 10 ppm at Figure 32.

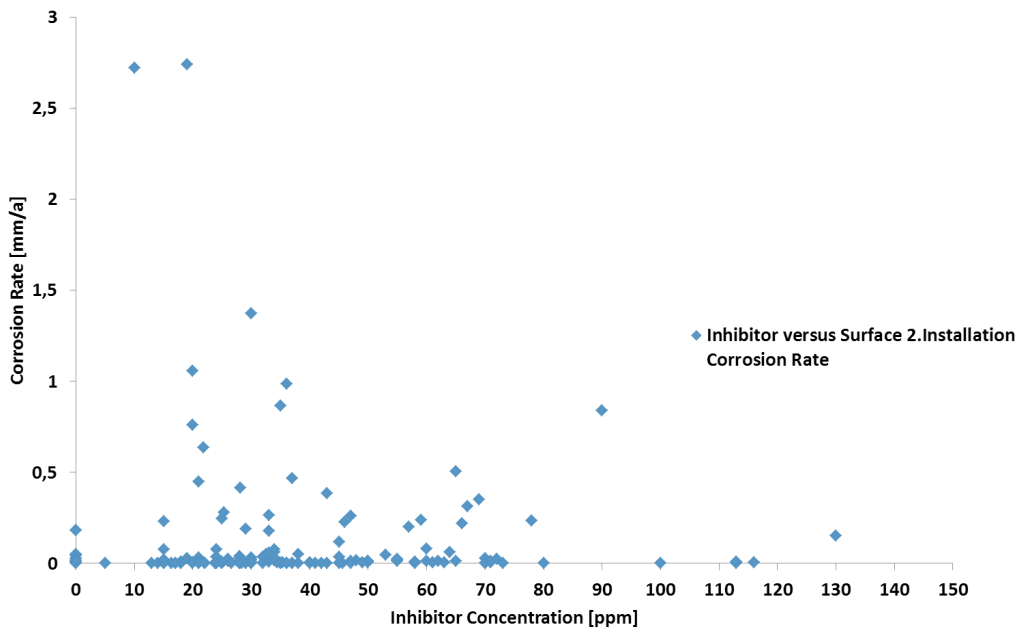


Figure 31 – FS1 versus Surface Corrosion Rates of 2nd Installation- Coupons for Watercuts > 80 % and Velocities > 0.15 m/s ⁵⁶

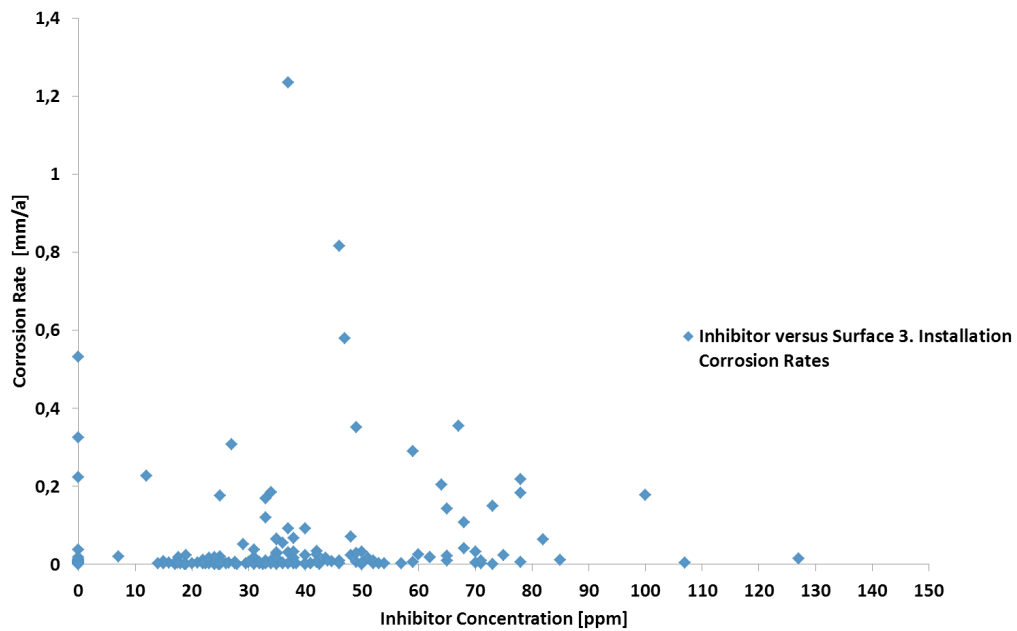


Figure 32 – FS1 versus Surface Corrosion Rates of 3rd Installation- Coupons for Watercuts > 80 % and Velocities > 0.15 m/s ⁵⁶

It has to be mentioned that there are corrosion rates exceeding corrosion limit within multiple measurements and have not been inhibited throughout the coupons evaluation phases. A reason for that can not be given.

List green Inhibitors

20 Wells are screened regarding corrosion behaviour in contact with FS1 and FS2 to realize a reliable comparison of inhibitors' field performance. As a matter of fact, coupons are installed in wellhead regions under same circumstances like Surface Installation 1- 3 data measurements. All wells are related to watercuts higher than 80 % and velocities higher than 0.15 m/s, so no filter was applied.

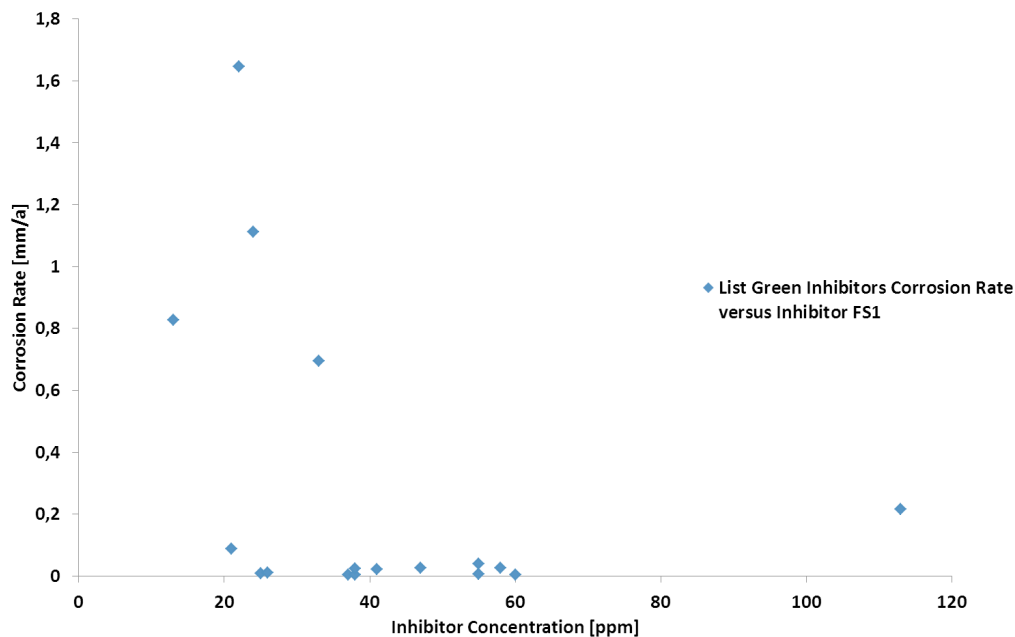


Figure 33 – Inhibitor FS1 versus Corrosion Rates of “List Green Inhibitors”^{56,57}

Three wells were not qualified due to stimulations, damage of sucker rod pump or injection pump failure during measurement period. (well numbers 198, 196 and 206)

High corrosion rates of well- measurement number 193 with approximately 1.64 mm/a, well numbers 197, 199 and 203, with the lowest corrosion rate of approximately 0.7 mm/a, require special consideration and possibly raised amounts of inhibitor doses to decrease their corrosion rates.

Again, corrosion reducing impacts of FS1 can be expected. It has to be considered, that wells have been chosen specifically for that investigation and more care regarding data and coupons evaluation has been applied compared to “Surface Installation 1- 3” measurements, e.g..

Comparing third Installation evaluation plot, Figure 32, with Figure 33 from above, indeed similarities are visible. Maximum concentrations are located in approximately 100 ppm regions and concentration minimum values, neglecting uninhibited wells, of around 20 ppm are seen in both charts as well. An optimum dose of inhibition is expected roughly at 80 ± 30 ppm.

Inhibitor FS2 Evaluation

FS2 is the latest introduction of inhibitors in austrian oilfields. Here availability of data is more limited compared to FS1 performances. Investigations concerning FS2 are performed once more by internal report "List green Inhibitors"⁵⁷ with same wells like in FS1 measurements.

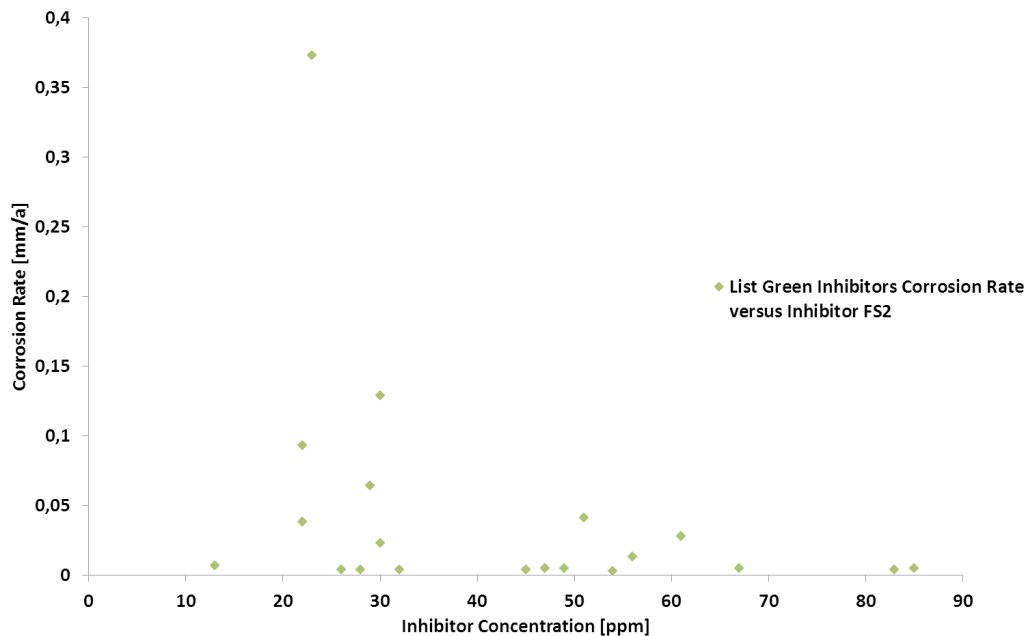


Figure 34 - Inhibitor FS2 versus Corrosion Rates of "List Green Inhibitors"^{56,57}

For FS2 evaluations same 20 wells were being chosen; fortunately no problems occurred in evaluation process making all 20 measurements valid. Same conditions during coupons measurements concerning duration, exposure area and coupons- material are found to have levels of comparison. Well- measurement number 206 , responsible for maximum corrosion rate in Figure 34 of 0.373, not able being evaluated in FS1 evaluations due to stimulations, could require also a higher concentration of inhibition for corrosion rate reduction. Two other wells not considered in FS1 plot (Figure 33), number 196 and 206, show low corrosion tendencies of 0.003 and 0.028 mm/a with advanced FS2 inhibitor doses of 54 and 61 ppm. Number 193, with approximately 1.64 mm/a (Figure 33), shows, with a dose of 22 ppm FS2, a surprisingly low corrosion rate of 0.038 mm/a in Figure 34. Well number 197, 199 and 203 on the other hand still maintain the corrosive tendency already illustrated in FS1 Internal Report investigations and exceed corrosion limit of 0.05 mm/a.

The optimum dose via Figure 34 is determined as roughly 60 ± 10 ppm.

Comparison FS1 with FS2

58 wells were treated with FS2 by September 2010, most of them starting with September 2007, whereas only in 20 wells a coupon measurement for FS2 evaluation (List green Inhibitors) was performed. Report "List green Inhibitors"⁵⁷ processes performance of both inhibitors (FS1 and FS2) in the field and targets for strengthening the performed laboratory tests, published in report "COR20050025"⁵⁸, where FS2 succeeded already.

Figure 35 below shows both inhibitors in comparison, where immediately higher corrosion rates in FS1 inhibited wells are noted.

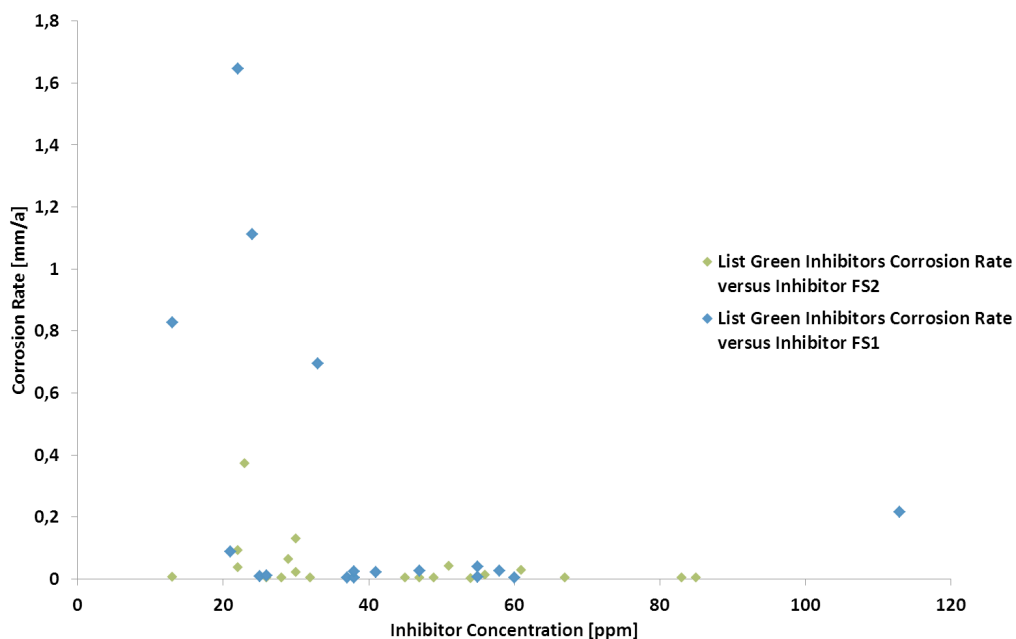


Figure 35 – Inhibitors FS1 and FS2 versus corresponding Corrosion Rates of "List Green Inhibitors"^{56, 57}

A closer look on differences of FS1 and FS2 inhibition has already been taken in the "FS2 Field Evaluation" chapter before. Additionally the changes of inhibition of relevant wells need to be screened, since basically, after gaining the results of FS1 investigations, adjustments of inhibitor FS2 (and a better result as a consequence), are possible. FS1 measurements have been performed approximately 6 months before FS2 measurements. Looking on average inhibitor doses of all Internal Report wells^{56, 57} equal doses of both approximately 42 ppm can be calculated. But considering the extremely high dose of well number 195, illustrated at Table 4, reasoned by the unexpected low production rate of 14.8 m³/day leading to a lower wellhead velocity of 0.17 m/s and excluding that value from the average, a difference of 6 ppm can be found.

Generally, slight deviations due to the flow rates are being faced. Nevertheless, FS2 corrosion rates are lower in average compared to FS1 treated coupons with respect to comparable inhibitor doses, since those deviations are, first of all, not to be prevented and, secondly, not considered as relevant.

Table 4 – Deviations of Concentrations between FS1 and FS2 Inhibitors of FS1 Wells exceeding Corrosion Limit^{56, 57}

Well Number	FS1 Dose [ppm]	FS1 Corr. Rate [mm/a]	FS2 Dose [ppm]	FS2 Corr. Rate [mm/a]
193	22	1.6	22	0.04
197	24	1.1	30	0.1
199	13	0.8	29	0.06
203	33	0.7	22	0.09
195	113	0.2	45	0.004
207	21	0.09	30	0.02

In order to have an alternative view on both inhibitors and their ability to reduce metal deterioration, the rate of Workover was selected as a parameter. The parameter “WO per year” is not valid to be correlated to corrosion processes as such, since not all failures, registered in databanks, are described explicitly whether corrosion was involved or not; however, differences regarding maintenance operations of FS1 and FS2 still have to be explored because of a direct relationship to runtime and costs.

Table 5 – Comparison of Inhibitors FS1 and FS2 via alternative Parameters^{56, 59}

Parameter	Inhibitor FS2	Inhibitor FS1
WO/year	0,433	0,481

Table 5 shows clearly a positive impact of FS2 regarding Workover. In that analysis, additionally a time factor needs to be considered. Whereas earliest FS2 applications were started in 2007, a lot of FS1 treatments have been performed in the 1990s in some wells for the first time. For FS1 investigations, a lower time limit of January 1999 has been set. For wells, where inhibition took place after 1999, the date of first injection has been taken. Within that time interval, relevant changes in well or reservoir conditions have been taken care of and time interval was adjusted, if necessary. So the average time interval of investigation of FS2 inhibition is 991 days (2.7 years) and for FS1 2040 days (5.5 years).

4 Experimental

Reliable conclusions, supported alone by field data investigations, can not be drawn due to their deviation to literature outputs of certain parameters. The maturity of field data definitely is an issue; the latest measurements have been performed approximately 10 years ago and recreating equivalent measurement- environments to corresponding evaluation dates is of limited reliability, obviously. Missing coupons to prove created theses, is another problem not to be solved in that scenario. That is why an experimental investigation was added to have an extra perspective on critical data that was not providing a satisfying match to the literature. The following experiments were emphasized on partial pressures of CO₂, temperatures and inhibitor performance of FS1 with help of Autoclave Pressure Cells. To obtain comparisons between FS1 and FS2, FS2 was tested at 80 °C with variations in partial pressures.

4.1 Materials

The material used as specimen was an API- L80⁶⁰ sucker rod with a diameter of 1 1/8". Before it was cut by saw to a sample- cylinder of 10 mm height, the bar was turned to remove irregularities from its surface. 24 hours before installation into the pressure cell, samples were grinded wet at all planes and edges by three types of sandpaper with grain sizes of 120, 220 and finally 320. After each type, the samples were degreased with ethanol and dried. After the last sandpaper interval, the samples were stored in an oven at 120 °C (for 24 hours). Before installation, the samples' weight, height and diameter was determined. The chemical composition and mechanical properties of used steel is shown at Table 6 and Table 7.

Table 6 – L80 Steel Composition^{61, 62}

L80 Steel										
Element	C	Si	Mn	P	S	Cu	Cr	Ni	Mo	Al
Content [Weight%]	0.26	0.25	0.68	0.01	0.008	0.02	0.98	0.03	0.19	0.032

Table 7 – L80 Steel mechanical Properties^{61, 62}

L80 Steel Mechanical Properties		
Yield Strength Rt 0.5 [MPa]	Ultimate Tensile Strength Rm [MPa]	Hardness [HRC]
597	738	21

Dimensions and an image of a sample and its microstructure are shown from Background Data 29 to Background Data 31. Dimensions vary due to treatments like turning and sandpapering. All samples were equipped with specific numbers to prevent confusion.

4.2 Autoclave Testing

Three pressure cells with an inner diameter of 6.7 cm, a height of 67 cm and an inner volume of 2362 cm³ were filled with 1.5 l of electrolyte each. The electrolyte contained distilled water with 27 g/l NaCl content. Exceeding 3 weight% of NaCl at room temperature, corrosion rate is finally expected to decrease within aerated conditions, since oxygen solubility is being decreased.⁶³ The dose of NaCl creates a worst case scenario regarding chlorides, since same behaviour regarding solubility of CO₂ is assumed. In the field, an average of approximately 12000 ppm of chloride concentration is calculated, since all fields are being injected with water containing that specific chloride concentration.⁵¹ Closed autoclaves were purged with CO₂ with 1 l/min (1 bar) for 5 hours, to evacuate oxygen. Afterwards, samples were installed in a glass specimen holder, preventing metal to metal contact of sample and autoclave (or sample to samples) and then dropped into the electrolyte, creating permanent exposure and full coverage of the metal by the liquid. If necessary, inhibitor doses were injected by means of a pipette and stirred, before specimens were installed into the autoclave. The experiments were performed under static conditions and thus samples were always covered in liquid. Autoclaves were finally closed for the corrosion measurement and purged with CO₂ again for 1 hour to remove again freshly migrated oxygen. After purging, the cell was pressurized and put into a heating oven, if higher temperatures were required for evaluations. A leak detection spray (Herbert Torrey) was used in order to check valve and autoclave tightness. Testing time was set to 6 days (144 hours). At the end of the testing time, the samples were extracted from the autoclave and immediately cleaned with ethanol and dried. After the second weighing procedure, samples were exposed to a staining agent⁶⁴ (Background Data 32) for 5 minutes, neutralized with water and then again purged with ethanol. At the end, they were brushed with a rubber brush to remove possible residuals on the surface, once more purged with ethanol, dried and weighed for the third and final time. All samples were stored in a desiccator. The testing conditions, the samples are exposed to, are illustrated in Table 8.

Table 8 – Testing Conditions for Autoclave Experiments

	Variation			
Partial Pressure CO₂ [bar]	1	3	10	
Temperature [°C]	20	80	120	
Inhibitor Doses [ppm]	0	30	100	300

4.3 Evaluation

The weight difference between weighing procedure 1 and weighing procedure 3 has been computed and was used as a basis for calculation of corrosion rates. The scale used is only valid up to unit [mg], which was rounded to the hundredth digit after computation of the uniform mass loss.

Three specimens were installed into one autoclave per experiment. The following formula was applied to calculate the mean corrosion rate CR [mm/a] of each sample.

$$CR = \frac{365 \cdot \Delta m}{\rho_{Fe} \cdot t \cdot A} \quad \text{Equation 50}$$

where Δm describes the mass loss [g], ρ_{Fe} the density of the iron [g/mm³], t for the elapsed time [days] and A represents the surface area of the samples [mm²].

For each experiment, the arithmetic mean was calculated, creating a single value for every investigation.

5 Experimental Results

5.1 Repeatability

Like already mentioned before, three samples were assembled inside the autoclave for achievement of reliable results.

All results need to be able to be repeated for validity. That is why the standard deviation is calculated for every measurement and inserted as “error bars” into respective plots, to see how widely values are dispersed from the average value. If no error bar is visible at certain data points, error bars are smaller than data points’ plotting area.

The formula used for standard deviation based on a sample is shown at Equation 51:

$$\sigma_s = \sqrt{\frac{\sum (x - \bar{x})^2}{(n-1)}} \quad \text{Equation 51}$$

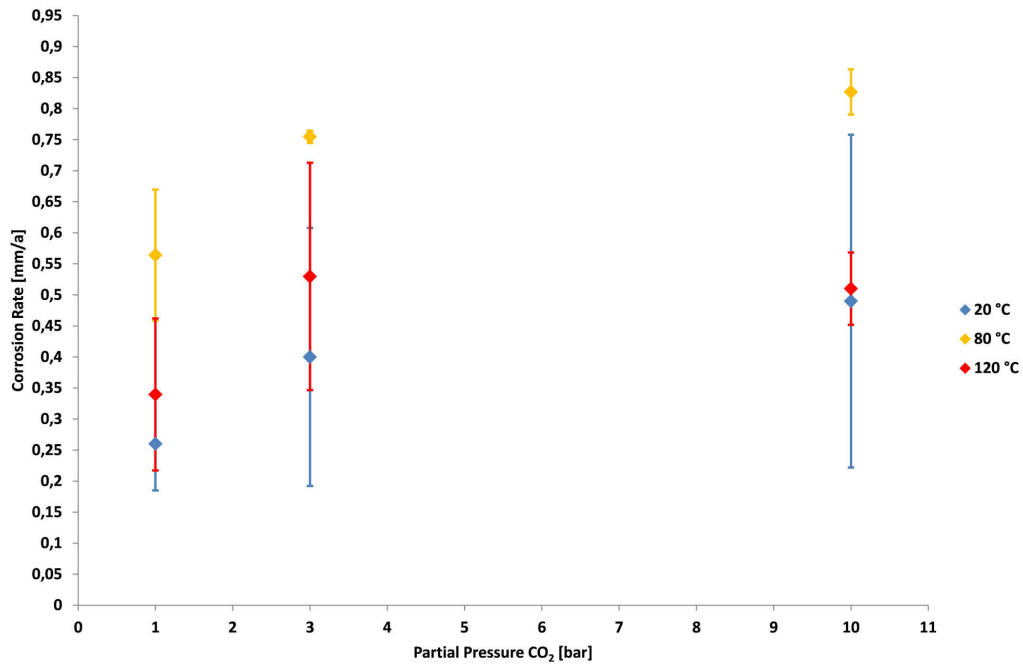
where x is the sample value, \bar{x} refers to the mean of all samples and n to the total amount of samples.

5.2 Partial Pressure CO₂

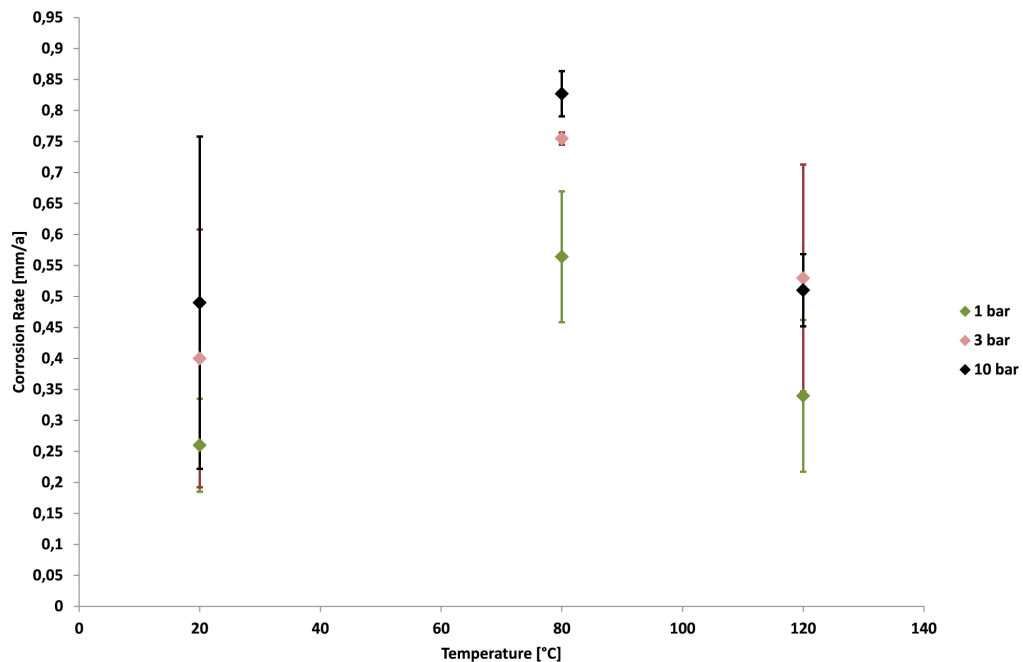
Figure 36 shows the corrosion rate as a function of partial pressure of CO₂ at varying temperatures. Basically it shows that with increasing partial pressure, corrosion rates increase. The corrosion rate can not be connected to the partial pressure in a linear manner, but more in a logarithmic manner. That logarithmic distribution was already visualized in Figure 2, within “2 Theory of CO₂ Corrosion” and can be explained by de Waard’s Equation 12, connecting the pH value logarithmically to partial pressure CO₂. The pH value, accelerating the cathodic reaction if lowered, is not changing significantly between 3 and 10 bar, whereas variations of 1 to 3 bar are more effective in pH decrease.

The standard deviation of 20 °C experiments is high compared to other results and ranges from approximately 0.21 (relative standard deviation of 51 %) at 3 bar to 0.27 (relative standard deviation of 54 %) at 10 bar.

Additionally, logarithmic distributions are independent of temperatures. Deeper analysis of temperature influences are found in chapter 5.3.

Figure 36 – Partial Pressure CO₂ Distribution with Variations in Temperature from Autoclave Experiments

5.3 Temperature

Figure 37 – Temperature Distribution with Variations in Partial Pressure CO₂ from Autoclave Experiments

As already stated above, corrosion rates are proportional to partial pressure of CO₂. Looking at temperature distribution within Figure 37, also a correlation according to literature outputs, like shown within Figure 6, can be seen. Precipitation of FeCO₃, acting as a protective film, leads to a reduced corrosion rate at 120 °C. Background Data 34 illustrates the mentioned black FeCO₃ layer, which was found on all samples exposed to maximum temperature. In maximum

temperature region, corrosion rates of 3 bar is slightly higher than corrosion rates of 10 bar. This can be referred to measurement inconsistencies, considering high relative standard deviations of 1 and 3 bar of both approximately 35 %. The maximum corrosion rate is illustrated at 80 °C. Again, highest standard deviations are under room temperature at 3 and 10 bar.

5.4 Inhibitor Performance

Figure 38, Figure 39 and Figure 40 illustrate the Inhibitor FS1 performance under 20, 80 and 120 °C at different partial pressures of CO₂. At room temperature, corrosion rate decreases significantly by addition of FS1. Nevertheless, corrosion rate reduction, not violating 0.05 mm/a threshold, is not feasible by means of 30 ppm doses, independent of created laboratory conditions. With increasing concentration of inhibitor up to 100 and 300 ppm, corrosion rates decrease below the corrosion limit, showing up the measurement limits of 0.01 mm/a, since the applied scale is only valid up to unit [mg] and rounded, which was already mentioned before. As can be seen in Background Data 33, difference of 100 ppm inhibitor dose at 1 and 3 bar still is significant, even though difference is only 0.01 mm/a. 300 ppm creates maximum protection compared to the other concentrations at corresponding partial pressures. At room temperature, standard deviations decrease with increasing doses of inhibitor.

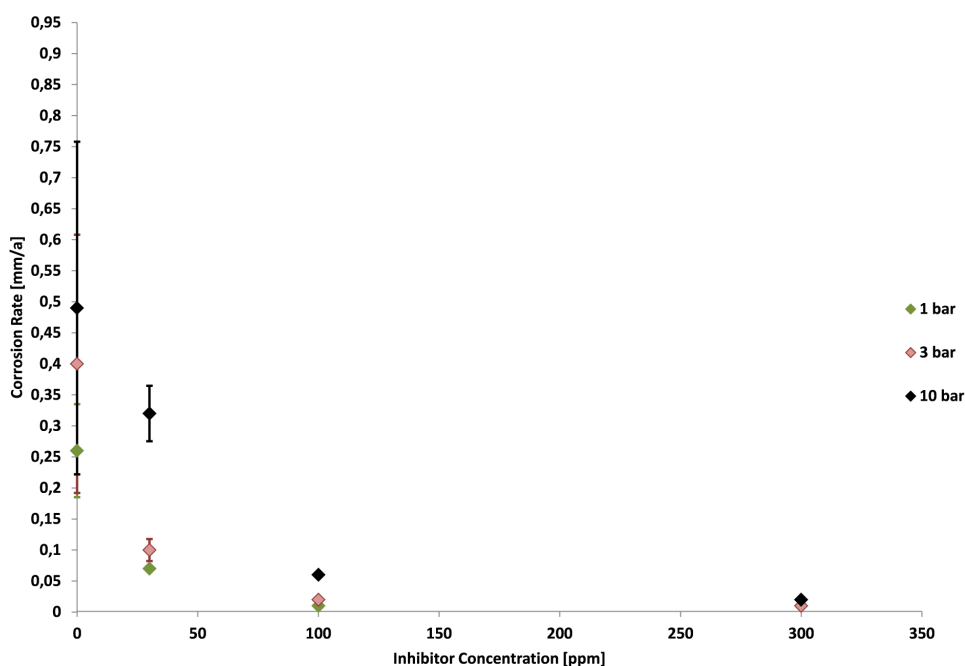


Figure 38 – Inhibitor FS1 Performance with Variations in Partial Pressures at Roomtemperature

Efficiency of FS1 is reduced at 80 °C, like Figure 39 or Background Data 35 shows. No injected concentration is able to keep corrosion rates below the corrosion limit. 30 ppm show low protection- tendencies at 3 and 10 bar and also at 1 bar corrosion rates are of higher dimensions. Comparing 100 ppm results with others, it can be seen that corrosion rates are being reduced significantly at 1 and 3 bar and do not change significantly at a raise to 300 ppm.

Additionally, with concentrations of 300 ppm, results of 10 bar can be “shifted” to the same corrosion rate- level than already realized with 100 ppm at 1 and 3 bar.

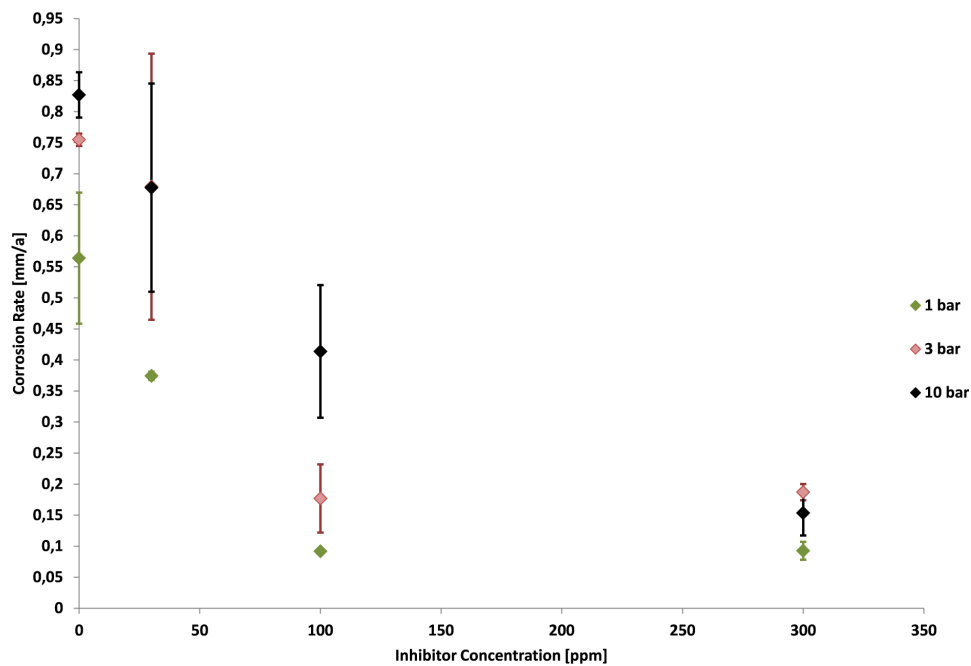


Figure 39 – FS1 Performance with Variations in Partial Pressures at 80 °C

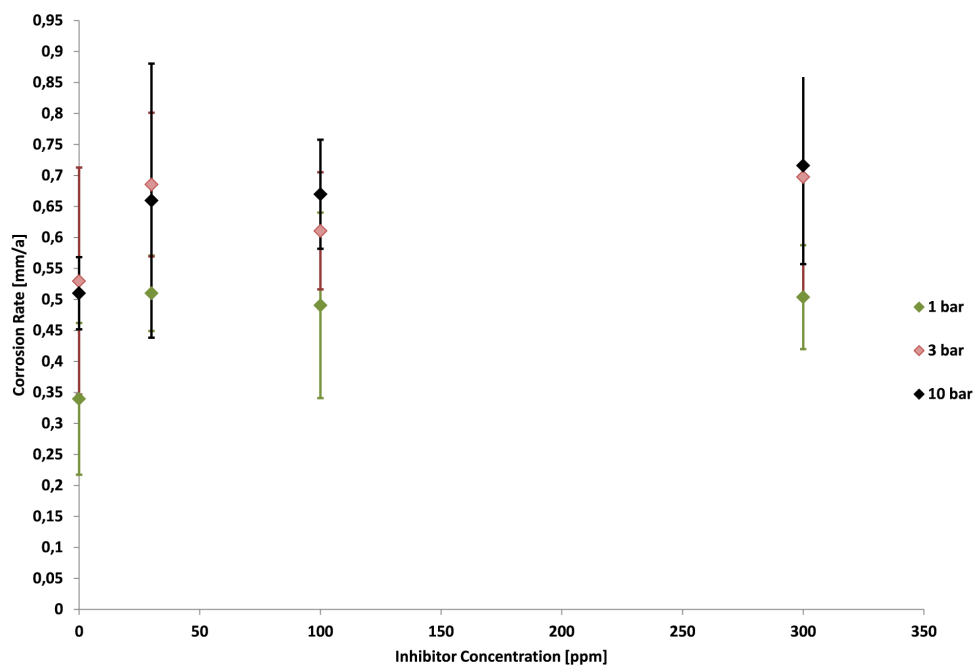


Figure 40 – FS1 Performance with Variations in Partial Pressures at 120 °C

At 120 °C results (Figure 40), inhibitor does, independent of partial pressures, not reduce corrosion rates significantly. At 100 ppm, a slight reduction can be seen, but facing error bars and its standard deviation, the slight reduction can be considered as measurement- variation. As already mentioned, the reason for lower corrosion rates compared to 80 °C can be connected to the precipitation of FeCO_3 and the connected creation of a protective film.

However, Figure 40 shows slightly lowered corrosion rates at uninhibited measurements compared to measurements with injected inhibitor FS1. Inhibitors can influence homogeneity of siderite (FeCO_3) layers significantly⁶⁵ and thus deteriorate the protection potential of respective films. During evaluation procedures, FeCO_3 layers of inhibited samples were removed much easier than FeCO_3 layers of uninhibited samples.

FS2

To continue comparison between inhibitor FS1 and FS2, like performed in the “Field Data” sector, an additional experiment screening FS2 and its performance under 80 °C with variations in partial pressures has been made. Comparing inhibitors’ performances under same autoclave conditions, FS2 evidences once more the improved performance regarding corrosion inhibition.

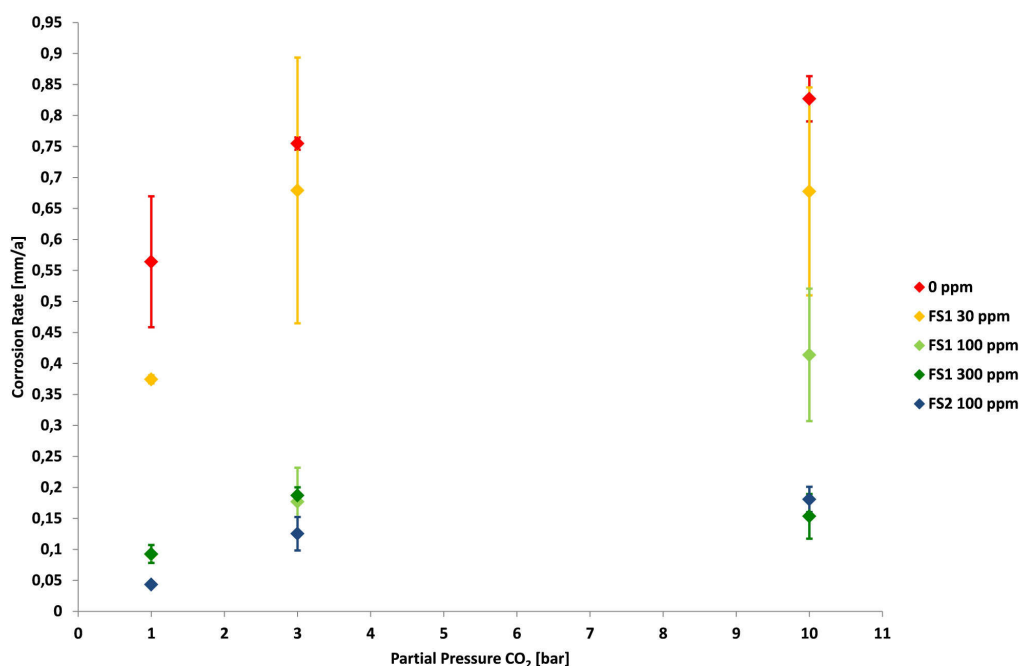


Figure 41 – Comparison FS1 to FS2 with Variations in Inhibitor Doses of FS1 at 80 °C

FS2 is, independent of exposed partial pressures, lowering corrosion rates more efficiently than inhibitor FS1. As a matter of fact, results of 100 ppm FS2 and 300 ppm of FS1 can be considered as equal. This shows additionally an improved performance under highest pressure.

6 Discussion

After gaining the experimental results, literature and field data are to be discussed and verified for proper outputs.

6.1 Watercut

Watercut investigations by means of field data show corrosion- inhibitive properties of oil at watercuts lower than 80 %. This result reflects investigations of Smith et al.¹⁴ and shows that in fields of Austria, generally no inhibition support of oil can be expected, since the average watercut is near 90 %.

Furthermore, watercuts measured in wells can be influenced by its flow rate or velocity. That means, with increasing production rates more water is sucked into the borehole and oil is not able to accumulate and segregate downhole, which would lead to an artificial decrease of watercut.

6.2 Fluid Velocity

The dependency of the watercut on the velocity makes the identification of the net- influence of velocity an issue. Furthermore, only by removal of H₂S containing wells a weak correlation according to literature could be found. Basically, corrosion rates are considered to increase with increasing velocity.^{11, 28, 29} The analysis of velocity influence additionally was simplified by exclusion of gas and linked slug flow. Knowing all that and keeping in mind that the presence of FeS films and the connected extraction of wells is highly speculative, reliable outputs (except the dependency of watercut) regarding fluid velocity can not be made. Nevertheless, velocity thresholds, also with respect to watercut, can be presented. At wellhead velocities lower than 0.15 m/s and tubing velocities lower than 0.11 m/s corrosion rates stay below "0.05 mm/a- limit".

6.3 CO₂ and H₂S Partial Pressure

Like already mentioned in experimental introduction, partial pressures CO₂, gained via field analysis, are not to be correlated to literature outputs. That is why experimental investigations have been added in order to verify field data. Basically, literature outputs of partial pressures CO₂ can be repeated and prove a misleading picture of field analysis. But field analysis still is helpful talking about classification of partial pressure relevance. Whereas 1 and 3 bar partial pressures are common in lower tubing areas (Figure 16), 10 bar is not registered in corresponding oil wells' analysis. Knowing that most CO₂ partial pressures are lower than 3 bar, further steps regarding well management need to be taken with respect to that threshold value.

H₂S partial pressures as well as analyzed " P_{CO_2} / P_{H_2S} " ratios show, according to numerous literature citations, a strong indication of FeS precipitation.^{20, 21, 22, 23, 24, 26}

Additionally, by analysis of H₂S wells, a lot of low corrosion rates could be explained under advanced velocities and higher CO₂ partial pressures. Removing H₂S wells, weak correlations of those parameters according to literature were found (Figure 23 to Figure 26). Like mentioned several times already, installed coupons are not available to prove that hypothesis, which makes assumptions still highly speculative. Whatsoever, H₂S influence needs to be considered in future, since FeS on coupons' surface can falsify measurement results. FeS is not supportive in corrosion prevention and needs to be taken seriously. It increases pitting probability, since FeS layers are not always homogeneous and H₂S as such is referred to cause Sulfide Stress Cracking (SSC).^{14, 19}

6.4 Temperature

Temperature was another parameter to be explored separately by means of laboratory experiments. Surface temperatures were considered to be constant, whereas downhole temperatures were calculated on basis of common "3.3 °C/100 m" gradient in oilfields. No connections of field data to literature were found. With help of experiments, temperature can be considered as proportional to corrosion rates until 80 °C, where peak corrosion rates are experienced. With further increase, corrosion rates finally decrease due to FeCO₃ formation. This has also been experienced in numerous scientific articles.^{1, 2, 25, 30, 46} Again, field data is supportive regarding qualification of temperature. That means that temperatures of 120 °C are not found at lowest tubing location; highest temperatures are calculated to approximately 60 °C (Figure 27 and Figure 28).

Once more, the appearance of protective scales can not be guaranteed in oil fields, since a lot of parameters, like velocity or pH, can influence protectiveness negatively.

6.5 Inhibitor Performance

The last point to be discussed is the inhibitor performance of FS1 and FS2. Starting with FS1, clear trends regarding an optimum dose of respective inhibitor could not be found via provided data of austrian fields (Figure 30 to Figure 33). Emphasizing on laboratory results and considering harshest conditions present downhole, 100 ppm of FS1 show optimum efficiency regarding corrosion rate reduction. At room temperature, as well as at elevated temperatures of 80 °C, 100 ppm shows satisfying results at 1 and 3 bar. As already mentioned in chapter "5 Experimental Results", under higher partial pressures of 10 bar, concentrations of 300 ppm show better performance than lower concentrations. Focussing on tubing protection, 10 bar of partial pressure CO₂ is excludable, like field investigations have shown. With temperatures of 120 °C, inhibitor performance breaks down showing no metal protection tendencies. Additionally, the inhibitor seems to decrease capabilities of protection of the FeCO₃ scale within the created laboratory conditions. This could be explained via adsorption of the inhibitor on FeCO₃ particles, leading to a decrease of grip of FeCO₃ on metal surfaces, explaining the easy removal of FeCO₃ films at inhibited samples within the evaluation phase. Furthermore, with increasing amounts of FeCO₃ particles, surfaces that need to be covered by the inhibitor is

increased, decreasing available inhibitor amounts to protect the metal surface. Like already mentioned, inhibitors are able to change FeCO_3 layers' porosity as well as other physical parameters.⁶⁵

Focussing now on FS2, an improved reduction of corrosion rates can be evidenced from field investigations, by means of "List Green Inhibitors", as well as from laboratory analyses. Especially at 10 bar CO_2 partial pressure and 80 °C, FS2 is able to halve the accomplished corrosion rate of FS1. To obtain more reliable properties of the inhibitor FS2, further investigations accordingly are necessary. Once more, description of differing compounds of respective inhibitor is being found at Background Data 28.

7 Conclusions

With field analyses alone only few reliable outputs were gained. With support of autoclave experiments, the following reliable results and findings can be published in order to understand critical parameters.

- Coupon measurements with watercuts lower than 80 % show significantly lower corrosion rates compared to the ones with higher watercuts. Knowing the average watercut of 90 % of Austrian oilfields, large inhibitive support from oil can not be expected.
- Velocity threshold values of 0.15 m/s for surface and 0.11 m/s for downhole are being defined. Below those threshold values corrosion is not proven and expected, since also watercuts depend on velocity.
- The precipitation of FeS can not be proven, due to missing coupons. Nevertheless, there are strong indicators from literature, underlining a high probability of FeS presence on relevant coupons.
- Field data analyses show insufficient trends and correlations with respect to partial pressure CO₂ and H₂S, velocity and temperature.
- Temperature and partial pressure CO₂ autoclave experiments show outputs according to literature.
- 30 ppm of FS1- inhibition is not sufficient in terms of optimum protection against corrosion, like experiments have shown.
- For most efficient protection of production tubings, 100 ppm of FS1 can be recommended. Dealing with higher CO₂ partial pressures of 10 bar and raised temperatures of 80 °C, an increase to 300 ppm improves metal conservation.
- At 120 °C, inhibitor FS1 is not efficient.
- Inhibitor FS2 performs better under 80 °C within autoclave experiments than FS1 and strengthens the results gained in field analyses.

8 Recommendations & Future Work

To achieve a higher reliability of field data, an independent record related to corrosion management is recommended. With an unified program, problems as well as benefits can be identified with less efforts.

8.1 Measurement Concept

Monitoring the corrosion rate alone does not provide the full overview on corrosive problems. The influence of wear by coupling of pumps e.g., can provide a synergism increasing the conventional corrosion rate, which can not be computed via coupons measurements.^{66, 67} That is why the additional implementation of “meantime between failure” (MBF) to corrosion analysis is strongly recommended. By inclusion of MBF or “Workover per Year”, also mechanical forces like abrasion or possible erosion can be considered and weaknesses in corrosion operations can be discovered more easily.

8.1.1 Start

All wells need to be screened and adjustments on inhibition need to be performed. For that, a three phase coupons- measurement cycle, each with a duration of one month minimum, like “surface measurements 1- 3”, for evaluating inhibitor doses, is recommended. Minimum doses of inhibition were already concluded previously. After that, an optimum treatment of the corrosion processes as such is expected. Coupons surface measurements are preferred to downhole measurements, since results can be achieved faster with fewer efforts.

8.1.2 Frequency

- MBF

The limit for workover was set to 0.33 WO/a providing also a good basis for evaluation frequency. This value was determined with respect to the average MBF of Table 5. That is why every third year, all wells are to be screened for workover linked to corrosion damage and are to be compared to previous years.

- Surface Coupons Measurement Cycle

After every workover, where signs of corrosion were being observed, surface coupons measurement cycles should be performed additionally to check for inhibitor efficiency. Furthermore, unplanned coupons- measurement cycles and inhibitor adjustments should be performed, if new conditions in the borehole, like perforation of new horizons, have been conducted. Basically, a well is recommended to be screened once in three years.

8.1.3 Documentation

To make sure that corresponding treatments can be justified via environmental background and to understand basic behaviour of a corrosive situation, important parameters have to be conserved.

- MBF

In order to evaluate workover caused by corrosion, exact documentation of workover data has to be done. That means, even if a workover is conducted due to a stuck pump e.g. and tubings as well as other downhole equipment is replaced due to signs of corrosion on that occasion, it needs to be documented and the key word "Corrosion Replacement" needs to be registered in workover reports.

- What type of damage
- Where is that damage located (Measured Depth)
- Pump type and setting depth
- Depth of perforation and perforated horizon
- CO₂ and H₂S content as well as pH of formation water
- Watercut and chloride average until last workover
- Average inhibitor concentration and type until last workover
- Average pump rate and production rate (liquid and gas) until last workover
- Average sediment production until last workover

- Surface Measurement Cycle

- Depth of perforation and perforated horizon
- CO₂ , H₂S content and pH value before start of first measurement cycle
- Chlorides before first measurement cycle
- Watercut average during each surface measurement cycle
- Average inhibitor concentration and type during each surface measurement phase
- Average pump rate and production rate (liquid and gas) during each surface measurement phase

All coupons installed need to be isolated to prevent corrosion and attached to corresponding measurement records. Of course, weight before and after installation needs to be recorded.

In addition, screening of sediment production must be conducted at least once a year for every well during conventional production, in order to evaluate the possibility of erosion or three body abrasion.

8.2 Future Work

8.2.1 FS2 Analysis

The inhibitor FS2 needs to be exposed to all conditions inhibitor FS1 has been exposed to within autoclave experiments in this work; that creates the optimum chance for comparison and provides the best level which one of the inhibitors performs better. Additionally, a field test like “List Green Inhibitors” needs to be performed with both inhibitors. Only the amount of treated wells needs to be increased to approximately 50 wells, compared to “List Green Inhibitors” test. Coupons need to be installed on surface for 1 month after corresponding well- system was saturated with respective inhibitor. There should be at least a time gap of 1 month between injections of different inhibitors.

8.2.2 FS1 and FS2 Performance connected to Sediments

Very often sediments tend to adhere inhibitors and reduce the accumulated amount on the metal surface, which causes a reduced protection. Inhibitors need to be screened for corresponding properties. For that, experiments, where autoclaves are being rotated, with variations of inhibitor doses and sediments representative of Austrian oilfields are recommended.

8.2.3 Proving protective Layers on Measurement Coupons in Wells

The existence of both FeCO_3 and FeS layers needs to be proven. Both layers can influence measurements and could lead to misinterpretations of well corrosivity as a consequence. Especially FeS layers at H_2S wells are to be treated with a lot of caution, like mentioned several times within this work. If layers are evident, proper consideration is of primary importance. Layers are not always homogeneous and can be removed by external forces. Critical areas in production streams need to be highlighted as well as layer integrity has to be determined along the production system. As a matter of fact, inhibitor performances in connection to FeS particles would be another step to be investigated.

8.2.4 Implementation and Verification of Measurement Concept

The recommendations suggested within 8.1 needs to be implemented and checked for applicability and validity. Especially the start requires maximum consistency and one single person in charge for surveillance. For that, a record form, containing all suggested parameters and considerations, needs to be created and every measurement needs to be controlled and recorded according to invented guidelines. Furthermore, problems, criticism and other concerns during the evaluation phase have to be registered and, as a result, innovations can be introduced. The monitoring concept should be a dynamic corpus that has to be maintained over decades with maximum consistency to lower corrosion rates in a standardized manner.

9 Appendix

9.1 Background Data

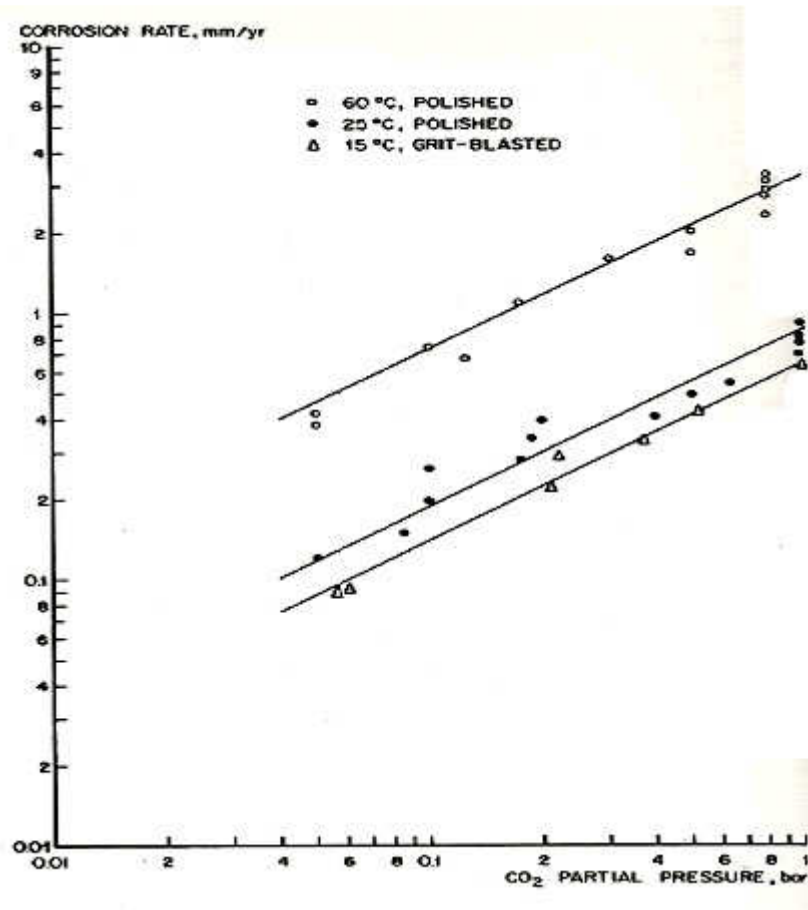
Component	Formation Water (ppm)	Chloride Containing Fluid (ppm)
Chloride	52,000	42500
SO ₄ ²⁻	10	
Bicarbonate	500	
Sodium	29,500	27540
Potassium	380	
Calcium	3200	
Magnesium	500	
Acetate	50	
pH	5.5-5.8	3.8-4.0

Background Data 1- Environments created at Investigations^{21,26}

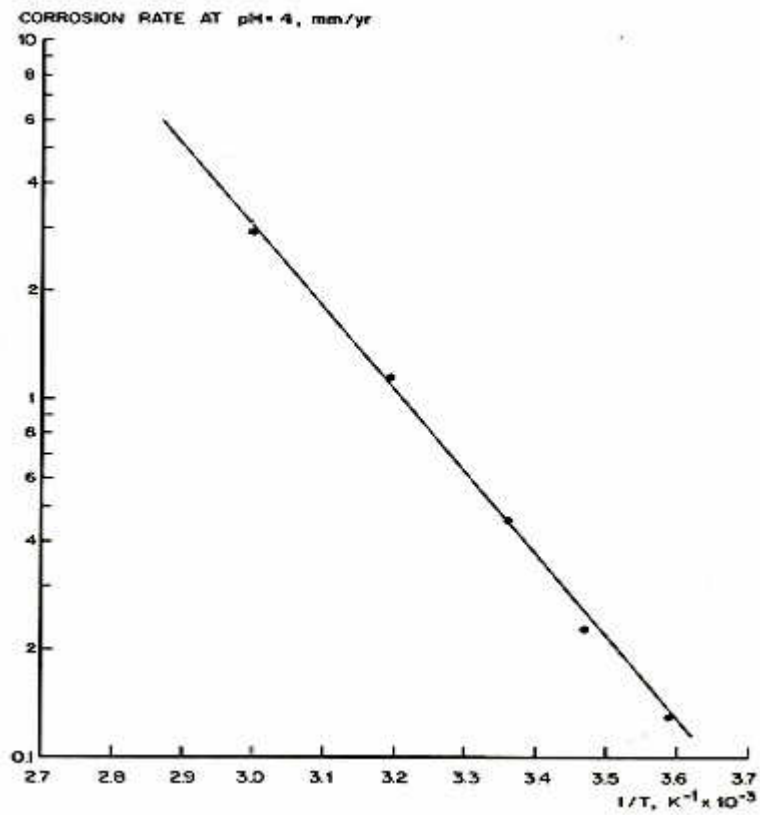
H₂S-CO₂ Corrosion Dominance and Prediction Guides (A Rule of Thumb)

CO ₂ /H ₂ S Ratio	Sub category	Operating Parameters	Dominating Corrosion Process	Primary Corrosion Product	Possible Pattern of Corrosion Damage	Corrosion Damage Risk Factor (A Rule of Thumb)
< 20	-	Known	H ₂ S	FeS	Low: Subject to the formation of a protective FeS	-
20 to 500		Known	Mixed H ₂ S/CO ₂	FeS and FeCO ₃	Mixed - the highest localised corrosion rate does not exceed predicted sweet corrosion rate.	CO ₂ Corrosion Model
	100	Fully known	Mixed H ₂ S/CO ₂	FeS and FeCO ₃	Mixed - Corrosion rate determined by the nature of FeS	CO ₂ Corrosion Model with possible reduction of 4
> 500		Known	CO ₂	FeCO ₃	CO ₂ driven	CO ₂ Corrosion Model with possible reduction of 4
	1000	Fully known	CO ₂	FeCO ₃	CO ₂ driven	CO ₂ Corrosion Model with possible reduction of 3
	10000	Fully known	CO ₂	FeCO ₃	CO ₂ driven	CO ₂ Corrosion Model with possible reduction of 3
	> 10000	Fully known	CO ₂	FeCO ₃	CO ₂ driven	CO ₂ Corrosion Model

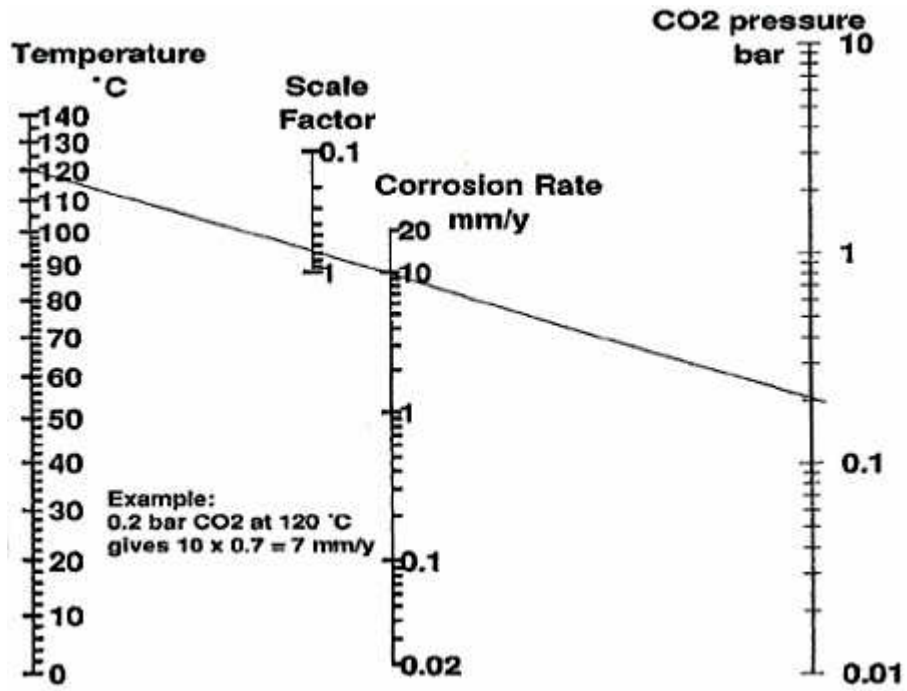
Background Data 2- Pots' Rule of Thumb for CO₂- H₂S Corrosion Prediction^{21,26}



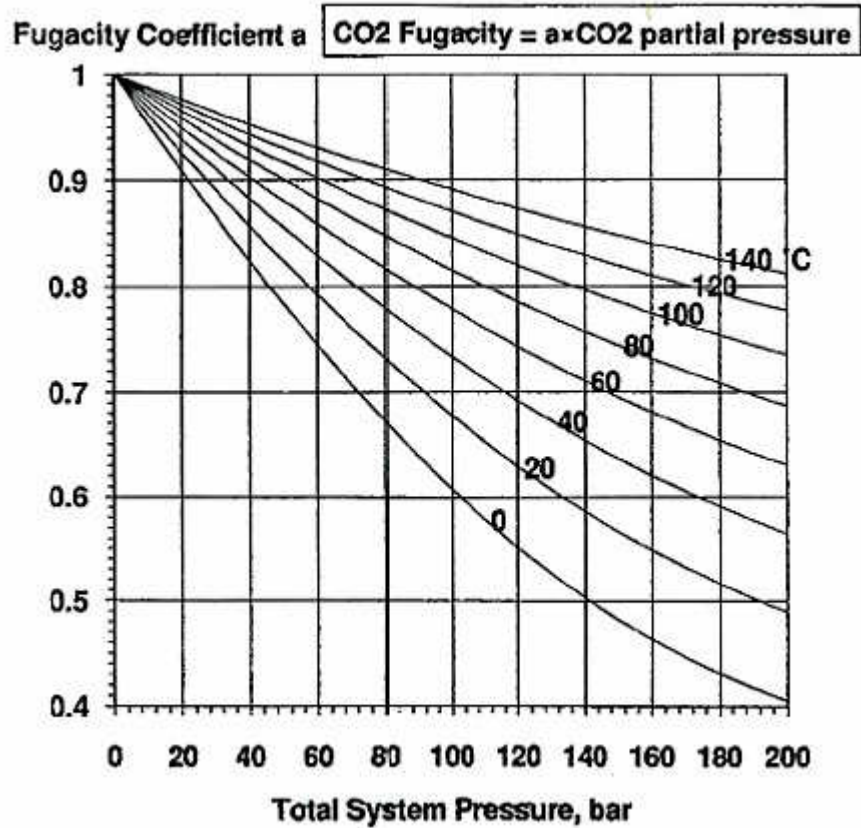
Background Data 3 – Influence of CO₂ Partial Pressure on Corrosion Rates¹⁷



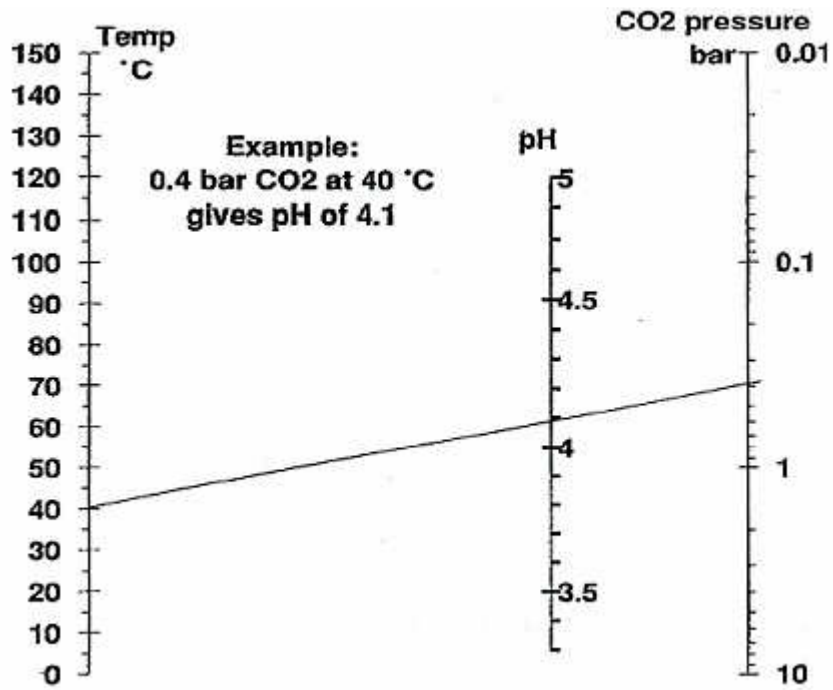
Background Data 4 – Arrhenius Plot of Corrosion Rates normalized to pH = 4 (grit blasted samples)¹⁷



Background Data 5 – Nomogram for CO₂ Corrosion⁴⁶



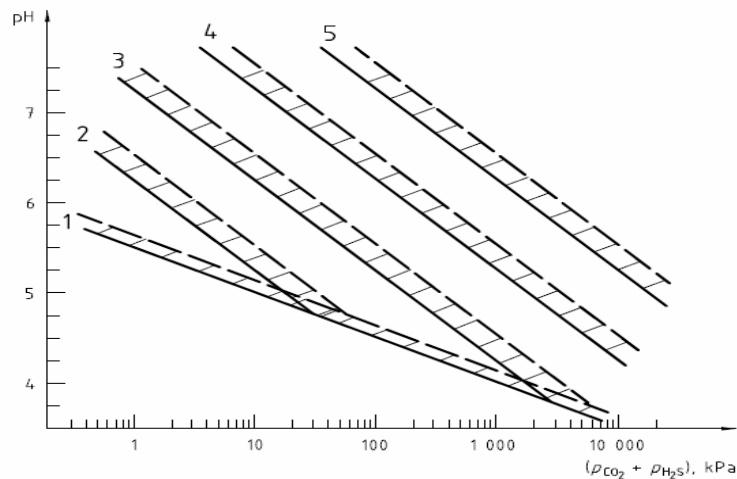
Background Data 6 – Fugacity Coefficient for CO₂ in Methane for Gas Mixtures less than 5 mol % CO₂⁴⁶



Background Data 7 – Nomogram for pH of Water and CO₂ as a function of CO₂ Pressure (Fugacity) and Temperature⁴⁶

Temperature °C	K _t
5	0,42
15	1,59
20	4,762
40	8,927
60	10,695
80	9,949
90	6,250
120	7,770
150	5,203

Background Data 8 – Constant K_t of NORSOK¹⁸



Key
 1 $\text{HCO}_3^- = 0 \text{ meq/l}$
 2 $\text{HCO}_3^- = 0,1 \text{ meq/l}$
 3 $\text{HCO}_3^- = 1 \text{ meq/l}$
 4 $\text{HCO}_3^- = 10 \text{ meq/l}$
 5 $\text{HCO}_3^- = 100 \text{ meq/l}$
 - - - - - $T = 100 \text{ }^\circ\text{C}$
 ———— $T = 20 \text{ }^\circ\text{C}$

Background Data 9 – The pH of condensed Water (wet Gas) or Formation Waters containing Bicarbonate (undersaturated in CaCO_3) under CO_2 and H_2S Pressure⁶⁸

Temperature °C	pH	f(pH)
5	$3,5 \leq \text{pH} < 4,6$	$f(\text{pH}) = 2,0676 - (0,2309 \times \text{pH})$
5	$4,6 \leq \text{pH} \leq 6,5$	$f(\text{pH}) = 4,342 - (1,051 \times \text{pH}) + (0,0708 \times \text{pH}^2)$
15	$3,5 \leq \text{pH} < 4,6$	$f(\text{pH}) = 2,0676 - (0,2309 \times \text{pH})$
15	$4,6 \leq \text{pH} \leq 6,5$	$f(\text{pH}) = 4,986 - (1,191 \times \text{pH}) + (0,0708 \times \text{pH}^2)$
20	$3,5 \leq \text{pH} < 4,6$	$f(\text{pH}) = 2,0676 - (0,2309 \times \text{pH})$
20	$4,6 \leq \text{pH} \leq 6,5$	$f(\text{pH}) = 5,1885 - (1,2353 \times \text{pH}) + (0,0708 \times \text{pH}^2)$
40	$3,5 \leq \text{pH} < 4,6$	$f(\text{pH}) = 2,0676 - (0,2309 \times \text{pH})$
40	$4,6 \leq \text{pH} \leq 6,5$	$f(\text{pH}) = 5,1885 - (1,2353 \times \text{pH}) + (0,0708 \times \text{pH}^2)$
60	$3,5 \leq \text{pH} < 4,6$	$f(\text{pH}) = 1,836 - (0,1818 \times \text{pH})$
60	$4,6 \leq \text{pH} \leq 6,5$	$f(\text{pH}) = 15,444 - (6,1291 \times \text{pH}) + (0,8204 \times \text{pH}^2) - (0,0371 \times \text{pH}^3)$
80	$3,5 \leq \text{pH} < 4,6$	$f(\text{pH}) = 2,6727 - (0,3636 \times \text{pH})$
80	$4,6 \leq \text{pH} \leq 6,5$	$f(\text{pH}) = 331,68 \times e^{(-1,2618 \times \text{pH})}$
90	$3,5 \leq \text{pH} < 4,57$	$f(\text{pH}) = 3,1355 - (0,4673 \times \text{pH})$
90	$4,57 \leq \text{pH} < 5,62$	$f(\text{pH}) = 21254 \times e^{(-2,1811 \times \text{pH})}$
90	$5,62 \leq \text{pH} \leq 6,5$	$f(\text{pH}) = 0,4014 - (0,0538 \times \text{pH})$
120	$3,5 \leq \text{pH} < 4,3$	$f(\text{pH}) = 1,5375 - (0,125 \times \text{pH})$
120	$4,3 \leq \text{pH} < 5$	$f(\text{pH}) = 5,9757 - (1,157 \times \text{pH})$
120	$5 \leq \text{pH} \leq 6,5$	$f(\text{pH}) = 0,546125 - (0,071225 \times \text{pH})$
150	$3,5 \leq \text{pH} < 3,8$	$f(\text{pH}) = 1$
150	$3,8 \leq \text{pH} < 5$	$f(\text{pH}) = 17,634 - (7,0945 \times \text{pH}) + (0,715 \times \text{pH}^2)$
150	$5 \leq \text{pH} \leq 6,5$	$f(\text{pH}) = 0,037$

Background Data 10 – pH Function of NORSOK¹⁸

Parameter	Units	Range	Comments
Temperature	°C	5 to 150	
	°F	68 to 302	
Total pressure	bar	1 to 1000	
	psi	14,5 to 14500	
Total mass flow	kmole/h	10^{-3} to 10^8	Only relevant when CO ₂ is given in kmole/h.
CO ₂ fugacity in the gas phase	bar	0,1 to 10	The CO ₂ partial pressure shall be \leq the total pressure. The allowed ranges of mole% and kmole/h CO ₂ are dependent on the total pressure.
	psi	1,45 to 145	
	mole%	variable	
	kmole/h	variable	
Wall shear stress	Pa	1 to 150	Can be calculated by use of other input parameters, see 7.2.1.
PH		3,5 to 6,5	Can be calculated by use of other input parameters, see 7.2.2.
Glycol concentration	weight%	0 to 100	
Inhibitor efficiency	%	0 to 100	See NORSOK M-001

Background Data 11 – Basic Input Parameters of NORSOK¹⁸

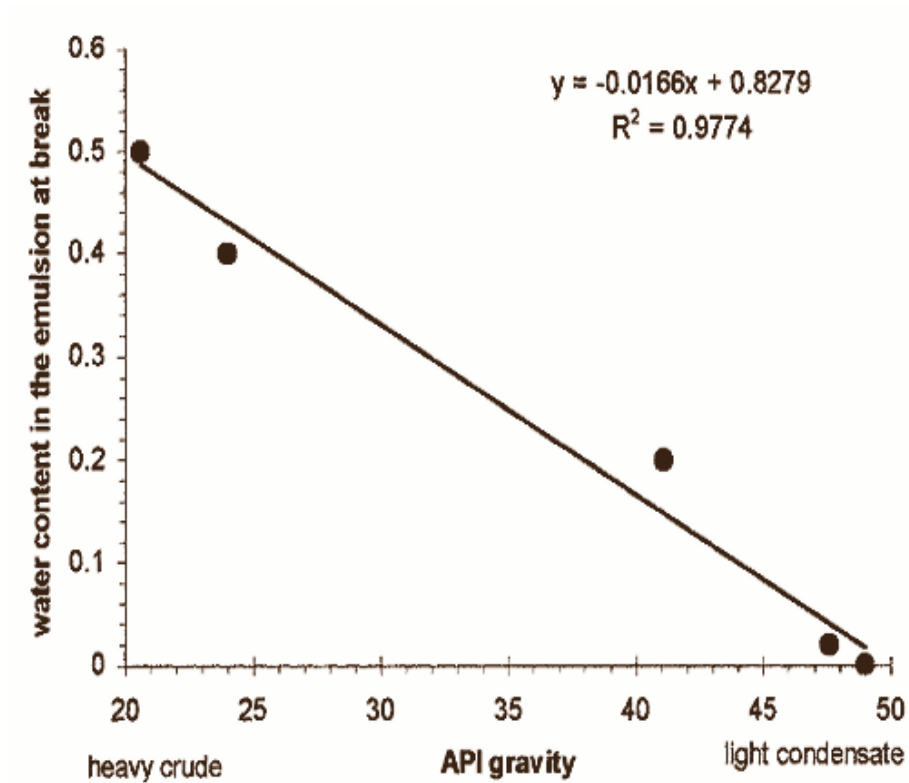
Parameter	Units	Range	Comments
Temperature	°C	5 to 150	
	°F	41 to 302	
Total pressure	bar	1 to 1000	
	psi	14,5 to 14500	
Superficial liquid velocity/ Liquid flow	m/s Sm ³ /d	0 to 20 (depends on internal pipe diameter)	Requirement: turbulent flow, i.e. Re > 2300
Superficial gas velocity/ Gas flow	m/s MSm ³ /d	0 to 40 (depends on internal pipe diameter)	Requirement: turbulent flow, i.e. Re > 2300
Watercut, ϕ	%	0 to 100	
Internal pipe diameter	mm	All diameters	Requirement: turbulent flow, i.e. Re > 2300

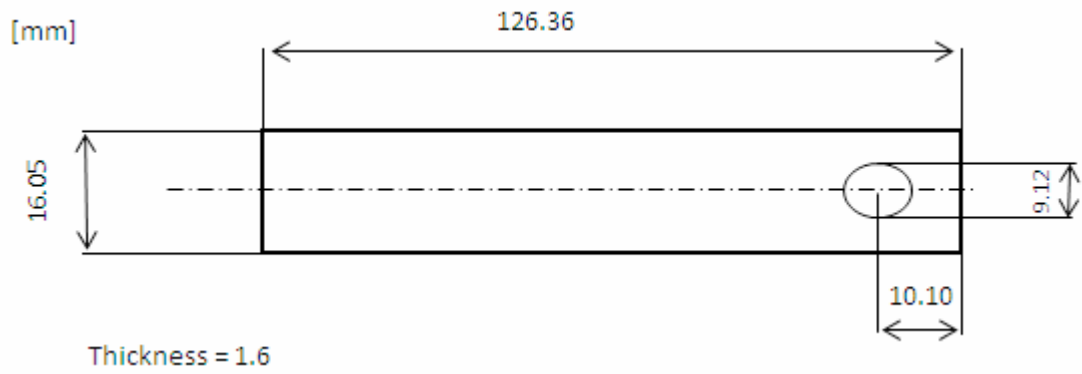
Background Data 12 – Input Parameters for simplified Calculation of Wall Shear Stress of NORSOK¹⁸

Parameter	Units	Range	Default value
Roughness	μm	0 to 100	50
Compressibility		0,8 to 1	0,9
Specific gravity of gas relative to air		0,5 to 1	0,8
Water density, ρ_w	kg/m ³	995 to 1050	1024
Oil density, ρ_o	kg/m ³	600 to 1100	850
Gas density, ρ_g	kg/m ³	1 to 1700	calculated
Water viscosity, μ_w	cp	0,17 to 1,1	calculated
	N s/m ²	0,00017 to 0,0011	
Oil viscosity, μ_o	cp	0,2 to 200	1,1
	N s/m ²	0,0002 to 0,2	
Gas viscosity, μ_g	cp	0,02 to 0,06	0,03
	N s/m ²	0,00002 to 0,00006	
Watercut at inversion point, ϕ_c		0,3 to 0,9	0,5
Maximum relative liquid viscosity, μ_{relmax}		1 to 100	7,06

Background Data 13 – Input Parameters for accurate Calculation of Wall Shear Stress of NORSOK¹⁸

Parameter	Unit	Range	Default values	Comments
Temperature	°C °F	5 to 150 41 to 302		
Total pressure	bar psi	1 to 1000 14,5 to 14500		
Total mass flow	kmole/h	10 ⁻³ to 10 ⁶		Only relevant when CO ₂ is given in kmole/h.
CO ₂ fugacity	bar psi mole% kmole/h	0 to 10 0 to 145 variable variable		The CO ₂ partial pressure shall be < the total pressure. The allowed ranges of mole% and kmole/h CO ₂ are dependent on the total pressure.
Bicarbonate (HCO ₃ ⁻)	mg/l mM	0 to 20000 0 to 327	0	Default values for formation water.
Ionic strength/salinity	g/l M	0 to 175 0 to 3	50	Default values for formation water.

Background Data 14 – Input Parameters for pH Calculations of NORSOK¹⁸Background Data 15 – Watercut Readings in Emulsions at the Point where at least 10% of the total Water has separated from Oil Water Emulsions³



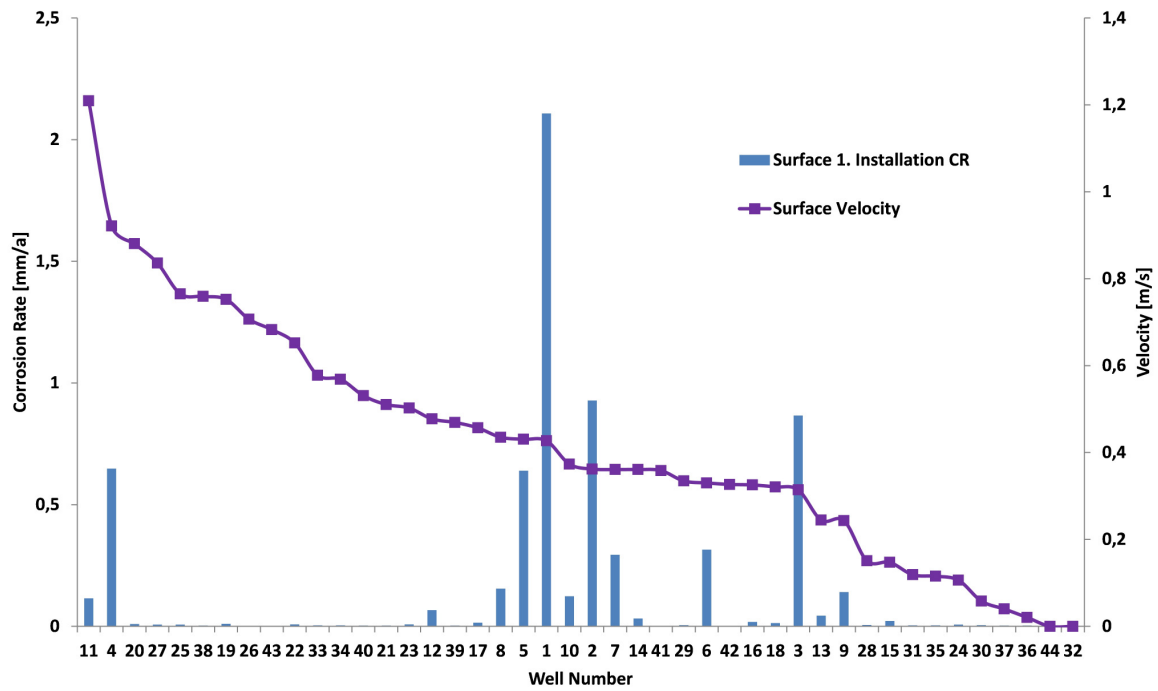
Background Data 16 – Dimensions and Content of an original C1020 Coupon⁶⁹



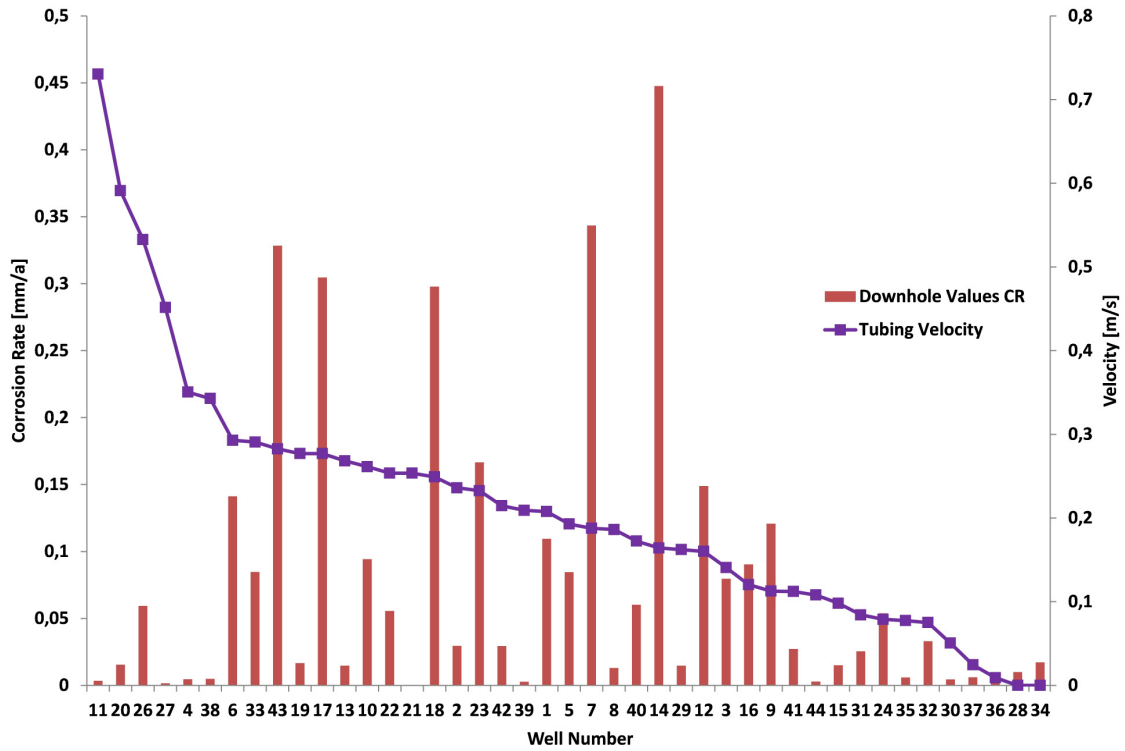
Background Data 17 – Example Picture of Surface/ Wellhead Coupons Installation of Prottes 109



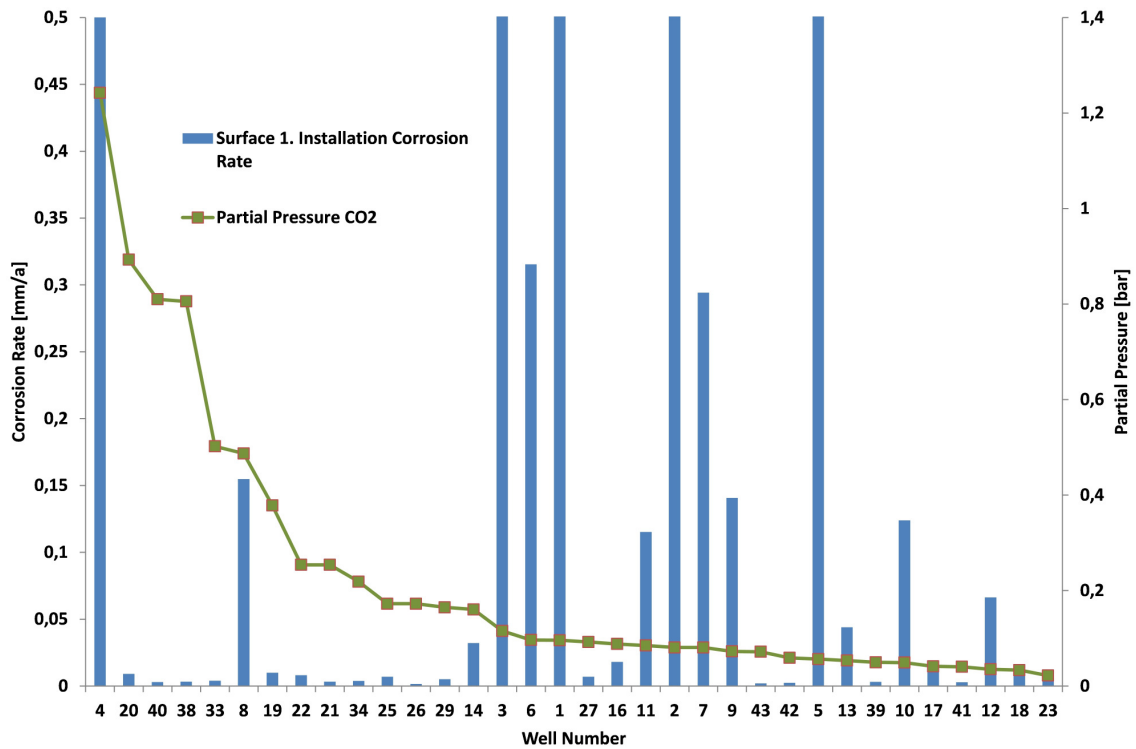
Background Data 18 – Example Picture of Downhole Coupons Installation in Tailpipe



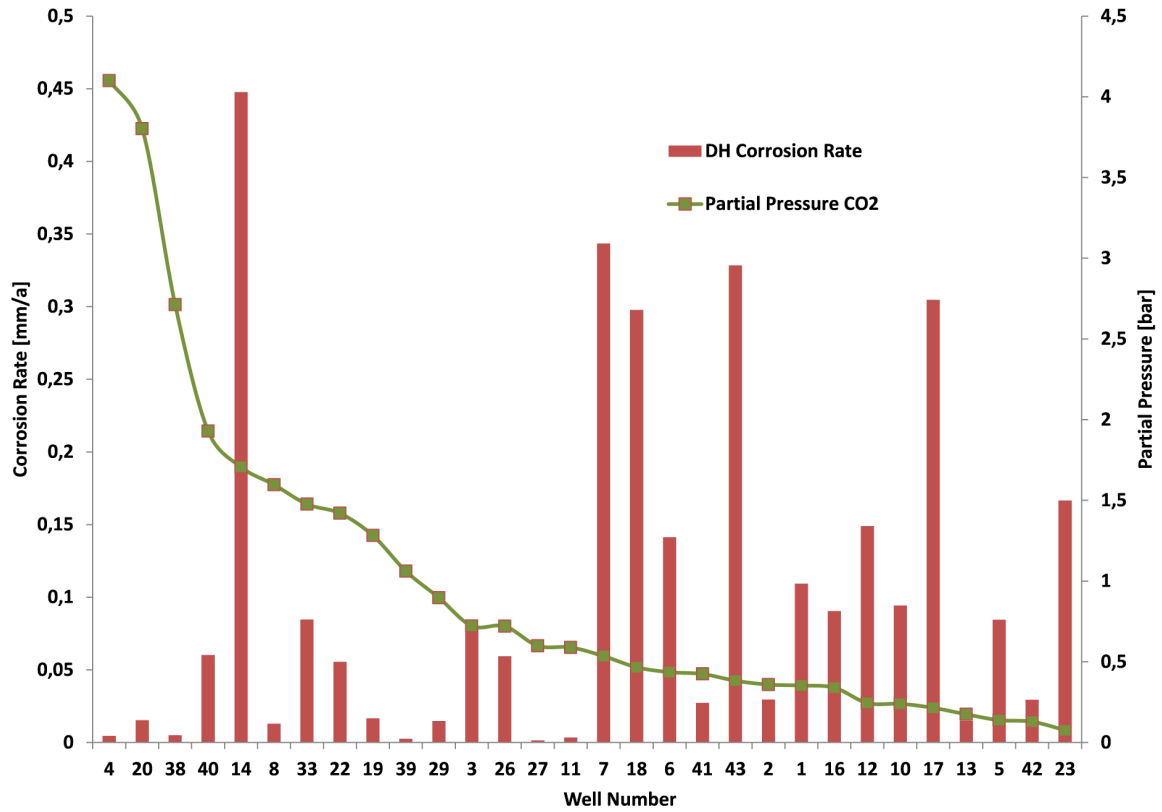
Background Data 19 – Numbered “Surface 1. Installation” Corrosion Rate versus Wellhead Velocity⁵¹



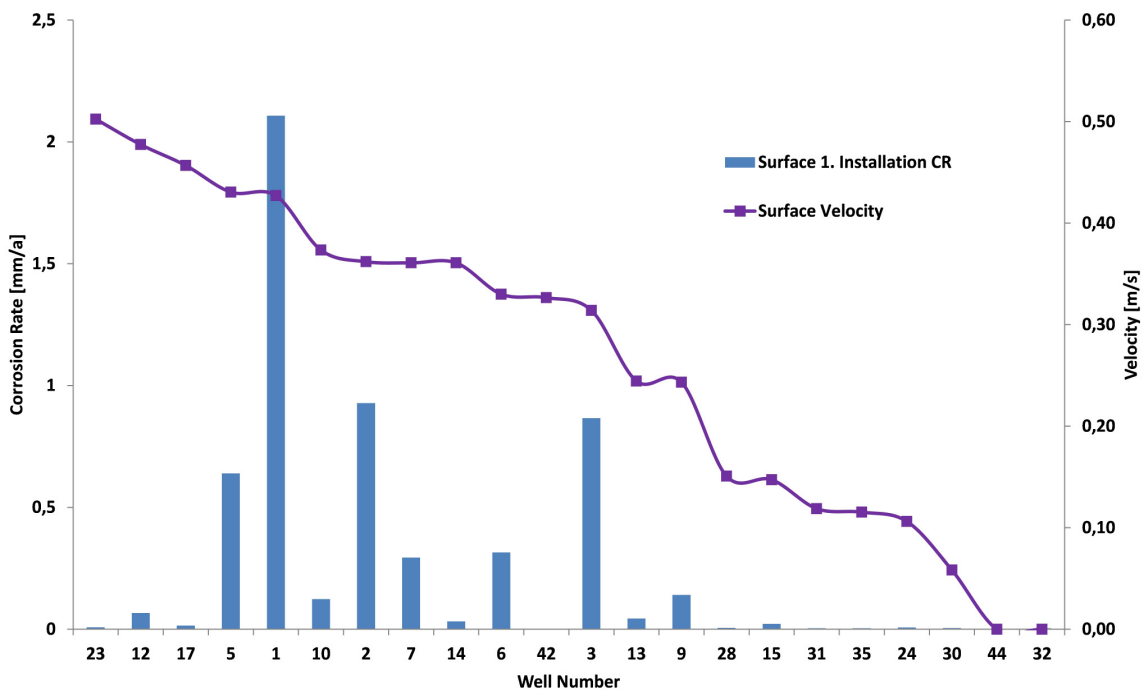
Background Data 20 – Numbered Downhole Corrosion Rate versus Tubing Velocity⁵¹



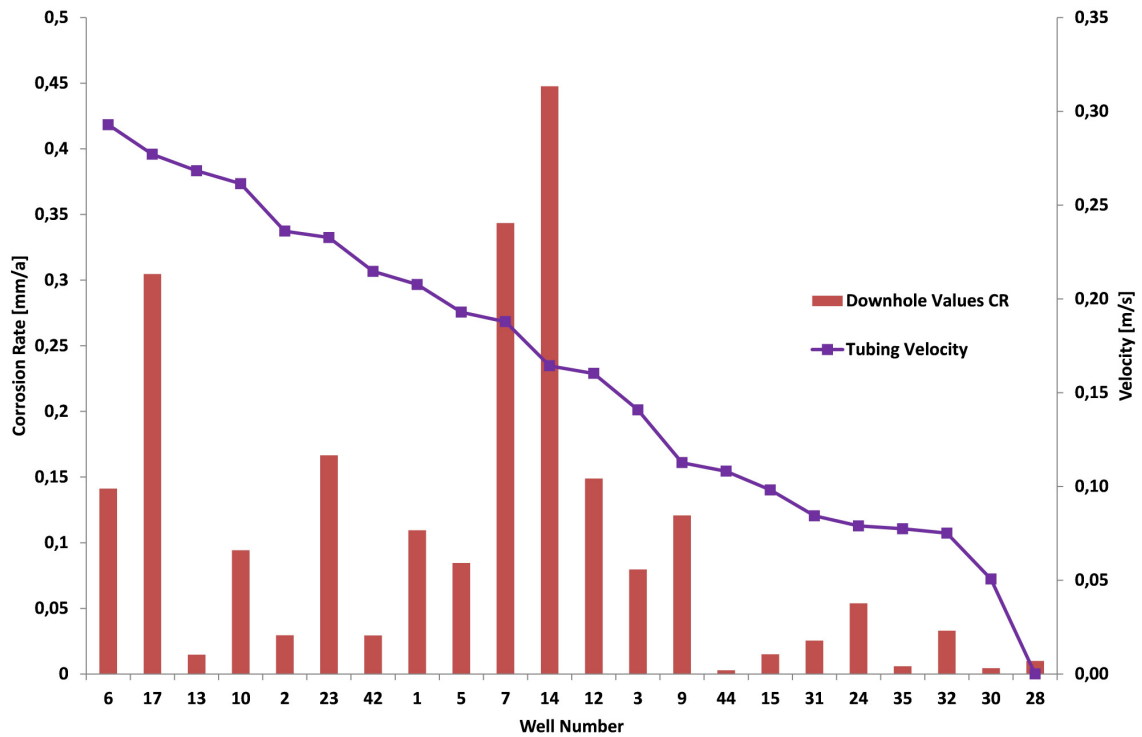
Background Data 21 – “Surface 1. Installation” Corrosion Rates versus numbered CO₂ Partial Pressures for Watercuts > 80 % and Velocities > 0.15 m/s⁵¹



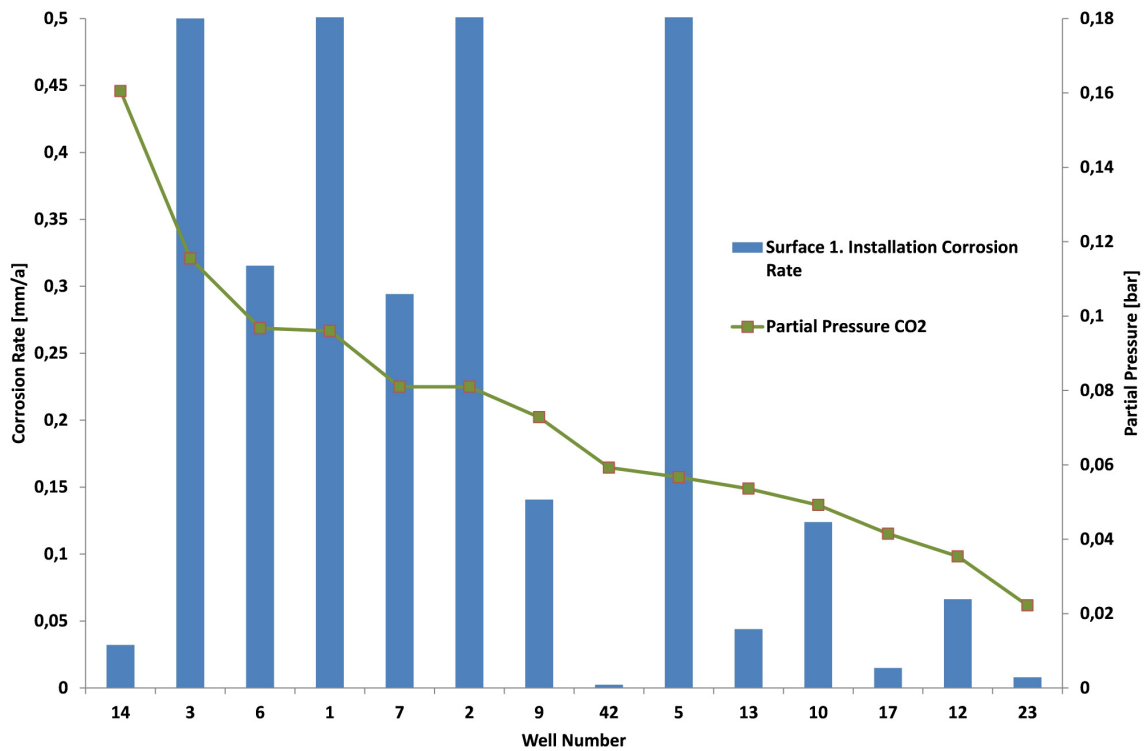
Background Data 22 – Downhole Corrosion Rates versus numbered CO₂ Partial Pressures for Watercuts > 80 % and Velocities > 0.11 m/s⁵¹



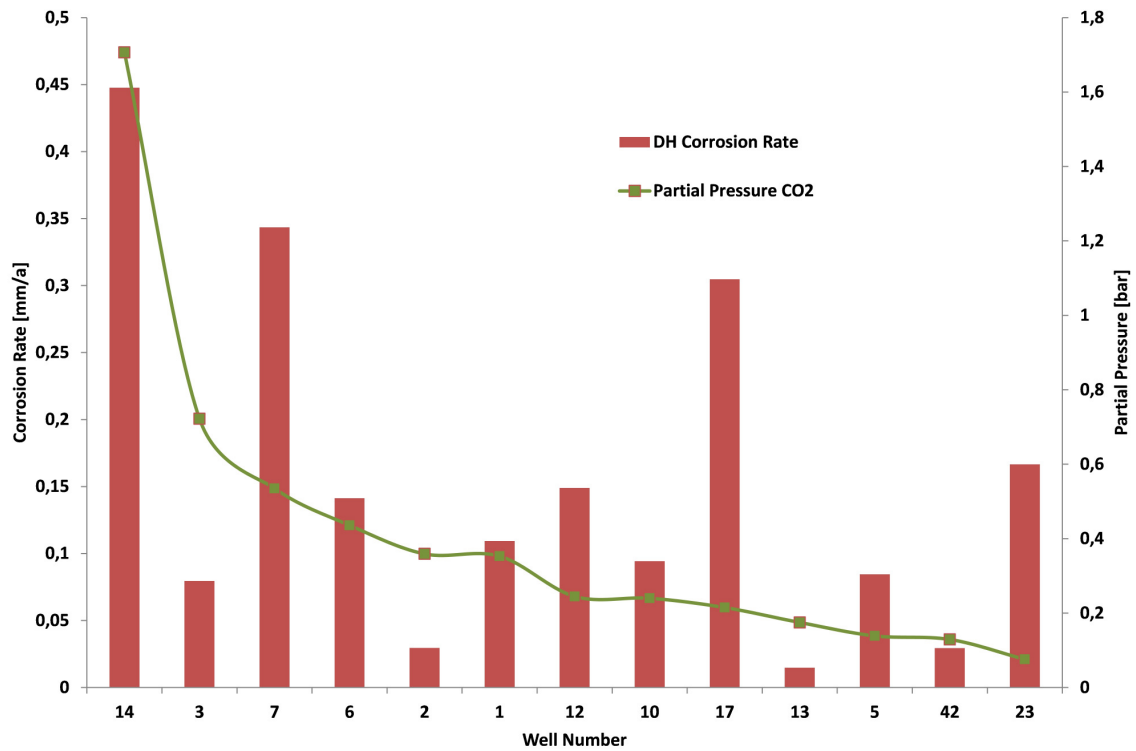
Background Data 23 – Wellhead Velocity versus numbered “Surface 1. Installation” Corrosion Rate without H₂S Wells⁵¹



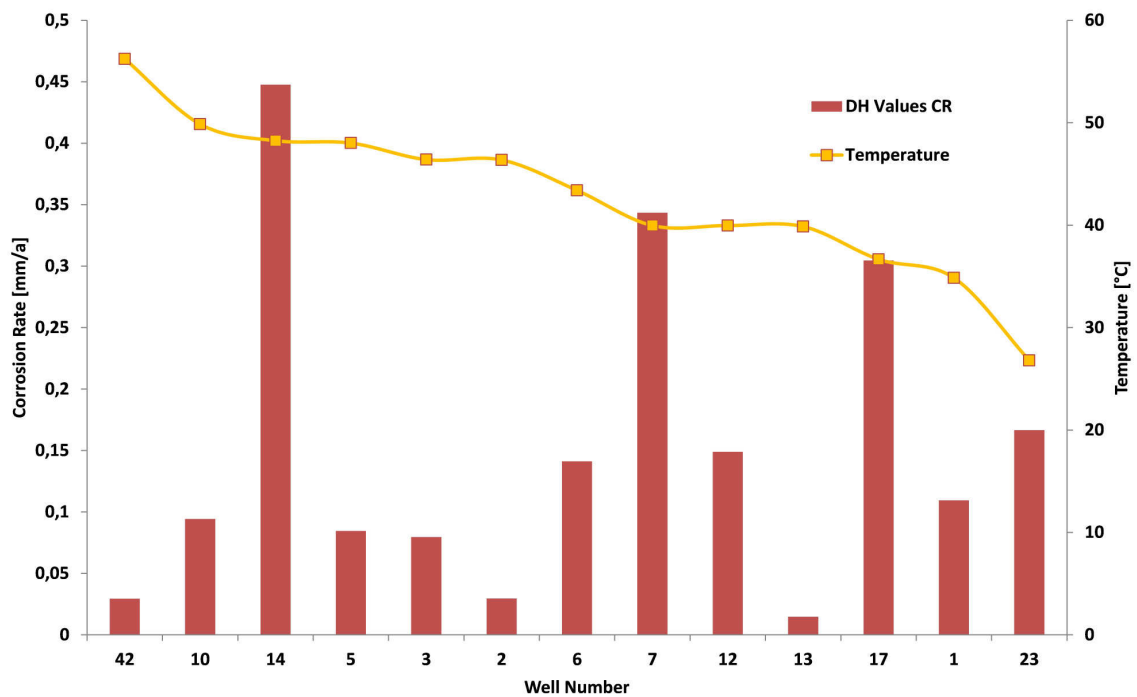
Background Data 24 – Tubing Velocity versus numbered Downhole Corrosion Rates without H₂S Wells⁵¹



Background Data 25 – Partial Pressure CO₂ versus numbered “Surface 1. Installation” Corrosion Rate for Watercuts > 80 % and Velocity > 0.15 m/s without H₂S Wells⁵¹

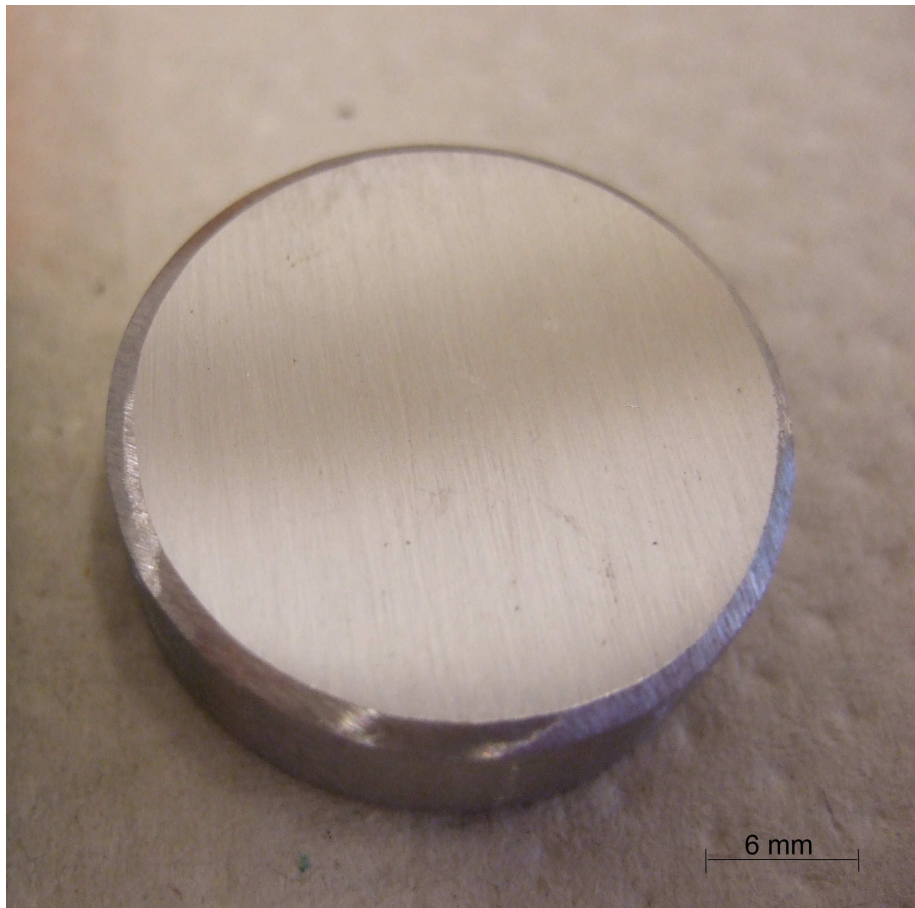


Background Data 26 – Partial Pressure CO₂ versus numbered Downhole Corrosion Rate for Watercuts > 80 % and Velocity > 0.11 m/s without H₂S Wells⁵¹

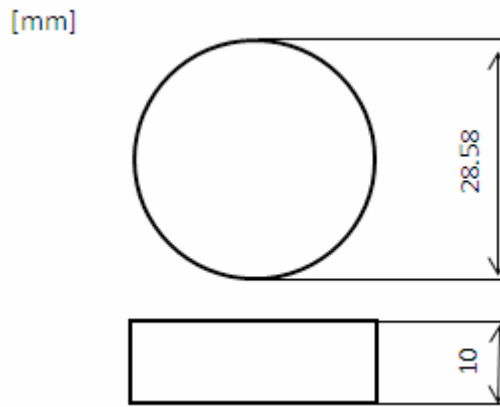


Background Data 27 – Temperature versus numbered Downhole Corrosion Rate for Watercuts > 80% and Tubing Velocities > 0.11 m/s without H₂S Wells⁵¹

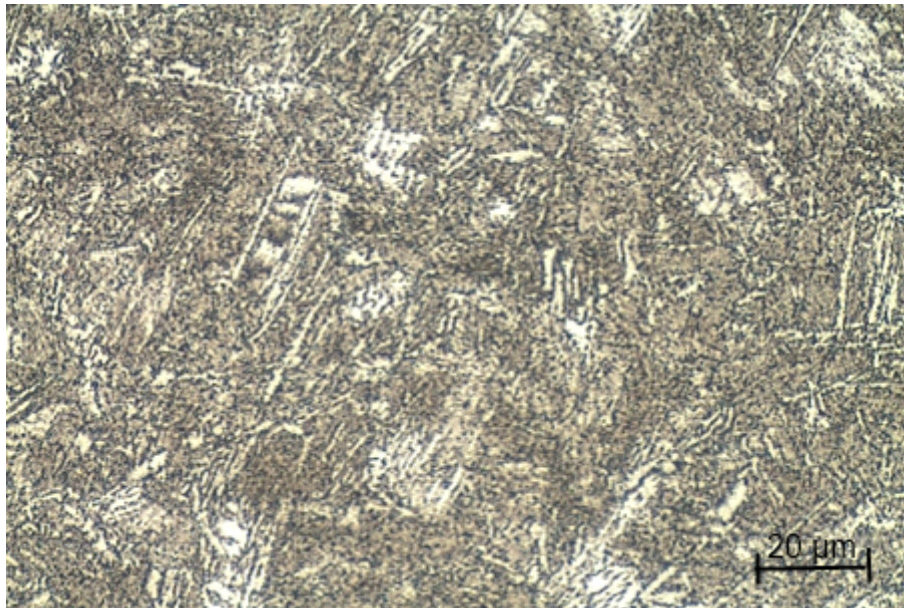
Inhibitor	Tradename	Compounds	Content [%]
FS1	Champion Technologies CK 347- HD	2,2'- Oxybisethanol	10 – 30
		2-(2-Ethoxyethoxy)ethanol	10 – 30
		Alcohol, ethoxylated, phosphated, neutralized	10 – 30
		Quarternary ammonium compounds	10 – 30
FS2	M-I Swaco	Alkylaminesalts	30 – 60
	KI 350	Others	40 – 70

Background Data 28 – Composition of Inhibitors FS1 and FS2⁷⁰

Background Data 29 – Sample for Autoclave Experiments



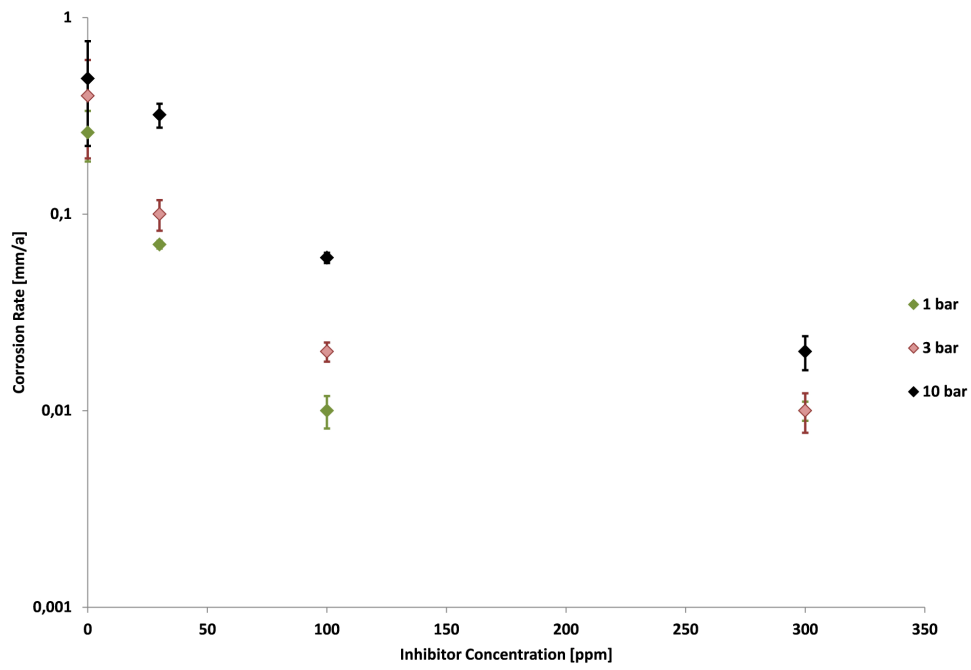
Background Data 30 – Dimensions of Specimen for Autoclave Experiments



Background Data 31 – Microstructure of L80 Steel

Components	Content [ml]
H ₂ O	660
HCl	330
“Sparbeize Sorte NFS”	10

Background Data 32 – Staining Agent (Bühler GmbH, Düsseldorf, Germany) for Autoclave Tests⁶⁴



Background Data 33 – Corrosion Rates at Room Temperature versus Inhibitor Dose with Variations in Partial Pressure CO₂ (log- scale)



Background Data 34 – FeCO₃ layered Sample representative for all Samples after Exposure to 120 °C Environment

Dose [ppm]	Efficiency FS1 [%] Room Temperature			Efficiency FS1 [%] 80 [°C]			Efficiency FS1 [%] 120 [°C]		
	P CO ₂ 1 [bar]	P CO ₂ 3 [bar]	P CO ₂ 10 [bar]	P CO ₂ 1 [bar]	P CO ₂ 3 [bar]	P CO ₂ 10 [bar]	P CO ₂ 1 [bar]	P CO ₂ 3 [bar]	P CO ₂ 10 [bar]
	0								
30	73	75	35	34	10	18	0	0	0
100	96	95	88	84	77	50	0	0	0
300	96	98	96	84	75	81	0	0	0

Background Data 35 – Efficiency of Inhibitor FS1 within Autoclave Experiments

9.2 Spreadsheets

FS1 = CK347 HD
 FS2 = KI350

Data 1st Installation

SONDENNAME	Well Number	Inhibitor 1.Installation [ppm]	1. Installation CR [mm/a]	1. Installation [date]	1. Installation Removal [date]
MATZEN 157	1	0	2,108	16.01.1996	05.03.1996
SCHOENKIRCHEN 119	2	0	0,9281	23.01.1996	18.03.1996
BOCKFLIESS 069	3	0	0,8664	07.06.1995	16.08.1995
BOCKFLIESS 101	4	0	0,6483	22.07.1997	17.09.1997
PROTTES 095	5	0	0,6394	17.01.1996	07.03.1996
SCHOENKIRCHEN 098	6	0	0,3155	14.06.1995	16.08.1995
SCHOENKIRCHEN 194	7	0	0,2943	23.01.1996	18.03.1996
BOCKFLIESS 056	8	0	0,1549	24.02.1994	28.04.1994
BOCKFLIESS 165	9	0	0,1408	16.01.1996	05.03.1996
SCHOENKIRCHEN 065	10	0	0,1239	08.06.1995	08.08.1995
MATZEN 168	11	0	0,1153	16.01.1996	05.03.1996
SCHOENKIRCHEN 196	12	0	0,0663	08.06.1995	08.08.1995
SCHOENKIRCHEN 096	13	0	0,044	17.01.1996	07.03.1996
BOCKFLIESS 067	14	0	0,0322	09.09.1994	23.09.1994
PROTTES 094	15	0	0,0222	11.07.1996	04.09.1996
MATZEN 164	16	0	0,0181	22.07.1997	17.09.1997
SCHOENKIRCHEN 042	17	0	0,015	08.06.1995	08.08.1995
MATZEN 154	18	0	0,0137	07.06.1995	16.08.1995
BOCKFLIESS 055	19	0	0,01	14.09.1995	09.11.1995
BOCKFLIESS 031	20	0	0,0092	14.09.1995	09.11.1995
BOCKFLIESS 028	21	0	0,0033	22.07.1997	17.09.1997
BOCKFLIESS 028	22	0	0,0082	16.06.1998	25.08.1998
MATZEN 445	23	0	0,008	25.02.1994	02.05.1994
SCHOENKIRCHEN 017	24	0	0,0073	14.06.1995	16.08.1995
BOCKFLIESS 095	25	0	0,007	07.01.1999	02.03.1999
BOCKFLIESS 095	26	0	0,0016	08.06.1999	10.08.1999
MATZEN 166	27	0	0,007	16.06.1998	25.08.1998
BOCKFLIESS 140	28	0	0,0053	09.07.1996	29.08.1996
BOCKFLIESS 120	29	0	0,0052	24.02.1994	27.04.1994
MATZEN 297	30	0	0,0045	16.01.1996	05.03.1996
SCHOENKIRCHEN 111	31	0	0,0043	17.01.1996	07.03.1996
SCHOENKIRCHEN 321	32	0	0,0042	23.01.1996	18.03.1996

BOCKFLIESS 006a	33	0	0,0041	16.01.1996	05.03.1996
BOCKFLIESS 038	34	0	0,0039	07.01.1999	02.03.1999
BOCKFLIESS 083	35	0	0,0038	09.07.1996	29.08.1996
MATZEN 351	36	0	0,0034	14.09.1995	09.11.1995
MATZEN 083	37	0	0,0034	22.07.1997	17.09.1997
BOCKFLIESS 110	38	0	0,0033	22.07.1997	17.09.1997
MATZEN 285	39	0	0,0032	29.01.1997	20.03.1997
BOCKFLIESS 074	40	0	0,003	14.09.1995	09.11.1995
MATZEN 195	41	0	0,0029	07.06.1995	16.08.1995
SCHOENKIRCHEN 078	42	0	0,0025	18.01.1996	07.03.1996
MATZEN 176	43	0	0,0021	27.07.1994	23.09.1994
MATZEN 417	44	0	0,0016	27.07.1994	23.09.1994
SCHOENKIRCHEN 111	45	45,2	0,0078	08.06.1995	08.08.1995
BOCKFLIESS 034	46	18	0,0076	16.01.1996	05.03.1996
BOCKFLIESS 059	47	4	0,1335	26.07.1994	23.09.1994
BOCKFLIESS 001	48	40	0,0097	07.01.1999	02.03.1999
BOCKFLIESS 005	49	32,6	0,0027	24.02.1994	29.04.1994
BOCKFLIESS 014	50	10	0,004	14.09.1995	09.11.1995
BOCKFLIESS 025	51	18	0,002	18.05.1993	21.07.1993
BOCKFLIESS 030	52	33	0,0017	08.06.1999	10.08.1999
BOCKFLIESS 035	53	18	0,004	07.01.1999	02.03.1999
BOCKFLIESS 036	54	18	0,0027	07.01.1999	02.03.1999
BOCKFLIESS 037	55	30	0,0019	08.06.1999	10.08.1999
BOCKFLIESS 041	56	20	0,3702	14.09.1995	09.11.1995
BOCKFLIESS 041	57	31	0,1428	16.06.1998	25.08.1998
BOCKFLIESS 045	58	32	0,0032	16.01.1996	05.03.1996
BOCKFLIESS 049	59	21,8	3,6003	24.02.1994	27.04.1994
BOCKFLIESS 051	60	27	0,0095	29.01.1997	20.03.1997
BOCKFLIESS 053	61	34	0,0052	29.01.1997	20.03.1997
BOCKFLIESS 061	62	24	0,103	29.01.1997	20.03.1997
BOCKFLIESS 063	63	31	0,0021	08.06.1999	10.08.1999
BOCKFLIESS 064	64	25	0,0038	09.07.1996	29.08.1996
BOCKFLIESS 066	65	29	0,0053	16.06.1998	25.08.1998
BOCKFLIESS 067	66	28	0,1217	14.09.1995	09.11.1995
BOCKFLIESS 067	67	34	0,0298	16.06.1998	25.08.1998
BOCKFLIESS 068	68	31	0,0049	16.06.1998	25.08.1998
BOCKFLIESS 069	69	60	0,0117	16.01.1996	05.03.1996
BOCKFLIESS 073	70	50	0,0017	26.07.1994	23.09.1994
BOCKFLIESS 075	71	22	0,0018	07.01.1999	02.03.1999
BOCKFLIESS 079	72	15	0,0259	09.07.1996	29.08.1996
BOCKFLIESS 081	73	18	0,1798	07.06.1995	16.08.1995
BOCKFLIESS 081	74	29	0,4098	09.07.1996	29.08.1996
BOCKFLIESS 081	75	35	0,9256	16.01.1996	05.03.1996
BOCKFLIESS 089	76	33	0,0027	22.07.1997	17.09.1997
BOCKFLIESS 091	77	28,4	0,0008	24.02.1994	28.04.1994

BOCKFLIESS 104	78	17	0,004	18.05.1993	21.07.1993
BOCKFLIESS 109	79	30	0,0054	16.06.1998	25.08.1998
BOCKFLIESS 112	80	28,1	2,1675	24.02.1994	28.04.1994
BOCKFLIESS 115a	81	20	0,0034	09.07.1996	29.08.1996
BOCKFLIESS 118	82	15	0,0023	16.01.1996	05.03.1996
BOCKFLIESS 119	83	25	0,0015	24.02.1994	27.04.1994
BOCKFLIESS 121	84	45,6	0,0017	24.02.1994	28.04.1994
BOCKFLIESS 122	85	21	0,0525	08.06.1999	10.08.1999
BOCKFLIESS 126	86	16,3	0,0043	24.02.1994	27.04.1994
BOCKFLIESS 130	87	25	0,0221	16.06.1998	25.08.1998
BOCKFLIESS 133	88	41	0,002	19.05.1993	21.07.1993
BOCKFLIESS 134	89	10	0,145	22.07.1997	17.09.1997
BOCKFLIESS 137	90	50	0,003	14.09.1995	09.11.1995
BOCKFLIESS 139	91	19	0,102	18.05.1993	21.07.1993
BOCKFLIESS 139	92	58	0,0076	26.07.1994	23.09.1994
BOCKFLIESS 139	93	64	0,0191	14.09.1995	09.11.1995
BOCKFLIESS 144	94	75	0,0018	16.01.1996	05.03.1996
BOCKFLIESS 149	95	49	0,009	18.05.1993	21.07.1993
BOCKFLIESS 152	96	14	0,001	24.02.1994	28.04.1994
BOCKFLIESS 157	97	64,3	0,0012	24.02.1994	29.04.1994
BOCKFLIESS 160	98	100	0,0012	07.06.1995	16.08.1995
BOCKFLIESS 165	99	27	0,0654	09.07.1996	29.08.1996
BOCKFLIESS 178	100	35,4	0,0044	24.02.1994	29.04.1994
BOCKFLIESS T 002	101	23	0,9976	14.09.1995	09.11.1995
BOCKFLIESS T 002	102	55	0,0027	26.07.1994	23.09.1994
BOCKFLIESS T 002	103	80	0,0093	07.01.1999	02.03.1999
HOCHLEITEN 003	104	25	0,0014	30.01.1997	19.03.1997
HOCHLEITEN 012	105	25	0,0019	30.01.1997	19.03.1997
HOCHLEITEN 032	106	25	0,0007	30.01.1997	19.03.1997
HOCHLEITEN 045	107	50	0,0313	10.07.1996	02.09.1996
HOCHLEITEN 050	108	25	0,0046	10.07.1996	02.09.1996
MATZEN 052	109	353	0,002	19.05.1993	21.07.1993
MATZEN 092	110	22	0,0023	29.01.1997	20.03.1997
MATZEN 153	111	20	0,0049	07.06.1995	16.08.1995
MATZEN 157	112	25	0,0623	09.07.1996	29.08.1996
MATZEN 159	113	19	0,0043	08.06.1999	10.08.1999
MATZEN 160	114	20	0,0014	07.06.1995	16.08.1995
MATZEN 161	115	23,8	0,0008	25.02.1994	29.04.1994
MATZEN 185	116	51	0,002	08.06.1999	10.08.1999
MATZEN 197	117	37	0,0023	29.01.1997	29.01.1997
MATZEN 201	118	43	0,0036	05.02.1997	07.04.1997
MATZEN 222	119	19	0,0021	07.01.1999	02.03.1999
MATZEN 223	120	25	0,1342	16.01.1996	05.03.1996
MATZEN 284	121	18	0,1143	14.09.1995	09.11.1995
MATZEN 284	122	27	0,0143	16.06.1998	25.08.1998

MATZEN 291	123	25,3	0,0069	25.02.1994	29.04.1994
MATZEN 300	124	26,6	0,001	25.02.1994	02.05.1994
MATZEN 312	125	20	0,0041	07.06.1995	16.08.1995
MATZEN 339	126	25	0,0016	08.06.1999	10.08.1999
MATZEN 357	127	15	0,0026	08.06.1999	10.08.1999
MATZEN 360	128	34,4	0,0027	25.02.1994	02.05.1994
MATZEN 379	129	45	0,0011	07.06.1995	16.08.1995
MATZEN 417	130	25	0,002	19.05.1993	21.07.1993
MATZEN 434	131	28	0,015	19.05.1993	21.07.1993
MATZEN 452	132	81	0,0012	07.06.1995	16.08.1995
MATZEN 504	133	16	0,0175	29.01.1997	20.03.1997
PROTTES 029	134	17	0,0377	23.01.1996	18.03.1996
PROTTES 037	135	23	0,0193	18.01.1996	07.03.1996
PROTTES 049	136	59	0,0266	12.07.1996	04.09.1996
PROTTES 065	137	23,1	3,15	08.06.1995	08.08.1995
PROTTES 080	138	59	0,0031	11.07.1996	04.09.1996
PROTTES 095	139	52	0,056	30.01.1997	19.03.1997
PROTTES 095	140	74	1,1441	11.07.1996	04.09.1996
PROTTES 096	141	37	0,0024	18.01.1996	07.03.1996
PROTTES 103	142	24	0,0052	17.01.1996	07.03.1996
SCHOENKIRCHEN 008	143	61	0,003	05.02.1997	07.04.1997
SCHOENKIRCHEN 019	144	24	0,007	14.06.1995	16.08.1995
SCHOENKIRCHEN 025	145	27	0,3327	25.07.1996	04.09.1996
SCHOENKIRCHEN 049	146	23	0,0072	23.01.1996	18.03.1996
SCHOENKIRCHEN 052	147	32,9	0,0016	08.06.1995	08.08.1995
SCHOENKIRCHEN 053	148	29	0,9555	18.01.1996	07.03.1996
SCHOENKIRCHEN 054	149	46,8	0,0082	08.06.1995	08.08.1995
SCHOENKIRCHEN 064	150	26	0,0027	14.06.1995	16.08.1995
SCHOENKIRCHEN 068	151	25	0,3805	17.01.1996	07.03.1996
SCHOENKIRCHEN 068	152	52	0,0074	11.07.1996	04.09.1996
SCHOENKIRCHEN 077	153	23	0,5491	14.06.1995	16.08.1995
SCHOENKIRCHEN 077	154	33	0,0136	23.01.1996	18.03.1996
SCHOENKIRCHEN 077	155	46	0,3395	25.07.1996	04.09.1996
SCHOENKIRCHEN 077	156	65	0,1582	05.02.1997	07.04.1997
SCHOENKIRCHEN 079	157	34	0,0382	25.07.1996	04.09.1996
SCHOENKIRCHEN 079	158	65	0,1582	05.02.1997	07.04.1997
SCHOENKIRCHEN 081	159	60	0,07	11.07.1996	04.09.1996
SCHOENKIRCHEN 082	160	36	0,0036	30.01.1997	19.03.1997
SCHOENKIRCHEN 082	161	51	0,651	12.07.1996	04.09.1996
SCHOENKIRCHEN 094	162	54	0,0033	05.02.1997	07.04.1997
SCHOENKIRCHEN 094	163	61	0,0165	25.07.1996	04.09.1996
SCHOENKIRCHEN 096	164	56	0,2642	11.07.1996	04.09.1996
SCHOENKIRCHEN 096	165	88	0,2249	30.01.1997	19.03.1997
SCHOENKIRCHEN 098	166	18	1,2369	23.01.1996	18.03.1996
SCHOENKIRCHEN 098	167	64	2,4341	25.07.1996	04.09.1996

SCHOENKIRCHEN 098	168	70	0,0469	05.02.1997	07.04.1997
SCHOENKIRCHEN 106	169	38	0,027	30.01.1997	19.03.1997
SCHOENKIRCHEN 106	170	40	0,1555	10.07.1996	04.09.1996
SCHOENKIRCHEN 116	171	23	0,0138	23.01.1996	18.03.1996
SCHOENKIRCHEN 119	172	31	0,4658	25.07.1996	04.09.1996
SCHOENKIRCHEN 119	173	55	0,0299	05.02.1997	07.04.1997
SCHOENKIRCHEN 126	174	56	0,0646	25.07.1996	04.09.1996
SCHOENKIRCHEN 126	175	106	0,0314	05.02.1997	07.04.1997
SCHOENKIRCHEN 138	176	45	0,0079	23.01.1996	18.03.1996
SCHOENKIRCHEN 192	177	34	0,0071	25.07.1996	04.09.1996
SCHOENKIRCHEN 195	178	21	0,0145	23.01.1996	18.03.1996
SCHOENKIRCHEN 196	179	25	0,0122	10.07.1996	04.09.1996
SCHOENKIRCHEN 196	180	40	0,0141	30.01.1997	19.03.1997
SCHOENKIRCHEN 211	181	46	0,004	25.07.1996	04.09.1996
SCHOENKIRCHEN 235	182	37	0,004	25.07.1996	04.09.1996
SCHOENKIRCHEN 254	183	43	0,0025	30.01.1997	19.03.1997
SCHOENKIRCHEN 286	184	39	0,0035	25.07.1996	04.09.1996
SCHOENKIRCHEN 287	185	32,4	0,0052	08.06.1995	08.08.1995
SCHOENKIRCHEN 303	186	17	0,0035	23.01.1996	18.03.1996
ST.ULRICH 094	187	42	0,0005	14.06.1995	17.08.1995
ST.ULRICH 284	188	40	0,0022	14.06.1995	17.08.1995

Data 2nd Installation

SONDENNAME	Well Number	Inhibitor 2.Installation [ppm]	2. Installation CR [mm/a]	2. Installation [date]	2. Installation Removal [date]
MATZEN 157	1	15	0,2305	05.03.1995	23.04.1996
SCHOENKIRCHEN 119	2	55	0,0118	18.03.1996	09.05.1996
BOCKFLIESS 069	3	25	0,2474	16.08.1995	03.10.1995
BOCKFLIESS 101	4	21	0,4487	17.09.1997	30.10.1997
PROTTES 095	5	69	0,3495	07.03.1996	25.04.1996
SCHOENKIRCHEN 098	6	24	0,0786	16.08.1995	17.10.1995
SCHOENKIRCHEN 194	7	43	0,3866	18.03.1996	09.05.1996
BOCKFLIESS 056	8	0	0,1805	28.04.1994	29.06.1994
BOCKFLIESS 165	9	50	0,0123	05.03.1995	23.04.1996
SCHOENKIRCHEN 065	10	0	0,006	08.08.1995	04.10.1995
MATZEN 168	11	15	0,0761	05.03.1995	23.04.1996
SCHOENKIRCHEN 196	12	0	0,0429	08.08.1995	04.10.1995
SCHOENKIRCHEN 096	13	46	0,2272	07.03.1996	25.04.1996
BOCKFLIESS 067	14	0	0,0505	23.09.1994	24.11.1994
PROTTES 094	15	0	0,0028	04.09.1996	23.10.1996
MATZEN 164	16	0	0,1816	17.09.1997	30.10.1997

SCHOENKIRCHEN 042	17	0	0,0076	08.08.1995	04.10.1995
MATZEN 154	18	0	0,0059	16.08.1995	03.10.1995
BOCKFLIESS 055	19	0	0,0065	09.11.1995	31.01.1996
BOCKFLIESS 031	20	0	0,0052	09.11.1995	31.01.1996
BOCKFLIESS 028	21	0	0,0069	17.09.1997	30.10.1997
BOCKFLIESS 028	22	0	0,0084	25.08.1998	13.10.1998
MATZEN 445	23	0	0,0288	02.05.1994	30.06.1994
SCHOENKIRCHEN 017	24	43	0,0051	16.08.1995	17.10.1995
BOCKFLIESS 095	25	0	0,0077	02.03.1999	19.04.1999
BOCKFLIESS 095	26	18	0,002	10.08.1999	05.10.1999
MATZEN 166	27	0	0,0045	25.08.1998	13.10.1998
BOCKFLIESS 140	28	0	0,004	29.08.1996	25.10.1996
BOCKFLIESS 120	29	0	0,0245	27.04.1994	29.06.1994
MATZEN 297	30	0	0,0041	05.03.1996	23.04.1996
SCHOENKIRCHEN 111	31	0	0,0125	07.03.1996	25.04.1996
SCHOENKIRCHEN 321	32	0	0	18.03.1996	09.05.1996
BOCKFLIESS 006a	33	0	0,0044	05.03.1995	23.04.1996
BOCKFLIESS 038	34	0	0,0104	02.03.1999	19.04.1999
BOCKFLIESS 083	35	0	0,0033	29.08.1996	25.10.1996
MATZEN 351	36	0	0,0133	09.11.1995	31.01.1996
MATZEN 083	37	0	0,0033	17.09.1997	30.10.1997
BOCKFLIESS 110	38	0	0,0039	17.09.1997	30.10.1997
MATZEN 285	39	0	0,0037	20.03.1997	21.05.1997
BOCKFLIESS 074	40	0	0,0126	09.11.1995	31.01.1996
MATZEN 195	41	0	0,0041	16.08.1995	03.10.1995
SCHOENKIRCHEN 078	42	0	0,0032	07.03.1996	25.04.1996
MATZEN 176	43	0	0,004	23.09.1994	24.11.1994
MATZEN 417	44	22	0,002	23.09.1994	24.11.1994
SCHOENKIRCHEN 111	45	45,2	0,0049	08.08.1995	04.10.1995
BOCKFLIESS 034	46	0	0,0128	05.03.1995	23.04.1996
BOCKFLIESS 059	47	5	0,0016	23.09.1994	24.11.1994
BOCKFLIESS 001	48	48	0,0174	02.03.1999	19.04.1999
BOCKFLIESS 005	49	32,6	0,0522	29.04.1994	30.06.1994
BOCKFLIESS 014	50	10	2,7218	09.11.1995	31.01.1996
BOCKFLIESS 025	51	18	0,003	21.07.1993	21.09.1993
BOCKFLIESS 030	52	13	0,0023	10.08.1999	05.10.1999
BOCKFLIESS 035	53	24	0,0027	02.03.1999	19.04.1999
BOCKFLIESS 036	54	22	0,0017	02.03.1999	19.04.1999
BOCKFLIESS 037	55	37	0,0023	10.08.1999	05.10.1999
BOCKFLIESS 041	56	28	0,0131	25.08.1998	13.10.1998
BOCKFLIESS 041	57	19	2,7419	09.11.1995	31.01.1996
BOCKFLIESS 045	58	30	0,0026	05.03.1995	23.04.1996
BOCKFLIESS 049	59	21,8	0,6369	27.04.1994	29.06.1994
BOCKFLIESS 051	60	24	0,0022	20.03.1997	21.05.1997
BOCKFLIESS 053	61	33	0,0095	20.03.1997	21.05.1997

BOCKFLIESS 061	62	24	0,0371	20.03.1997	21.05.1997
BOCKFLIESS 063	63	28	0,0021	10.08.1999	05.10.1999
BOCKFLIESS 064	64	31	0,0026	29.08.1996	25.10.1996
BOCKFLIESS 066	65	36	0,0024	25.08.1998	13.10.1998
BOCKFLIESS 067	66	34	0,0635	25.08.1998	13.10.1998
BOCKFLIESS 067	67	28	0,0388	09.11.1995	31.01.1996
BOCKFLIESS 068	68	37	0,0025	25.08.1998	13.10.1998
BOCKFLIESS 069	69	50	0,0145	05.03.1995	23.04.1996
BOCKFLIESS 073	70	70	0,0013	23.09.1994	24.11.1994
BOCKFLIESS 075	71	35	0,0014	02.03.1999	19.04.1999
BOCKFLIESS 079	72	28	0,0264	29.08.1996	25.10.1996
BOCKFLIESS 081	73	20	1,059	16.08.1995	03.10.1995
BOCKFLIESS 081	74	34	0,0757	29.08.1996	25.10.1996
BOCKFLIESS 081	75	20	0,7616	05.03.1995	23.04.1996
BOCKFLIESS 089	76	38	0,0027	17.09.1997	30.10.1997
BOCKFLIESS 091	77	28,4	0,0021	28.04.1994	29.06.1994
BOCKFLIESS 104	78	17	0,003	21.07.1993	21.09.1993
BOCKFLIESS 109	79	50	0,0079	25.08.1998	13.10.1998
BOCKFLIESS 112	80	28,1	0,4146	28.04.1994	29.06.1994
BOCKFLIESS 115a	81	20	0,004	29.08.1996	25.10.1996
BOCKFLIESS 118	82	15	0,0035	05.03.1995	23.04.1996
BOCKFLIESS 119	83	25	0,0029	27.04.1994	29.06.1994
BOCKFLIESS 121	84	45,6	0,0027	28.04.1994	29.06.1994
BOCKFLIESS 122	85	21	0,033	10.08.1999	05.10.1999
BOCKFLIESS 126	86	16,3	0,0016	27.04.1994	29.06.1994
BOCKFLIESS 130	87	35	0,0025	25.08.1998	13.10.1998
BOCKFLIESS 133	88	41	0,002	21.07.1993	21.09.1993
BOCKFLIESS 134	89	26	0,0231	17.09.1997	30.10.1997
BOCKFLIESS 137	90	50	0,0038	09.11.1995	31.01.1996
BOCKFLIESS 139	91	70	0,0289	09.11.1995	31.01.1996
BOCKFLIESS 139	92	19	0,03	21.07.1993	21.09.1993
BOCKFLIESS 139	93	55	0,0184	23.09.1994	24.11.1994
BOCKFLIESS 144	94	100	0,0024	05.03.1995	23.04.1996
BOCKFLIESS 149	95	49	0,005	21.07.1993	21.09.1993
BOCKFLIESS 152	96	14	0,0015	28.04.1994	29.06.1994
BOCKFLIESS 157	97	64,3	0,0055	29.04.1994	30.06.1994
BOCKFLIESS 160	98	60	0,0015	16.08.1995	03.10.1995
BOCKFLIESS 165	99	30	0,0327	29.08.1996	25.10.1996
BOCKFLIESS 178	100	35,4	0,0053	29.04.1994	30.06.1994
BOCKFLIESS T 002	101	63	0,0063	02.03.1999	19.04.1999
BOCKFLIESS T 002	102	70	0,002	23.09.1994	24.11.1994
BOCKFLIESS T 002	103	30	1,3753	09.11.1995	31.01.1996
HOCHLEITEN 003	104	25	0,003	19.03.1997	04.06.1997
HOCHLEITEN 012	105	25	0,0026	19.03.1997	04.06.1997
HOCHLEITEN 032	106	25	0,0089	19.03.1997	04.06.1997

HOCHLEITEN 045	107	50	0,0036	02.09.1996	23.10.1996
HOCHLEITEN 050	108	0	0	abg.Behandlung	
MATZEN 052	109	353	0,004	21.07.1993	21.09.1993
MATZEN 092	110	21	0,0021	20.03.1997	21.05.1997
MATZEN 153	111	18	0,0096	16.08.1995	03.10.1995
MATZEN 157	112	32	0,0354	29.08.1996	25.10.1996
MATZEN 159	113	24	0,0024	10.08.1999	05.10.1999
MATZEN 160	114	20	0,0022	16.08.1995	03.10.1995
MATZEN 161	115	23,8	0,0024	29.04.1994	30.06.1994
MATZEN 185	116	43	0,0025	10.08.1999	05.10.1999
MATZEN 197	117	46	0,0019	20.03.1997	21.05.1997
MATZEN 201	118	58	0,0032	07.04.1997	04.06.1997
MATZEN 222	119	15	0,0015	02.03.1999	19.04.1999
MATZEN 223	120	30	0,0218	05.03.1995	23.04.1996
MATZEN 284	121	26	0,0119	25.08.1998	13.10.1998
MATZEN 284	122	15	0,1283	09.11.1995	31.01.1996
MATZEN 291	123	25,3	0,2784	29.04.1994	30.06.1994
MATZEN 300	124	26,6	0,0036	02.05.1994	30.06.1994
MATZEN 312	125	28	0,0015	16.08.1995	03.10.1995
MATZEN 339	126	29	0,0023	10.08.1999	05.10.1999
MATZEN 357	127	17	0,0027	10.08.1999	05.10.1999
MATZEN 360	128	34,4	0,0066	02.05.1994	30.06.1994
MATZEN 379	129	45	0,0016	16.08.1995	03.10.1995
MATZEN 417	130	25	0,002	21.07.1993	21.09.1993
MATZEN 434	131	28	0,006	21.07.1993	21.09.1993
MATZEN 452	132	80	0,0024	16.08.1995	03.10.1995
MATZEN 504	133	15	0,0214	20.03.1997	21.05.1997
PROTTES 029	134	34	0,01872	18.03.1996	09.05.1996
PROTTES 037	135	47	0,0114	07.03.1996	25.04.1996
PROTTES 049	136	60	0,0115	04.09.1996	23.10.1996
PROTTES 065	137	36	0,0025	08.08.1995	04.10.1995
PROTTES 080	138	59	0,0027	04.09.1996	23.10.1996
PROTTES 095	139	67	0,3123	19.03.1997	04.06.1997
PROTTES 095	140	35	0,8668	04.09.1996	23.10.1996
PROTTES 096	141	73	0,0032	07.03.1996	25.04.1996
PROTTES 103	142	47	0,0027	07.03.1996	25.04.1996
SCHOENKIRCHEN 008	143	71	0,0048	07.04.1997	04.06.1997
SCHOENKIRCHEN 019	144	21,1	0,0066	16.08.1995	17.10.1995
SCHOENKIRCHEN 025	145	29	0,19	04.09.1996	11.11.1996
SCHOENKIRCHEN 049	146	45	0,0355	18.03.1996	09.05.1996
SCHOENKIRCHEN 052	147	40	0,001	08.08.1995	04.10.1995
SCHOENKIRCHEN 053	148	78	0,2357	07.03.1996	25.04.1996
SCHOENKIRCHEN 054	149	34	0,0175	08.08.1995	04.10.1995
SCHOENKIRCHEN 064	150	22	0,0012	16.08.1995	17.10.1995
SCHOENKIRCHEN 068	151	59	0,2378	07.03.1996	25.04.1996

SCHOENKIRCHEN 068	152	113	0,0031	04.09.1996	23.10.1996
SCHOENKIRCHEN 077	153	64	0,0618	07.04.1997	04.06.1997
SCHOENKIRCHEN 077	154	65	0,5065	18.03.1996	09.05.1996
SCHOENKIRCHEN 077	155	47	0,2621	04.09.1996	11.11.1996
SCHOENKIRCHEN 077	156	33	0,2645	16.08.1995	17.10.1995
SCHOENKIRCHEN 079	157	45	0,1169	07.04.1997	04.06.1997
SCHOENKIRCHEN 079	158	33	0,1766	04.09.1996	11.11.1996
SCHOENKIRCHEN 081	159	62	0,014	04.09.1996	23.10.1996
SCHOENKIRCHEN 082	160	37	0,4672	04.09.1996	23.10.1996
SCHOENKIRCHEN 082	161	34	0,0328	19.03.1997	04.06.1997
SCHOENKIRCHEN 094	162	53	0,0483	07.04.1997	04.06.1997
SCHOENKIRCHEN 094	163	71	0,0144	04.09.1996	11.11.1996
SCHOENKIRCHEN 096	164	116	0,0069	19.03.1997	04.06.1997
SCHOENKIRCHEN 096	165	130	0,1515	04.09.1996	23.10.1996
SCHOENKIRCHEN 098	166	90	0,84	18.03.1996	09.05.1996
SCHOENKIRCHEN 098	167	66	0,2186	04.09.1996	11.11.1996
SCHOENKIRCHEN 098	168	61	0,0047	07.04.1997	04.06.1997
SCHOENKIRCHEN 106	169	32	0,0033	04.09.1996	23.10.1996
SCHOENKIRCHEN 106	170	33	0,0586	19.03.1997	04.06.1997
SCHOENKIRCHEN 116	171	72	0,0237	18.03.1996	09.05.1996
SCHOENKIRCHEN 119	172	60	0,0808	07.04.1997	04.06.1997
SCHOENKIRCHEN 119	173	36	0,9878	04.09.1996	11.11.1996
SCHOENKIRCHEN 126	174	57	0,2023	04.09.1996	11.11.1996
SCHOENKIRCHEN 126	175	113	0,0104	07.04.1997	04.06.1997
SCHOENKIRCHEN 138	176	50	0,0202	18.03.1996	09.05.1996
SCHOENKIRCHEN 192	177	34	0,003	04.09.1996	11.11.1996
SCHOENKIRCHEN 195	178	55	0,0252	18.03.1996	09.05.1996
SCHOENKIRCHEN 196	179	38	0,0502	19.03.1997	04.06.1997
SCHOENKIRCHEN 196	180	30	0,0099	04.09.1996	23.10.1996
SCHOENKIRCHEN 211	181	28	0,0022	04.09.1996	11.11.1996
SCHOENKIRCHEN 235	182	58	0,0111	04.09.1996	11.11.1996
SCHOENKIRCHEN 254	183	43	0,0025	19.03.1997	04.06.1997
SCHOENKIRCHEN 286	184	48	0,002	04.09.1996	11.11.1996
SCHOENKIRCHEN 287	185	30	0,0027	08.08.1995	04.10.1995
SCHOENKIRCHEN 303	186	65	0,0117	18.03.1996	09.05.1996
ST.ULRICH 094	187	42	0,001	17.08.1995	17.10.1995
ST.ULRICH 284	188	40	0,0039	17.08.1995	17.10.1995

Data 3rd Installation

SONDENNAME	Well Number	Inhibitor 3.Installation [ppm]	3. Installation CR [mm/a]	3. Installation [date]	3. Installation Removal [date]
MATZEN 157	1	7	0,0205	23.04.1996	11.06.1996
SCHOENKIRCHEN 119	2	33	0,1195	09.05.1996	24.06.1996
BOCKFLIESS 069	3	35	0,0041	03.10.1995	30.11.1995
BOCKFLIESS 101	4	21	0,0042	30.10.1997	09.12.1997
PROTTES 095	5	73	0,1498	25.04.1996	18.06.1996
SCHOENKIRCHEN 098	6	25	0,0013	17.10.1995	06.12.1996
SCHOENKIRCHEN 194	7	85	0,0117	09.05.1996	24.06.1996
BOCKFLIESS 056	8	38,4	0,0019	29.06.1994	01.09.1994
BOCKFLIESS 165	9	35	0,0639	23.04.1996	11.06.1996
SCHOENKIRCHEN 065	10	24	0,0006	04.10.1995	06.12.1995
MATZEN 168	11	16	0,0046	23.04.1996	11.06.1996
SCHOENKIRCHEN 196	12	0	0,0008	04.10.1995	06.12.1995
SCHOENKIRCHEN 096	13	46	0,816	25.04.1996	18.06.1996
BOCKFLIESS 067	14	0	0,5319	24.11.1994	25.01.1995
PROTTES 094	15	0	0,0038	23.10.1996	11.12.1996
MATZEN 164	16	0	0,3252	30.10.1997	09.12.1997
SCHOENKIRCHEN 042	17	0	0,0119	04.10.1995	06.12.1995
MATZEN 154	18	23	0,0165	03.10.1995	30.11.1995
BOCKFLIESS 055	19	0	0,0065	31.01.1996	26.03.1996
BOCKFLIESS 031	20	0	0,0126	31.01.1996	26.03.1996
BOCKFLIESS 028	21	0	0,0056	30.10.1997	09.12.1997
BOCKFLIESS 028	22	0	0,0038	13.10.1998	14.12.1998
MATZEN 445	23	0	0,0176	30.06.1994	31.08.1994
SCHOENKIRCHEN 017	24	43	0,0013	17.10.1995	06.12.1996
BOCKFLIESS 095	25	0	0,2233	19.04.1999	11.06.1999
BOCKFLIESS 095	26	22,5	0,002	05.10.1999	17.12.1999
MATZEN 166	27	0	0,0027	13.10.1998	14.12.1998
BOCKFLIESS 140	28	0	0,0027	25.10.1996	11.12.1996
BOCKFLIESS 120	29	0	0,0017	29.06.1994	01.09.1994
MATZEN 297	30	0	0,0046	23.04.1996	11.06.1996
SCHOENKIRCHEN 111	31	0	0	Packereinbau	
SCHOENKIRCHEN 321	32	0	0	nicht eingeb.	
BOCKFLIESS 006a	33	0	0,0072	23.04.1996	11.06.1996
BOCKFLIESS 038	34	0	0,009	19.04.1999	11.06.1999
BOCKFLIESS 083	35	0	0,0017	25.10.1996	11.12.1996
MATZEN 351	36	0	0,0077	31.01.1996	26.03.1996
MATZEN 083	37	0	0,0052	30.10.1997	09.12.1997
BOCKFLIESS 110	38	0	0,0039	30.10.1997	09.12.1997

MATZEN 285	39	0	0,0038	21.05.1997	30.06.1997
BOCKFLIESS 074	40	0	0,0052	31.01.1996	26.03.1996
MATZEN 195	41	0	0,0056	03.10.1995	30.11.1995
SCHOENKIRCHEN 078	42	52	0,0034	25.04.1996	18.06.1996
MATZEN 176	43	0	0,0036	24.11.1994	25.01.1995
MATZEN 417	44	39	0,001	24.11.1994	25.01.1995
SCHOENKIRCHEN 111	45	0	0,0372	04.10.1995	06.12.1995
BOCKFLIESS 034	46	0	0,0076	23.04.1996	11.06.1996
BOCKFLIESS 059	47	0	0,0015	24.11.1994	25.01.1995
BOCKFLIESS 001	48	50	0,0332	19.04.1999	11.06.1999
BOCKFLIESS 005	49	43,6	0,016	30.06.1994	31.08.1994
BOCKFLIESS 014	50	12	0,2276	31.01.1996	26.03.1996
BOCKFLIESS 025	51	18	0,0033	21.09.1993	23.11.1993
BOCKFLIESS 030	52	29,5	0,0025	05.10.1999	17.12.1999
BOCKFLIESS 035	53	23	0,0025	19.04.1999	11.06.1999
BOCKFLIESS 036	54	24	0,003	19.04.1999	11.06.1999
BOCKFLIESS 037	55	22	0,0107	05.10.1999	17.12.1999
BOCKFLIESS 041	56	33	0,0098	13.10.1998	14.12.1998
BOCKFLIESS 041	57	25	0,1759	31.01.1996	26.03.1996
BOCKFLIESS 045	58	33	0,0034	23.04.1996	11.06.1996
BOCKFLIESS 049	59	26,5	0,0041	29.06.1994	01.09.1994
BOCKFLIESS 051	60	31	0,0124	21.05.1997	30.06.1997
BOCKFLIESS 053	61	34	0,0103	21.05.1997	30.06.1997
BOCKFLIESS 061	62	31	0,0182	21.05.1997	30.06.1997
BOCKFLIESS 063	63	32	0,0023	05.10.1999	17.12.1999
BOCKFLIESS 064	64	31	0,0016	25.10.1996	11.12.1996
BOCKFLIESS 066	65	35	0,0013	13.10.1998	14.12.1998
BOCKFLIESS 067	66	35	0,0268	13.10.1998	14.12.1998
BOCKFLIESS 067	67	27	0,3086	31.01.1996	26.03.1996
BOCKFLIESS 068	68	40	0,0023	13.10.1998	14.12.1998
BOCKFLIESS 069	69	46	0,0097	23.04.1996	11.06.1996
BOCKFLIESS 073	70	40	0,0011	24.11.1994	25.01.1995
BOCKFLIESS 075	71	33	0,0022	19.04.1999	11.06.1999
BOCKFLIESS 079	72	34	0,002	25.10.1996	11.12.1996
BOCKFLIESS 081	73	40	0,0915	03.10.1995	30.11.1995
BOCKFLIESS 081	74	37	0,0303	25.10.1996	11.12.1996
BOCKFLIESS 081	75	35	0,0314	23.04.1996	11.06.1996
BOCKFLIESS 089	76	36	0,0028	30.10.1997	09.12.1997
BOCKFLIESS 091	77	32,5	0,0008	29.06.1994	01.09.1994
BOCKFLIESS 104	78	17	0,0008	21.09.1993	23.11.1993
BOCKFLIESS 109	79	57	0,0031	13.10.1998	14.12.1998
BOCKFLIESS 112	80	37,9	0,01683	29.06.1994	01.09.1994
BOCKFLIESS 115a	81	19	0,0016	25.10.1996	11.12.1996
BOCKFLIESS 118	82	17	0,0036	23.04.1996	11.06.1996
BOCKFLIESS 119	83	27,6	0,0062	29.06.1994	01.09.1994

BOCKFLIESS 121	84	41	0,002	29.06.1994	01.09.1994
BOCKFLIESS 122	85	51	0,0172	05.10.1999	17.12.1999
BOCKFLIESS 126	86	18,7	0,0004	29.06.1994	01.09.1994
BOCKFLIESS 130	87	25	0,0017	13.10.1998	14.12.1998
BOCKFLIESS 133	88	41	0,0027	21.09.1993	23.11.1993
BOCKFLIESS 134	89	42	0,035	30.10.1997	09.12.1997
BOCKFLIESS 137	90	52	0,0092	31.01.1996	26.03.1996
BOCKFLIESS 139	91	65	0,0097	31.01.1996	26.03.1996
BOCKFLIESS 139	92	50	0,0017	21.09.1993	23.11.1993
BOCKFLIESS 139	93	48	0,0713	24.11.1994	25.01.1995
BOCKFLIESS 144	94	70	0,0036	23.04.1996	11.06.1996
BOCKFLIESS 149	95	49	0,0069	21.09.1993	23.11.1993
BOCKFLIESS 152	96	42,5	0,0009	29.06.1994	01.09.1994
BOCKFLIESS 157	97	69,2	0,0016	30.06.1994	31.08.1994
BOCKFLIESS 160	98	50	0,0012	03.10.1995	30.11.1995
BOCKFLIESS 165	99	40	0,0229	25.10.1996	11.12.1996
BOCKFLIESS 178	100	44,7	0,007	30.06.1994	31.08.1994
BOCKFLIESS T 002	101	60	0,0257	19.04.1999	11.06.1999
BOCKFLIESS T 002	102	50	0,0012	24.11.1994	25.01.1995
BOCKFLIESS T 002	103	49	0,351	31.01.1996	26.03.1996
HOCHLEITEN 003	104	26	0,0028	04.06.1997	09.07.1997
HOCHLEITEN 012	105	25	0,0198	04.06.1997	09.07.1997
HOCHLEITEN 032	106	25	0,0135	04.06.1997	09.07.1997
HOCHLEITEN 045	107	51	0,029	23.10.1996	11.12.1996
HOCHLEITEN 050	108	0	0		
MATZEN 052	109	353	0,0006	21.09.1993	23.11.1993
MATZEN 092	110	20	0,0033	21.05.1997	30.06.1997
MATZEN 153	111	15	0,0083	03.10.1995	30.11.1995
MATZEN 157	112	19	0,0233	25.10.1996	11.12.1996
MATZEN 159	113	24	0,0059	05.10.1999	17.12.1999
MATZEN 160	114	24	0,0015	03.10.1995	30.11.1995
MATZEN 161	115	24,7	0,0017	30.06.1994	31.08.1994
MATZEN 185	116	46	0,0027	05.10.1999	17.12.1999
MATZEN 197	117	58	0,0028	21.05.1997	30.06.1997
MATZEN 201	118	71	0,0031	04.06.1997	09.07.1997
MATZEN 222	119	15	0,0029	19.04.1999	11.06.1999
MATZEN 223	120	25	0,0114	23.04.1996	11.06.1996
MATZEN 284	121	25	0,0125	13.10.1998	14.12.1998
MATZEN 284	122	17	0,1481	31.01.1996	26.03.1996
MATZEN 291	123	17,6	0,0179	30.06.1994	31.08.1994
MATZEN 300	124	17,5	0,0036	30.06.1994	30.08.1994
MATZEN 312	125	22	0,0031	03.10.1995	30.11.1995
MATZEN 339	126	25	0,0019	05.10.1999	17.12.1999
MATZEN 357	127	14	0,0023	05.10.1999	17.12.1999
MATZEN 360	128	27,6	0,0021	30.06.1994	30.08.1994

MATZEN 379	129	40	0,0011	03.10.1995	30.11.1995
MATZEN 417	130	25	0,012	21.09.1993	23.11.1993
MATZEN 434	131	28	0,0016	21.09.1993	23.11.1993
MATZEN 452	132	50	0,0036	03.10.1995	30.11.1995
MATZEN 504	133	23	0,0157	21.05.1997	30.06.1997
PROTTES 029	134	35	0,0651	09.05.1996	24.06.1996
PROTTES 037	135	48	0,0232	25.04.1996	18.06.1996
PROTTES 049	136	62	0,0187	23.10.1996	11.12.1996
PROTTES 065	137	38	0,0019	04.10.1995	06.12.1995
PROTTES 080	138	60	0,0016	23.10.1996	11.12.1996
PROTTES 095	139	68	0,1086	04.06.1997	09.07.1997
PROTTES 095	140	37	0,0927	23.10.1996	11.12.1996
PROTTES 096	141	53	0,0028	25.04.1996	18.06.1996
PROTTES 103	142	42	0,0067	25.04.1996	18.06.1996
SCHOENKIRCHEN 008	143	107	0,0052	04.06.1997	08.07.1997
SCHOENKIRCHEN 019	144	22	0,0047	17.10.1995	06.12.1996
SCHOENKIRCHEN 025	145	31	0,0372	11.11.1996	17.12.1996
SCHOENKIRCHEN 049	146	44	0,0103	09.05.1996	24.06.1996
SCHOENKIRCHEN 052	147	31	0,0016	04.10.1995	06.12.1995
SCHOENKIRCHEN 053	148	78	0,0062	25.04.1996	18.06.1996
SCHOENKIRCHEN 054	149	30	0,0069	04.10.1995	06.12.1995
SCHOENKIRCHEN 064	150	24	0,018	17.10.1995	06.12.1996
SCHOENKIRCHEN 068	151	82	0,0639	25.04.1996	18.06.1996
SCHOENKIRCHEN 068	152	59	0,0058	23.10.1996	11.12.1996
SCHOENKIRCHEN 077	153	71	0,01	04.06.1997	08.07.1997
SCHOENKIRCHEN 077	154	65	0,1437	09.05.1996	24.06.1996
SCHOENKIRCHEN 077	155	59	0,2894	11.11.1996	17.12.1996
SCHOENKIRCHEN 077	156	33	0,1692	17.10.1995	06.12.1996
SCHOENKIRCHEN 079	157	49	0,0282	04.06.1997	08.07.1997
SCHOENKIRCHEN 079	158	47	0,5797	11.11.1996	17.12.1996
SCHOENKIRCHEN 081	159	68	0,0405	23.10.1996	11.12.1996
SCHOENKIRCHEN 082	160	38	0,067	23.10.1996	11.12.1996
SCHOENKIRCHEN 082	161	34	0,1845	04.06.1997	08.07.1997
SCHOENKIRCHEN 094	162	75	0,023	04.06.1997	08.07.1997
SCHOENKIRCHEN 094	163	65	0,0213	11.11.1996	17.12.1996
SCHOENKIRCHEN 096	164	127	0,0147	04.06.1997	08.07.1997
SCHOENKIRCHEN 096	165	78	0,218	23.10.1996	11.12.1996
SCHOENKIRCHEN 098	166	100	0,1784	09.05.1996	24.06.1996
SCHOENKIRCHEN 098	167	67	0,3555	11.11.1996	17.12.1996
SCHOENKIRCHEN 098	168	64	0,2049	04.06.1997	08.07.1997
SCHOENKIRCHEN 106	169	36	0,0556	23.10.1996	11.12.1996
SCHOENKIRCHEN 106	170	35	0,0165	04.06.1997	08.07.1997
SCHOENKIRCHEN 116	171	32	0,0063	09.05.1996	24.06.1996
SCHOENKIRCHEN 119	172	62	0,0177	23.06.1997	08.07.1997
SCHOENKIRCHEN 119	173	37	1,2348	11.11.1996	17.12.1996

SCHOENKIRCHEN 126	174	78	0,1826	11.11.1996	17.12.1996
SCHOENKIRCHEN 126	175	70	0,0329	04.06.1997	08.07.1997
SCHOENKIRCHEN 138	176	89	0,0091	09.05.1996	24.06.1996
SCHOENKIRCHEN 192	177	33	0,0072	11.11.1996	17.12.1996
SCHOENKIRCHEN 195	178	42	0,0249	09.05.1996	24.06.1996
SCHOENKIRCHEN 196	179	38	0,0327	04.06.1997	09.07.1997
SCHOENKIRCHEN 196	180	29	0,051	23.10.1996	11.12.1996
SCHOENKIRCHEN 211	181	33	0,003	11.11.1996	17.12.1996
SCHOENKIRCHEN 235	182	42	0,0059	11.11.1996	17.12.1996
SCHOENKIRCHEN 254	183	34	0,0035	04.06.1997	08.07.1997
SCHOENKIRCHEN 286	184	41	0,0023	11.11.1996	17.12.1996
SCHOENKIRCHEN 287	185	54	0,0027	04.10.1995	06.12.1995
SCHOENKIRCHEN 303	186	36	0,0036	09.05.1996	24.06.1996
ST.ULRICH 094	187	73	0,0016	17.10.1995	06.12.1996
ST.ULRICH 284	188	37	0,0034	17.10.1995	06.12.1996

Data Downhole Measurement and Deviations

Well Number	DH Installation [date]	DH Removal [date]	Downhole CR [mm/a]	Deviation 1 [Downhole CR/Surface1]	Deviation 2 [Downhole CR/Surface2]	Deviation 3 [Downhole CR/Surface3]
1	15.10.1990	12.04.1991	0,10942675	0,051910224	0,474736449	5,337890322
2	27.05.1994	25.07.1995	0,02955414	0,031843702	2,504588146	0,24731498
3	09.12.1992	03.02.1994	0,07961783	0,091895007	0,321818247	19,418984
4	17.01.1991	28.07.1995	0,00458599	0,007073866	0,010220609	1,091901729
5	24.08.1995	23.07.1997	0,08458599	0,132289627	0,242019992	0,564659461
6	06.11.1995	05.05.1997	0,14127389	0,447777767	1,797377676	108,6722195
7	27.04.1995	02.10.1995	0,34343949	1,166970746	0,888358744	29,3538026
8	06.02.1991	02.02.1994	0,01299363	0,083883993	0,071986873	6,838752933
9	11.02.1993	28.06.1993	0,12076433	0,857701216	9,81823831	1,889895637
10	16.06.1994	25.02.1997	0,09426752	0,76083548	15,71125265	157,1125265
11	05.07.1993	18.11.1996	0,00343949	0,029830793	0,045196984	0,747715314
12	22.03.1994	23.02.1995	0,1489172	2,246111575	3,471263344	186,1464968
13	09.04.1996	03.02.1998	0,01477707	0,335842501	0,065039921	0,018109154
14	14.06.1994	25.01.1995	0,44764331	13,90196621	8,864224002	0,841592991
15	30.11.1995	23.05.1997	0,01503185	0,677110231	5,368516833	3,955749246
16	20.06.1995	15.11.1995	0,09044586	4,997008833	0,498049889	0,2781238
17	24.04.1991	26.07.1991	0,30471338	20,31422505	40,09386524	25,60616603
18	10.11.1993	12.09.1994	0,29783439	21,73973685	50,48040592	18,05056939
19	08.10.1991	12.12.1996	0,0166879	1,668789809	2,567368937	2,567368937
20	20.04.1995	14.04.1998	0,01541401	1,675436167	2,964233219	1,223334344
21				0	0	0
22	09.12.1987	05.08.1992	0,0555414	6,773341619	6,61207158	14,61615823

23	08.06.1993	12.05.1995	0,1666242	20,82802548	5,785562633	9,467284308
24	19.09.1994	20.09.1995	0,05388535	7,381554838	10,56575496	41,45026948
25				0	0	0
26	17.02.1992	25.06.1996	0,05936306	37,10191083	29,68152866	29,68152866
27	19.01.1988	04.01.1995	0,00152866	0,218380346	0,33970276	0,566171267
28	13.05.1992	23.07.1993	0,00993631	1,874774667	2,484076433	3,680113234
29	27.03.1991	17.10.1997	0,01477707	2,841744243	0,603145717	8,692394155
30	20.12.1990	16.12.1996	0,0044586	0,990799717	1,087463104	0,969260593
31	19.06.1996	07.01.1998	0,02547771	5,925048141	2,038216561	
32	04.01.1993	16.06.1993	0,03299363	7,855626327		
33	05.10.1987	13.06.1990	0,08471338	20,66179897	19,25303995	11,76574664
34	31.03.1993	19.05.1993	0,01719745	4,409603136	1,653601176	1,910828025
35	13.08.1992	31.10.1995	0,00585987	1,54207174	1,775718973	3,446983889
36	15.10.1991	26.06.1995	0,00165605	0,48707381	0,124515109	0,215071553
37	31.01.1991	13.10.1993	0,00611465	1,798426377	1,852924146	1,17589417
38	14.12.1990	05.05.1992	0,00496815	1,505500869	1,27388535	1,27388535
39	17.06.1986	14.06.1993	0,00267516	0,835987261	0,72301601	0,703989273
40	04.07.1989	04.01.1993	0,06025478	20,08492569	4,782125164	11,58745713
41	20.11.1996	06.11.1997	0,02726115	9,400395344	6,649060121	4,868061874
42	24.04.1996	14.11.1997	0,02942675	11,77070064	9,195859873	8,654926939
43	25.06.1992	18.08.1993	0,32840764	156,3845921	82,10191083	91,22434536
44	24.11.1995	02.07.1996	0,00280255	1,751592357	1,401273885	2,802547771
45				0	0	0
46	02.02.1993	18.02.1993	0,05261146	6,92256118	4,110270701	6,92256118
47	28.08.1995	05.07.1996	0,04700637	0,352107636	29,37898089	31,33757962
48	23.06.1995	14.05.1998	0,00802548	0,827368836	0,461234351	0,241731256
49	10.01.1991	03.01.1996	0,00394904	1,462609106	0,075652195	0,246815287
50	03.03.1995	07.09.1995	0,03452229	8,630573248	0,012683626	0,15167967
51	08.01.1991	15.05.1992	0,4011465	200,5732484	133,7154989	121,5595445
52	28.05.1979	17.07.1992	0,00025478	0,149868865	0,110772639	0,101910828
53	21.03.1988	05.07.1996	0,02242038	5,605095541	8,303845247	8,968152866
54	02.12.1987	20.03.1992	0,05910828	21,89195565	34,76957662	19,70276008
55	13.12.1988	11.04.1995	0,06	31,57894737	26,08695652	5,607476636
56				0	0	0
57	26.08.1993	11.09.1995	0,00165605	0,011596995	0,000603979	0,00941473
58	18.04.1995	20.02.1997	0,01184713	3,702229299	4,556589907	3,484451105
59	11.10.1993	14.01.1994	0,08420382	0,023388001	0,132208858	20,53751748
60	06.12.1991	31.05.1996	0,07974522	8,394233993	36,2478286	6,431066365
61	21.03.1990	02.06.1992	0,0011465	0,220480157	0,120683875	0,11131037
62	05.10.1993	20.08.1996	0,00522293	0,050708058	0,140779783	0,286974172
63	19.10.1995	17.11.1995	0,03630573	17,28844404	17,28844404	15,78510108
64	28.02.1993	25.06.1998	0,01095541	2,883003688	4,213620774	6,847133758
65	22.05.1986	01.04.1992	0,00216561	0,408604735	0,902335456	1,665850073
66				0	0	0
67				0	0	0

68	16.02.1993	25.03.1993	0,03694268	7,539321461	14,77707006	16,06203268
69				0	0	0
70	15.05.1991	11.03.1992	0,12318471	72,4615961	94,75747183	111,9861031
71	21.12.1994	14.01.1998	0,0166879	9,271054494	11,91992721	7,585408222
72	14.12.1990	01.08.1994	0,04866242	1,87885793	1,843273499	24,33121019
73				0	0	0
74				0	0	0
75	02.07.1991	17.06.1996	0,00382166	0,004128842	0,005017931	0,121708791
76	11.04.1988	26.06.1990	0,05171975	19,15546119	19,15546119	18,47133758
77	12.09.1989	16.11.1990	0,46280255	578,5031847	220,3821656	578,5031847
78	28.06.1989	07.06.1990	0,31171975	77,92993631	103,9065817	389,6496815
79	22.03.1996	30.01.1998	0,01146497	2,123142251	1,451261792	3,698376824
80	10.02.1993	18.04.1995	0,08050955	0,03714397	0,194186093	4,783693056
81	19.12.1994	17.03.1998	0,00573248	1,686024728	1,433121019	3,582802548
82	11.11.1991	20.03.1995	0,13452229	58,48795348	38,43494086	37,36730361
83	07.08.1990	21.11.1995	0,03324841	22,1656051	11,46496815	5,362646394
84	25.05.1992	19.03.1998	0,00356688	2,098164106	1,321066289	1,78343949
85	10.06.1986	27.06.1990	0,00292994	0,055808311	0,088785949	0,170345134
86	30.06.1994	19.12.1996	0,00433121	1,007258184	2,707006369	10,82802548
87	17.06.1993	12.06.1996	0,08140127	3,68331556	32,56050955	47,88310229
88	04.01.1996	28.02.1997	0,00229299	1,146496815	1,146496815	0,8492569
89	17.07.1992	20.09.1994	0,060115	0,414586207	2,602380952	1,717571429
90	29.10.1991	24.10.1994	0,0677707	22,59023355	17,8343949	7,366380504
91	06.12.1993	19.06.1997		0	0	0
92	06.12.1993	19.06.1997		0	0	0
93	06.12.1993	19.06.1997	0,00840764	0,440190749	0,456937137	0,117919261
94	06.06.1994	02.08.1995	0,09312102	51,7338995	38,80042463	25,86694975
95	28.03.1997	17.06.1997	0,0766879	8,520877565	15,33757962	11,11418813
96	14.03.1990	25.07.1990	0,59095541	590,955414	393,970276	656,6171267
97	05.10.1992	07.06.1993	0,69401274	578,343949	126,1841343	433,7579618
98	16.02.1995	26.02.1998	0,01605096	13,37579618	10,70063694	13,37579618
99				0	0	0
100	11.07.1991	24.08.1995	0,09719745	22,09033005	18,33914193	13,88535032
101				0	0	0
102				0	0	0
103	17.07.1995	30.07.1996	0,01312102	1,41086227	0,009540478	0,037381821
104	13.10.1995	07.04.1998	0,01541401	11,0100091	5,138004246	5,50500455
105	23.11.1989	16.01.1995	0,01006369	5,296681193	3,870651641	0,508267387
106	05.12.1996	30.06.1997	0,03872611	55,32302093	4,351248837	2,868601085
107	12.07.1993	11.02.1997	0,02420382	0,773285037	6,723283793	0,83461454
108	19.10.1995	26.06.1997	0,0089172	1,938521185		
109	29.03.1989	31.01.1990	0,02802548	14,01273885	7,006369427	46,70912951
110	22.02.1988	28.06.1996	0,02025478	8,806424813	9,645131938	6,137811233
111	26.08.1988	05.09.1990	0,20636943	42,11620954	21,49681529	24,86378636
112				0	0	0

113	06.04.1989	19.06.1998	0,01095541	2,547770701	4,564755839	1,856849833
114	16.11.1993	13.01.1998	0,04394904	31,3921747	19,97683845	29,29936306
115	06.08.1991	30.03.1992	0,14229299	177,866242	59,28874735	83,70176096
116	14.02.1990	01.04.1997	0,0044586	2,229299363	1,78343949	1,651332862
117	14.04.1988	08.04.1993	0,00420382	1,827748546	2,212537714	1,501364877
118	18.01.1995	24.05.1996	0,00815287	2,264685067	2,547770701	2,629956852
119	22.01.1986	24.05.1991	0,02318471	11,0403397	15,45647558	7,99472875
120	18.02.1997	12.05.1997	0,0266242	0,198391981	1,221293753	2,335456476
121				0	0	0
122	12.08.1991	10.04.1997	0,0033121	0,231615518	0,025815292	0,022363956
123	23.12.1988	28.11.1994	0,00165605	0,240007385	0,005948459	0,092516813
124	24.04.1990	11.06.1997	0,02535032	25,35031847	7,041755131	7,041755131
125	28.02.1996	08.06.1998	0,01095541	2,672052198	7,303609342	3,53400452
126	26.04.1988	08.03.1991	0,03082803	19,26751592	13,40348934	16,22527657
127	02.03.1988	27.01.1992	0,01757962	6,761391475	6,510969568	7,643312102
128	01.08.1990	20.11.1990	0,29146497	107,9499882	44,16135881	138,792842
129	18.10.1993	07.03.1994	0,38840764	353,0978576	242,7547771	353,0978576
130				0	0	0
131	05.04.1994	30.10.1996	0,01464968	0,976645435	2,441613588	9,156050955
132	04.03.1993	03.02.1994	0,22980892	191,507431	95,7537155	63,83581033
133	26.04.1989	20.04.1994	0,00063694	0,036396724	0,029763676	0,040569597
134	26.01.1996	08.09.1997	0,01923567	0,510229941	1,02754641	0,295478783
135	14.10.1994	23.02.1998	0,09350318	4,844724597	8,202033747	4,030309686
136	24.02.1995	18.08.1995	0,05898089	2,217326756	5,128773193	3,154058381
137	02.06.1995	07.04.1997	0,0122293	0,003882317	4,891719745	6,436473349
138	31.08.1993	11.03.1996	0,03757962	12,12245737	13,91837698	23,48726115
139				0	0	0
140	24.08.1995	23.07.1997	0,08458599	0,073932337	0,097584203	0,912470197
141	27.01.1994	08.11.1994	0,76038217	316,8259023	237,6194268	271,5650591
142	29.09.1994	03.08.1995	0,14878981	28,61342479	55,10733664	22,20743417
143	29.08.1995	29.08.1996	0,01414013	4,713375796	2,945859873	2,719255267
144	25.01.1995	09.06.1997	0,08254777	11,79253867	12,50723798	17,56335547
145	19.04.1996	11.12.1997	0,0256051	0,076961513	0,134763661	0,68830902
146	06.01.1995	15.03.1995	0,08343949	11,58881812	2,350408182	8,100921403
147	18.09.1996	17.04.1997	0,02089172	13,05732484	20,89171975	13,05732484
148	17.03.1995	07.03.1997	0,00878981	0,009199172	0,037292359	1,417711116
149	12.03.1997	13.02.1998	0,05707006	6,959763865	3,261146497	8,271023724
150	24.11.1994	27.08.1996	0,01299363	4,812455768	10,82802548	0,721868365
151				0	0	0
152	19.09.1996	25.09.1997	0,01783439	2,410053365	5,753030614	3,074895673
153				0	0	0
154				0	0	0
155				0	0	0
156	19.05.1994	17.01.1995	0,12522293	0,79154823	0,473432627	0,740088238
157				0	0	0

158	12.12.1995	24.04.1996	0,09273885	0,586212728	0,525135071	0,159977322
159	16.05.1990	05.11.1990	0,28012739	4,001819836	20,00909918	6,916725643
160				0	0	0
161	15.03.1994	14.07.1995	0,03146497	0,048333284	0,95929781	0,170541833
162				0	0	0
163	10.12.1997	18.05.1998	0,29031847	17,59505887	20,16100495	13,62997518
164				0	0	0
165				0	0	0
166				0	0	0
167				0	0	0
168				0	0	0
169				0	0	0
170	10.11.1995	28.08.1996	0,01375796	0,088475638	0,234777505	0,833815866
171	23.06.1994	20.03.1995	0,00394904	0,286162651	0,166626354	0,626832474
172				0	0	0
173				0	0	0
174				0	0	0
175	16.04.1997	06.04.1998	0,03949045	1,257657511	3,797158256	1,200317503
176	28.03.1995	05.12.1995	0,03974522	5,031040877	1,967585294	4,367606915
177	16.11.1995	10.04.1997	0,00191083	0,269130708	0,636942675	0,265392781
178	31.08.1994	23.01.1995	0,00942675	0,650120799	0,374077444	0,378584401
179				0	0	0
180				0	0	0
181	03.09.1997	30.04.1998	0,03834395	9,585987261	17,42906775	12,78131635
182	24.04.1997	27.08.1998	0,09286624	23,21656051	8,366328112	15,74004102
183	02.07.1996	17.04.1998	0,01528662	6,114649682	6,114649682	4,367606915
184	25.08.1992	08.02.1994	0,08878981	25,36851683	44,39490446	38,60426475
185	27.11.1992	21.07.1993	0,20394904	39,22097011	75,53668318	75,53668318
186	22.08.1995	24.11.1995	0,09974522	28,49863512	8,525232729	27,70700637
187	10.07.1996	12.06.1997	0,02280255	45,60509554	22,80254777	14,25159236
188	29.06.1990	10.12.1990	0,86280255	392,1829763	221,2314225	253,7654552

Data Watercuts, Chloride Content, Velocities, Tubing Sizes

Well No.	Watercut Surface [%]	Watercut Downhole [%]	Chloride Content [ppm]	Flowrate Surface [m ³ /day]	Flowrate Downhole [m ³ /day]	Velocity Surface [m/s]	Tubing OD ["]	Velocity Downhole [m/s]
1	90,64	90,42	12570	37,4	40,7	0,427	3,5	0,208
2	87,7	90,58	15480	31,7	30,8	0,362	2,875	0,236
3	95,27	92,47	13240	27,5	27,6	0,314	3,5	0,141
4	97,89	97,09	12995	80,7	68,7	0,922	3,5	0,351
5	89,92	88,36	15210	37,7	37,8	0,431	3,5	0,193
6	95,5	91,88	13205	28,9	38,2	0,330	2,875	0,293

7	94,3	90,00	12670	31,6	24,5	0,361	2,875	0,188
8	95,8	94,25	12500	38,1	36,5	0,435	3,5	0,186
9	84,98	76,87	16260	21,3	14,7	0,243	2,875	0,113
10	85,63	89,44	13840	32,7	34,1	0,373	2,875	0,261
11	98,3	98,60	11700	105,9	95,3	1,209	2,875	0,731
12	93,06	96,82	14770	41,8	31,4	0,477	3,5	0,160
13	93,93	93,14	14136	21,4	35	0,244	2,875	0,268
14	91,46	92,24	13630	31,6	32,2	0,361	3,5	0,164
15	80,62	89,58	15095	12,9	12,8	0,147	2,875	0,098
16	84,91	83,90	14415	28,5	23,6	0,325	3,5	0,120
17	95,75	95,51	13065	40	54,3	0,457	3,5	0,277
18	96,09	95,24	12440	28,1	32,5	0,321	2,875	0,249
19	94,84	92,69	12215	65,9	54,3	0,753	3,5	0,277
20	96,24	96,24	11565	77,1	77,1	0,880	2,875	0,591
21	93,51		11570	44,7		0,510		
22	92,99	87,93	11570	57,1	49,7	0,652	3,5	0,254
23	96,59	96,49	14485	44	45,6	0,502	3,5	0,233
24	82,2	84,47	15190	9,3	10,3	0,106	2,875	0,079
25	96,72		12500	67		0,765		
26	97,09	95,83	12500	61,9	69,5	0,707	2,875	0,533
27	93,03	90,66	11840	73,2	58,9	0,836	2,875	0,452
28	71,97	0,00	15690	13,2	0	0,151	2,875	0,000
29	92,15	89,62	12090	29,3	31,8	0,335	3,5	0,162
30	54,9	63,64	14340	5,1	6,6	0,058	2,875	0,051
31	77,88	77,64	13995	10,4	11	0,119	2,875	0,084
32	0	84,70	17750	0	9,8	0,000	2,875	0,075
33	90,32	89,57	12210	50,6	57	0,578	3,5	0,291
34	93,78	0,00	12070	49,8	0	0,569	3,5	0,000
35	69,31	69,31	15265	10,1	10,1	0,115	2,875	0,077
36	33,33	64,00	14630	1,8	1,2	0,021	2,875	0,009
37	22,86	18,75	9445	3,5	3,2	0,040	2,875	0,025
38	92,03	88,94	12355	66,5	67,2	0,759	3,5	0,343
39	90,2	87,07	11910	41,1	41	0,469	3,5	0,209
40	90,54	88,29	13705	46,5	33,8	0,531	3,5	0,172
41	97,45	90,00	10995	31,4	22	0,359	3,5	0,112
42	86,36	88,93	16720	28,6	28	0,327	2,875	0,215
43	95,32	93,50	11560	59,8	55,4	0,683	3,5	0,283
44	0	89,31	15690	0	14,1	0,000	2,875	0,108
45	89,74		13995	13,3		0,152		
46	89,31	0	11570	39,3	0	0,449	2,875	0,000
47	99,21	0	12496	113,9	0	0,650	2,875	0,000
48	87,57	94,92	16685	16,9	17,1	0,193	2,875	0,131
49	89,65	89,44	12215	36,7	36	0,419	2,875	0,276
50	96,93	96,79	12520	55,3	59,2	0,631	3,5	0,302
51	90,66	87,52	12210	47,1	52,1	0,538	2,875	0,399

52	95,97	91,59	11220	50,6	51,1	0,578	2,875	0,392
53	96,5	95,18	12110	99,9	45,6	1,141	3,5	0,233
54	98,29	96,86	11860	81,8	73,2	0,934	3,5	0,373
55	95,15	93,47	12080	61,9	56,7	0,707	3,5	0,289
56	95,06		12500	64,8		0,740		
57	97,79	95,55	12500	81,5	44,9	0,931	3,5	0,229
58	94,59	94,59	11710	66,5	66,5	0,759	3,5	0,339
59	97,01	97,09	12780	70,2	68,7	0,802	3,5	0,351
60	97,7	97,98	12780	78,3	69,3	0,894	2,875	0,531
61	96,84	95,62	12310	72,9	75,3	0,832	3,5	0,384
62	94,31	93,83	12280	72,1	48,6	0,823	3,5	0,248
63	89,1	65,41	11415	34,4	18,5	0,393	2,875	0,142
64	31,17	31,17	14650	7,7	7,7	0,088	2,875	0,059
65	83,94	88	12140	49,2	45	0,562	2,875	0,345
66	95,34		13630	60,1		0,686		
67	95,73		13630	58,6		0,669		
68	91,32	0	11640	38	0	0,434	3,5	0,000
69	94,49		13240	27,2		0,311		
70	86,71	85,81	12140	14,3	14,8	0,163	2,875	0,113
71	97,44	96,25	13100	66,5	56	0,759	3,5	0,286
72	86,8	83,55	12070	39,4	37,7	0,450	3,5	0,192
73	89,96		12640	44,8		0,512		
74	90,37		12640	59,2		0,676		
75	89,7	89,7	12640	43,2	43,2	0,493	3,5	0,220
76	92,36	85,59	11855	45,8	30,5	0,523	2,875	0,234
77	87,8	85,45	12495	50	25,5	0,571	2,875	0,195
78	96,65	96,78	11785	50,7	55,9	0,579	3,5	0,285
79	92,98	92,31	16045	17,1	16,9	0,195	2,875	0,130
80	88,84	87,22	12685	43	45,4	0,491	3,5	0,232
81	95,12	95,12	12070	43	43	0,491	3,5	0,219
82	94,35	92,2	11850	69	44,9	0,788	3,5	0,229
83	95,35	94,83	12790	47,3	46,4	0,540	3,5	0,237
84	90,4	90,4	12690	37,5	37,5	0,428	2,875	0,287
85	97,41	95,95	11640	41,6	34,6	0,475	3,5	0,177
86	93,6	93,6	14970	20,3	20,3	0,232	3,5	0,104
87	97,44	94,64	13135	43	23,6	0,491	2,875	0,181
88	95,91	0	15690	34,2	0	0,391	2,875	0,000
89	x	93,13		x	19,2		1,9	0,408
90	94,59	90,83	13820	38,8	36	0,443	2,875	0,276
91	95,5		14770	42,3		0,483		
92	95,5		14770	40,4		0,461		
93	95,5	95,21	14770	37,8	42,1	0,432	2,875	0,323
94	90,11	86,86	14050	26,3	13,7	0,300	2,875	0,105
95	88,83	86,56	13560	17,9	18,6	0,204	3,5	0,095
96	82,56	80,31	12425	19,6	19,3	0,224	3,5	0,098

97	63,44	63,44	12460	22,7	22,7	0,259	3,5	0,116
98	17,02	7,41	17395	4,7	2,7	0,054	2,875	0,021
99	87,72		16260	22,8		0,260		
100	95,3	95,3	14110	23,4	23,4	0,267	2,875	0,179
101	92,1		14480	36,7		0,419		
102	86,79		14480	21,2		0,242		
103	92,92	92,1	14480	36,7	36,7	0,419	3,5	0,187
104	80,56	76,12	5880	18	20,1	0,206	2,875	0,154
105	90,66	29,46	6980	25,7	11,2	0,293	3,5	0,057
106	87,86	87,86	8940	58,5	58,5	0,668	3,5	0,298
107	33,33	33,33	5960	9,6	9,6	0,110	3,5	0,049
108	50	50	8310	1,8	1,8	0,021	2,875	0,014
109	0	0	14415	0	0	0,000	2,875	0,000
110	91,96	91,6	11860	45,7	48,8	0,522	3,5	0,249
111	94,1	92,97	12990	28,8	30,2	0,329	2,875	0,232
112	90,74		12570	36,7		0,419		
113	94,78	97,55	11930	36,4	93,8	0,416	2,875	0,719
114	95,07	95,07	11710	56,8	56,8	0,649	2,875	0,435
115	97,94	97,47	12285	57	39,5	0,651	3,5	0,202
116	86,67	98,98	12205	34,6	68,6	0,395	2,875	0,526
117	87,67	86,44	14060	7,3	5,9	0,083	2,875	0,045
118	95,28	0	14555	33,9	0	0,387	2,875	0,000
119	95,41	93,1	11540	88,4	25,1	1,009	3,5	0,128
120	95,9	95,9	13490	26,8	26,8	0,306	2,875	0,205
121	98,52		12620	67,5		0,771		
122	0	98,01	12620	0	50,3	0,000	2,875	0,386
123	98,1	97,97	12500	68,3	73,8	0,780	3,5	0,377
124	98,68	98,68	11820	83,5	83,5	0,954	2,875	0,640
125	90,82	90,82	14840	20,7	20,7	0,236	2,875	0,159
126	97,24	97,56	11180	105,1	49,2	1,200	2,875	0,377
127	92,79	89,92	11595	50,1	49,6	0,572	3,5	0,253
128	91,5	89,92	13135	24,7	23,8	0,282	2,875	0,182
129	91,98	91,98	12275	26,2	26,2	0,299	3,5	0,134
130	84,62		15690	13		0,148		
131	93,37	94,06	14555	34,7	43,8	0,396	3,5	0,223
132	97,04	89,6	14630	16,9	17,3	0,193	3,5	0,088
133	98	97,01	12640	65	46,9	0,742	3,5	0,239
134	91,53	91,53	12570	42,5	42,5	0,485	2,875	0,326
135	89,53	89,53	13490	29,6	29,6	0,338	2,874	0,227
136	92,94	90,88	12990	34,8	27,4	0,397	3,5	0,140
137	93,77	90,6	13770	36,9	26,6	0,421	3,5	0,136
138	56,48	56,67	14520	10,8	6	0,123	2,875	0,046
139	89,34		15210	34,7		0,396		
140	87,99	88,36	15210	38,3	37,8	0,437	3,5	0,193
141	88,3	80,22	17250	14,2	9,1	0,162	2,875	0,070

142	90,35	91,43	14920	22,8	10,5	0,260	2,875	0,080
143	89,47	91,98	13770	30,4	21,2	0,347	2,875	0,163
144	85,48	85,48	15490	24,8	24,8	0,283	3,5	0,127
145	95,57	95,32	13500	60,9	51,3	0,695	3,5	0,262
146	93,16	91,81	15050	23,4	17,1	0,267	2,875	0,131
147	84,66	88,13	15520	17,6	16	0,201	2,875	0,123
148	94,21	94,21	12690	24,2	24,2	0,276	2,875	0,186
149	88,6	89,91	14200	30,9	31,7	0,353	3,5	0,162
150	93,94	93,94	13490	19,8	19,8	0,226	2,875	0,152
151	90,7		14765	35,5		0,405		
152	92,59	90,7	14765	21,6	35,5	0,247	2,875	0,272
153	95,82		13990	43,1		0,492		
154	95,82		13990	43,1		0,492		
155	95,82		13990	43,1		0,492		
156	95,81	95,82	13990	38,2	43,1	0,436	2,875	0,330
157	92,08		14410	46,7		0,533		
158	92,08	92,08	14410	46,7	46,7	0,533	3,5	0,238
159	90,52	89,84	14200	23,2	25,6	0,265	2,875	0,196
160	97,68		13695	51,8		0,592		
161	97,68	96,35	13695	51,8	38,4	0,592	2,875	0,294
162	82,93		16610	17		0,194		
163	84,62	85,14	16610	18,6	17,5	0,212	3,5	0,089
164	94,04		14135	28,5		0,325		
165	93,93		14135	21,4		0,244		
166	88,19		13205	41,5		0,474		
167	88,19		13205	41,5		0,474		
168	92,38		13205	42		0,480		
169	91,18		13420	36,4		0,416		
170	91,18	90,62	13420	36,4	37,3	0,416	2,875	0,286
171	94,8	94,12	13060	26,9	27,2	0,307	3,5	0,139
172	92		15480	30,9		0,353		
173	89,72		15480	30,9		0,353		
174	89,24		16645	28,8		0,329		
175	97,59	89,24	16645	13,7	28,8	0,156	2,875	0,221
176	89,06	68,97	16985	12,06	8,7	0,138	2,875	0,067
177	89,26	89,26	15395	12,1	12,1	0,138	2,875	0,093
178	92,83	92	16685	25,1	25	0,287	2,875	0,192
179	93,06		14770	41,8		0,477		
180	93,06		14770	41,8		0,477		
181	95,89	95,56	12110	56	27	0,639	3,5	0,138
182	95,17	95,17	13630	33,1	33,1	0,378	3,5	0,169
183	77,3	77,3	14380	8,1	8,1	0,092	2,875	0,062
184	81,48	84,13	15760	5,4	6,3	0,062	2,875	0,048
185	95,81	95,98	14530	31	22,4	0,354	2,875	0,172
186	95,54	94,44	14840	16,5	21,6	0,188	2,875	0,166

187	85,12	85,12	9510	41	41	0,468	2,875	0,314
188	93,08	87,05	4615	62,1	50,2	0,709	3,5	0,256

Data Watercuts CO₂ & H₂S Contents, Surface (Partial-) Pressures, Pump setting Depth, Casing Pressure

Well Number	CO ₂ Content [Vol%]	H ₂ S Content [ppm]	Wellhead Pressure [bar]	Partial Pressure CO ₂ Surface [bar]	Partial Pressure H ₂ S Surface [bar]	Dynamic Fluid Level [m]	Setting Depth Pump [m]	Casing Pressure [bar]
1	2,4		4	0,096		351	450	5,00
2	1,62		5	0,081		624	799	5,00
3	1,65		7	0,1155		415	800	6,00
4	15,53	50	8	1,2424	0,0004	410	618	6,00
5	0,63		9	0,0567		706	849	8,00
6	1,29		7,5	0,09675		446	709	8,00
7	1,62		5	0,081		309	605	4,00
8	6,09	130	8	0,4872	0,00104	519	715	7,00
9	1,82		4	0,0728		513	701	12,00
10	0,82		6	0,0492		678	905	7,00
11	2,84	50	3	0,0852	0,00015	468	649	3,00
12	0,59		6	0,0354		284	605	10,00
13	0,67		8	0,0536		397	602	6,00
14	3,21		5	0,1605		365	856	5,00
15	0,99		7,5	0,07425		814	997	7,00
16	2,21	50	4	0,0884	0,0002	485	601	4,00
17	0,83		5	0,0415		302	505	6,00
18	1,12	150	3	0,0336	0,00045	208	602	3,00
19	4,73	400	8	0,3784	0,0032	451	656	7,00
20	11,16	1200	8	0,8928	0,0096	427	703	7,00
21	5,08	400	5	0,254	0,002			
22	5,08	400	5	0,254	0,002	413	647	5,00
23	0,37		6	0,0222		48	206	5,00
24	1,37		5,5	0,07535		627	775	6,00
25	2,3	120	7,5	0,1725	0,0009			
26	2,3	120	7,5	0,1725	0,0009	450	698	7,00
27	2,31	800	4	0,0924	0,0032	414	648	3,00
28	0,25		9	0,0225		672	1205	7,00
29	3,3	120	5	0,165	0,0006	434	650	6,00
30	0,96		3	0,0288		830	1000	6,00
31	0,58		7,5	0,0435		110	1196	15,00
32			7,5			945	1183	4,00
33	5,58	850	9	0,5022	0,00765	474	652	9,00
34	5,47	200	4	0,2188	0,0008	309	555	4,00

35	0,69		7,5	0,05175		861	1155	10,00
36	2,01	10	4	0,0804	0,00005	1309	1367	3,00
37	2,22	20	4	0,0888	0,00008	1600	1612	3,80
38	10,07	80	8	0,8056	0,00064	450	643	8,00
39	1,66	300	3	0,0498	0,0009	393	1004	4,00
40	9	250	9	0,81	0,00225	497	634	8,00
41	1,35	100	3	0,0405	0,0003	521	801	4,00
42	0,79		7,5	0,05925		972	1098	4,00
43	2,4	200	3	0,072	0,0006	524	656	3,00
44	2,42		4,5	0,1089		958	1300	3,00
45	0,58		7,5	0,0435				
46	6,94	240	5	0,347	0,0012	73	654	6,00
47	2,47		6	0,1482		110	1100	15,00
48	0,87		4,5	0,03915		1000	1207	0,00
49	0,64	20	6	0,0384	0,00012	215	554	6,00
50	1,98		9	0,1782		493	720	5,00
51	2,14		4	0,0856		430	600	5,00
52	7,27	800	5	0,3635	0,004	446	598	5,00
53	4,98	80	6	0,2988	0,00048	416	595	5,00
54	17,12	30	7,5	1,284	0,000225	456	700	6,00
55	5,28	100	6	0,3168	0,0006	419	595	5,00
56	2,33	10	7,5	0,17475	0,000075			
57	2,33	10	7,5	0,17475	0,000075	373	552	5,00
58	4,22	100	7	0,2954	0,0007	500	708	7,00
59	5,06	50	6	0,3036	0,0003	437	669	5,00
60	3,94	10	5	0,197	0,00005	444	601	6,00
61	9,35		7	0,6545			647	
62	6,93	20	8	0,5544	0,00016	393	603	6,00
63	4,02	100	7	0,2814	0,0007	461	540	7,00
64	1,74	150	7	0,1218	0,00105	439	1050	10,00
65	3,66	20	7	0,2562	0,00014	423	657	7,00
66	3,21		5	0,1605				
67	3,21		5	0,1605		365	856	5,00
68	1,8	200	5	0,09	0,001	625	704	6,00
69	1,65		7	0,1155		415	800	6,00
70	2,07		9	0,1863		753	1103	5,00
71	14,16	100	7	0,9912	0,0007	523	698	7,00
72	3,87	20	4	0,1548	0,00008		606	
73	2,96		4,5	0,1332				
74	2,96		4,5	0,1332				
75	2,96		4,5	0,1332		422	639	5,00
76	2,56	450	6	0,1536	0,0027	408	1003	6,00
77	3,21	200	4,5	0,14445	0,0009	540	825	9,00
78	7,96	600	7,5	0,597	0,0045	433	599	7,00
79	0,4		6	0,024		1004	1056	9,00

80	5,1	10	7	0,357	0,00007	438	701	7,00
81	3,42	25	7	0,2394	0,000175	480	600	6,00
82	3,11	1200	6	0,1866	0,0072	465	656	7,00
83	4,72		6	0,2832		439	640	5,00
84	4,34		7	0,3038		501	602	7,00
85	5,03	100	7	0,3521	0,0007	501	603	6,00
86	2,3		7,5	0,1725		1057	1099	7,00
87	1,51		4	0,0604		693	850	6,00
88	1,26	150	5	0,063	0,00075	0	999	0,00
89	0,55		7,5	0,04125		330	345	7,00
90	2,6	20	7	0,182	0,00014	437	601	7,00
91	1,28		4	0,0512				
92	1,28		4	0,0512				
93	1,28		4	0,0512		559	999	5,00
94	1,39	100	8	0,1112	0,0008	815	1120	9,00
95	2,59		4,5	0,11655		788	1004	6,00
96	2,8	250	8,5	0,238	0,002125	426	701	6,00
97			5			423	653	6,00
98	0,31		8,5	0,02635		1165	1202	6,00
99	1,82		4	0,0728				
100			7,5			431	557	4,00
101	1,4		6,5	0,091				
102	1,4		6,5	0,091				
103	1,4		6,5	0,091		163	801	9,00
104	0,76		4	0,0304		897	915	4,00
105			3			315	850	16,00
106	4,15		7	0,2905		370	692	7,00
107			3,5			600	963	14,00
108	2,24		5	0,112		819	934	12,00
109	1,65		4	0,066		456	1418	5,00
110	1,82	200	4	0,0728	0,0008	127	722	6,00
111	2,02		6	0,1212		183	456	5,00
112	2,4		4	0,096				
113	13,63	900	4	0,5452	0,0036	381	620	5,00
114	2,25	700	5	0,1125	0,0035	394	573	4,00
115	2,16	70	3	0,0648	0,00021	430	651	5,00
116	3,94	100	3	0,1182	0,0003	454	682	3,00
117	4,61		3,5	0,16135		607	1201	4,00
118	1,3		4,5	0,0585			604	
119	8,93	250	3	0,2679	0,00075	393	1001	2,00
120	2,98		4	0,1192		203	1302	2,00
121	1,48		7,5	0,111				
122	1,48	20	7,5	0,111	0,00015	608	805	0,00
123	3,66	50	7,5	0,2745	0,000375	436	608	3,00
124	2,16	800	3	0,0648	0,0024	65	614	5,00

125	1,7		7,5	0,1275		974	1107	5,00
126	19,11	370	3	0,5733	0,00111	386	679	3,00
127	2,22	116	4,5	0,0999	0,000522	156	797	4,00
128	2,57		4	0,1028		139	405	4,00
129	1,68	300	4	0,0672	0,0012	429	801	3,00
130	2,42	50	4,5	0,1089	0,000225			
131	1,99		7,5	0,14925		242	504	3,00
132	0,49		4	0,0196		185	400	5,00
133	2,05	50	7,5	0,15375	0,000375	350	354	20,00
134	1,97		5	0,0985		294	399	6,00
135	1,21		5	0,0605		416	500	6,00
136	0,64		6	0,0384		247	775	1,00
137	0,96		6	0,0576		635	1050	5,00
138	0,94		11	0,1034		672	1002	7,00
139	0,63		9	0,0567				
140	0,63		9	0,0567		706	849	8,00
141	1,66		8	0,1328		729	1156	7,00
142	0,63		7,5	0,04725		825	1049	7,00
143	1,69		7,5	0,12675		580	701	4,00
144	1,43		5,5	0,07865		501	647	6,00
145	0,76		4	0,0304		115	251	6,00
146	1,01		7,5	0,07575		754	898	5,00
147	1,58		3,5	0,0553		813	997	6,00
148	1,72		6	0,1032		679	753	6,00
149	0,44		6,5	0,0286		406	1099	6,00
150	1,73		8	0,1384		615	797	6,00
151	0,77		8	0,0616				
152	0,77		5	0,0385		476	798	5,00
153	1,89		7	0,1323				
154	1,89		7	0,1323				
155	1,89		7	0,1323				
156	1,89		7	0,1323		513	651	5,00
157	1		4	0,04				
158	1		4	0,04		645	797	4,00
159	1,08		4	0,0432		592	756	7,00
160	0,95		7,5	0,07125				
161	0,95		7,5	0,07125		304	600	5,00
162	0,59		3,5	0,02065				
163	0,59		3,5	0,02065		376	1001	28,00
164	0,67		8	0,0536				
165	0,67		8	0,0536				
166	1,29		7,5	0,09675				
167	1,29		7,5	0,09675				
168	1,29		6	0,0774				
169	0,09		5	0,0045				

170	0,09		5	0,0045		500	805	6,00
171	0,93		7,5	0,06975		302	550	5,00
172	1,62		5	0,081				
173	1,62		5	0,081				
174	1,31		5	0,0655				
175	1,31		5	0,0655		757	953	6,00
176	0,73		5	0,0365		553	998	10,00
177	1,66		7,5	0,1245		962	1000	5,00
178	2,1	40	5	0,105	0,0002	723	846	4,00
179	0,59		6	0,0354				
180	0,59		6	0,0354				
181	1,45	70	2	0,029	0,00014	500	672	2,00
182			5			535	1002	4,00
183	2,12		4	0,0848		762	1110	5,00
184	0,95		2,5	0,02375		991	1155	5,00
185	1,07		4	0,0428		400	662	5,00
186	2,48		7,5	0,186		731	783	4,00
187	6,39		5	0,3195		1018	1046	0,00
188	14,23		5	0,7115		455	900	6,00

Data Watercuts Partial Pressures Downhole, P_{CO_2}/P_{H_2S} Ratio, Temperature

Well Number	Partial Pressure CO ₂ Downhole [bar]	Partial Pressure H ₂ S Downhole [bar]	PCO ₂ /PH ₂ S	Temperature Downhole [°C]
1	0,3530856			34,85
2	0,3591135			46,37
3	0,7221803			46,40
4	4,1006654	0,0013202	3106	40,39
5	0,1387783			48,02
6	0,4360239			43,40
7	0,5352091			39,97
8	1,5972608	0,0034096	468,4615	43,60
9	0,554059			43,13
10	0,2400033			49,87
11	0,5894732	0,0010378	568	41,42
12	0,2447916			39,97
13	0,1749404			39,87
14	1,7066639			48,25
15	0,2470278			52,90
16	0,3398892	0,000769	442	39,83
17	0,2150887			36,67

18	0,4664957	0,0062477	74,66667	39,87
19	1,2823267	0,0108442	118,25	41,65
20	3,802837	0,0408907	93	43,20
21			127	
22	1,4201343	0,0111822	127	41,35
23	0,0758493			26,80
24	0,2811076			45,58
25			191,6667	
26	0,7205624	0,0037595	191,6667	43,03
27	0,5995697	0,0207643	28,875	41,38
28	0,1482183			59,77
29	0,8972568	0,0032628	275	41,45
30	0,2176992			53,00
31	0,7049123			59,47
32				59,04
33	1,4765684	0,0224925	65,64706	41,52
34	1,5388532	0,0056265	273,5	38,32
35	0,2680057			58,12
36	0,174665	8,69E-05	2010	65,11
37	0,1104938	9,954E-05	1110	73,20
38	2,7121833	0,0021547	1258,75	41,22
39	1,0613891	0,0191817	55,33333	53,13
40	1,929573	0,0053599	360	40,92
41	0,424818	0,0031468	135	46,43
42	0,1292487			56,23
43	0,3827808	0,0031898	120	41,65
44	0,8845148			62,90
45				
46	4,3719293	0,0151191	289,1667	41,58
47	2,7693393			56,30
48	0,1766683			59,83
49	0,2512378	0,0007851	320	38,28
50	0,5399203			43,76
51	0,4638878			39,80
52	1,4475442	0,015929	90,875	39,73
53	1,123483	0,0018048	622,5	39,64
54	5,1251117	0,0008981	5706,667	43,10
55	1,1756237	0,0022266	528	39,64
56			2330	
57	0,5256457	0,0002256	2330	38,22
58	1,1564826	0,0027405	422	43,36
59	1,4046155	0,001388	1012	42,08
60	0,843227	0,000214	3940	39,83
61	5,9345105			41,35
62	1,8434493	0,000532	3465	39,90

63	0,592946	0,001475	402	37,82
64	1,2169403	0,0104909	116	54,65
65	1,0963676	0,0005991	1830	41,68
66				
67				
68	0,2474982	0,00275	90	43,23
69	0,7221803			
70	0,8142345			56,40
71	3,422118	0,0024168	1416	43,03
72	2,3006608	0,001189	1935	40,00
73				
74				
75	0,7781159			41,09
76	1,6478592	0,0289663	56,88889	53,10
77	1,1863679	0,0073917	160,5	47,23
78	1,8534542	0,0139708	132,6667	39,77
79	0,0564048			54,85
80	1,6728153	0,000328	5100	43,13
81	0,6078024	0,0004443	1368	39,80
82	0,8004238	0,0308845	25,91667	41,65
83	1,1666943			41,12
84	0,7338115			39,87
85	0,8051119	0,0016006	503	39,90
86	0,2557646			56,27
87	0,3231657			48,05
88	1,2348239	0,0147003	84	52,97
89	0,0465933			31,39
90	0,6002984	0,0004618	1300	39,83
91				
92				
93	0,6164992			52,97
94	0,540995	0,0038921	139	56,96
95	0,7042106			53,13
96	0,92337	0,0082444	112	43,13
97				41,55
98	0,0298521			59,67
99				
100				38,38
101				
102				
103	1,0022292			46,43
104	0,0438201			50,20
105				48,05
106	1,6014103			42,84
107				51,78

108	0,5215056			50,82
109	1,6396413			66,79
110	1,1715249	0,0128739	91	43,83
111	0,6419823			35,05
112				
113	3,8771762	0,0256013	151,4444	40,46
114	0,4850978	0,0150919	32,14286	38,91
115	0,5762902	0,0018676	308,5714	41,48
116	0,9994519	0,0025367	394	42,51
117	2,8707115			59,63
118	0,7702812			39,93
119	5,5048806	0,0154112	357,2	53,03
120	3,2723946			62,97
121				
122	0,2860204	0,0003865	740	46,57
123	0,7273591	0,0009937	732	40,06
124	1,271309	0,0470855	27	40,26
125	0,3068041			56,53
126	6,0661446	0,011745	516,4865	42,41
127	1,4847826	0,0077583	191,3793	46,30
128	0,7734312			33,37
129	0,6634858	0,011848	56	46,43
130			484	
131	0,5711738			36,63
132	0,1278484			33,20
133	0,4180442	0,0010196	410	31,68
134	0,3211199			33,17
135	0,1723088			36,50
136	0,3378995			45,58
137	0,4388304			54,65
138	0,3701062			53,07
139				
140	0,1387783			48,02
141	0,8115524			58,15
142	0,1825387			54,62
143	0,2682047			43,13
144	0,2906132			41,35
145	0,1469962			28,28
146	0,1931766			49,63
147	0,3799963			52,90
148	0,2280617			44,85
149	0,3255265			56,27
150	0,4126777			46,30
151				
152	0,2817291			46,33

153				
154				
155				
156	0,3503644			41,48
157				
158	0,189112			46,30
159	0,2493547			44,95
160				
161	0,3233572			39,80
162				
163	0,5269438			53,03
164				
165				
166				
167				
168				
169				
170	0,0323285			46,57
171	0,2727578			38,15
172				
173				
174				
175	0,3304816			51,45
176	0,3916779			52,93
177	0,1448815			53,00
178	0,3373923	0,0006427	525	47,92
179				
180				
181	0,2736614	0,0013211	207,1429	42,18
182				53,07
183	0,8297426			56,63
184	0,2003398			58,12
185	0,3285135			41,85
186	0,2257098			45,84
187	0,1755205			54,52
188	7,0658354			49,70

List Green Inhibitors Inhibitor Doses, Corrosion Rates and Watercut

Well Number	Name	Inhibitor KI350 [ppm]	KI350 CR [mm/a]	Inhibitor CK347 [ppm]	CK347 CR [mm/a]	Watercut [%]
199	Schönkirchen 085	29	0,064	13	0,828	97,54
207	Schönkirchen 249	30	0,023	21	0,089	95,27
193	Prottes 029	22	0,038	22	1,645	95,84
197	Schönkirchen 054	30	0,129	24	1,113	91,12
189	Bockfliess 049	28	0,004	25	0,008	82,62
192	Matzen 292	26	0,004	26	0,01	93,23
203	Schönkirchen 147	22	0,093	33	0,695	90,34
190	Bockfliess 053	13	0,007	37	0,005	88,6
194	Prottes 105	67	0,005	38	0,025	91,5
208	Schönkirchen 256	32	0,004	38	0,004	95,57
205	Schönkirchen 151	47	0,005	41	0,021	93,59
202	Schönkirchen 146	51	0,041	47	0,026	93,44
191	Bockfliess 139	49	0,005	55	0,007	97,23
201	Schönkirchen 126	85	0,005	55	0,04	94,46
200	Schönkirchen 113	56	0,013	58	0,027	92,15
204	Schönkirchen 150	83	0,004	60	0,005	94,22
195	Schönkirchen 019	45	0,004	113	0,217	84,76
196	Schönkirchen 052	54	0,003			
198	Schönkirchen 065	61	0,028			
206	Schönkirchen 217	23	0,373			

List Green Inhibitors Content CO₂ & H₂S, Velocity,**Partial Pressure CO₂**

Well Number	Velocity [m/s]	Pressure Wellhead [bar]	CO ₂ Content [Vol%]	H ₂ S Content [ppm]	Partial Pressure CO ₂ Wellhead [bar]
199	0,698168712	5	1,72	0	0,09
207	0,599899466			0	
193	0,620467448	4	1,97	10	0,08
197	0,412502299	5	0,44	0	0,02
189	0,199966489	5	5,06	0	0,25
192	0,523340867	4	3,34		0,13
203	0,25481444	5	0,43		0,02
190	0,395362315	4	9,35	0	0,37
194	0,253671774	9	0,14	1314	0,01
208	0,399932977	4			
205	0,317661051	6	0,57		0,03

202	0,255957105	2	0,55		0,01
191	0,57247549	4	1,28	0	0,05
201	0,353083686	4	1,31	0	0,05
200	0,418215628	6	0,66	0	0,04
204	0,171399847	6			
195	0,169114516	5	1,43	2	0,07
196	0,289094409	4	1,58	0	0,06
198	0,418215628	5	0,82	0	0,04
206	0,497059557	4	1,17		0,05

List Green Inhibitors Partial Pressure H₂S, Chloride Content, additional Info

Well Number	Partial Pressure H ₂ S_Wellhead [bar]	Flowrate [m ³ /day]	Water KI350 [%]	Q KI350 [m ³ /day]	Chlorides [ppm]
199		61,1			
207		52,5			
193	0,0000	54,3			13142
197		36,1			14107
189		17,5	83	16,3	12532
192		91,6			
203		22,3			17670
190		34,6	90,3	32	12670
194	0,0118	22,2			12605
208		35			15265
205		27,8			17680
202		22,4			15470
191		50,1			14677
201		30,9			15918
200		36,6			
204		15			17510
195		14,8			15212
196			92,6	27,2	
198			92,04	36,6	
206			92,73	43,5	

10 Literature

List of Symbols and Abbreviations

[bar]	Bar
[°C]	Degrees Celsius
[cp]	Centipoise
[,] and [.] in tables and figures	Both mean “comma”
CR	Corrosion Rate
e.g.	exempli gratia (for example)
[“]	Inch
Install.	Installation
[l]	Litre
[kg]	Kilogramm
M	Mille (1000)
[meq/l]	Milli- equivalent of solute per Litre of Solvent
[ml]	Milli- Litre
[mm/a] or [mm/y]	Millimetre per Year
[mpy]	Milli- inch (Mils) per Year
[m/s]	Meter per Second
[m ³ /day]	Cubic Meter per Day
No.	Number
O.C.	Oil Company
[Pa]	Pascal
[%]	Percent
P _{Gas}	Partial Pressure of Gas
[ppm]	Parts per Million
[psi]	Pounds per Square Inch
Rt	Yield Strength
Rm	Ultimate Tensile Strength
[WO/a]	Workover per Year

Conversion into metric Units

psi	= 0.0689 bar
Mpa	= 10 bar
mpy	= 0.0254 mm/a
(°F- 32)/1.8	= °C
cp	= 0.001 Pas

- ¹ D.A. Lopez, T. Perez, S.N. Simison, "The influence of microstructure and chemical composition of carbon and low alloy steels in CO₂ corrosion. A state-of-the-art appraisal", *Materials and Design* 24 (2003) , Pages 561-565
- ² M.B. Kermani, A. Morshed, "Carbon Dioxide Corrosion in Oil and Gas Production- A Compendium", *NACE, Corrosion* 59 (2003) No.8, Pages 659- 667, 678-679
- ³ C. de Waard, L. M. Smith, B.D. Craig, "The Influence of Crude Oils on Well Tubing Corrosion Rates", *NACE-Corrosion* 2003 No. 3629, Pages 1- 8
- ⁴ K. Videm, A.Dugstad, "Corrosion of Carbon Steel in an Aqueous Carbon Dioxide Environment. Part II: Film Formation", *Environment Treatment and Control, MP/ April* 1989, Pages 46- 50
- ⁵ J. Vera, "Oil Characteristics, Water/Oil wetting and Flow Influence on the Metal Loss Corrosion. Part 1: Effect of Oil and Flow on CO₂/H₂S Corrosion ", *NACE Corrosion Expo 2006- 61st Conference No.:*6113, Pages: 2-3
- ⁶ M. Castillo, "Protective Properties of Crude Oils in CO₂ and H₂S Corrosion", *NACE Corrosion 2000 No.:* 5, Pages: 2, 6
- ⁷ J.L. Crolet, "Which CO₂ Corrosion, Hence which Prediction?" – Predicting CO₂ Corrosion in the Oil and Gas Industry, *European Federation of Corrosion Publication No.:*13, London Institute of Materials, UK (1994), Pages: 8- 10
- ⁸ J.L. Crolet, M. Bonis, "Why so low free Acetic Acid Thresholds in sweet Corrosion at low Pressure CO₂?", *NACE Corrosion 2005 No.:*5272, Pages: 24- 25
- ⁹ K. Lewis, "Processing corrosive crude Oils", *NACE Corrosion 1999 No.:* 377, Pages :4- 6
- ¹⁰ P. Roberge, "Corrosion Engineering- Principles and Practice", McGraw- Hill, 2008, Pages: 15- 26
- ¹¹ J. Carew, A. Al- Sayegh, "The Effect of Watercut on the Corrosion Behaviour of L80 Carbon Steel under Downhole Conditions", *NACE Corrosion 2000 No.:*61, Pages: 1- 5
- ¹² J. Carew, A. Al- Hashem, "CO₂ Corrosion of L- 80 Steel in stimulated Oil Well Conditions", *NACE Corrosion 2002 No.:* 2299, Pages: 3- 4
- ¹³ B. Mishra, S. Al- Hassan, " Development of a predictive Model for activation controlled Corrosion of Steel in Solutions containing Carbon Dioxide", *NACE Corrosion 1997, Pages* 852- 859
- ¹⁴ L. Smith, K. de Waard, "Corrosion Prediction and Materials Selection for Oil and Gas producing Environments", *NACE Corrosion 2005 No.:*5648, Pages: 2- 14
- ¹⁵ S. Nestic, N. Thevenot, " Electrochemical Properties of Iron Dissolution in the Presence of CO₂ – Basics Revisited", *NACE Corrosion 1996 No.:* 3, Pages: 10; 11
- ¹⁶ K. Videm, A.Dugstad, "Corrosion of Carbon Steel in an Aqueous Carbon Dioxide Environment. Part I: Solution Effects", *Environment Treatment and Control, MP/ April* 1989, Pages: 64, 67
- ¹⁷ C. De Waard, D. E. Williams, "Carbonic Acid Corrosion of Steel", *NACE, Corrosion* 31 (1975) No.5, Pages 177- 181
- ¹⁸ NORSOK Standard M- 506, "CO₂ Corrosion Rate Calculation Model", *Standards Norway, Lysaker- Norge* (2005), Pages 5- 14
- ¹⁹ M. Oberndorfer, " Metallurgy and Corrosion for Petroleum Engineers", *University of Leoben 120.023, SS 2007, Pages:*7, 55, 59, 74, 127
- ²⁰ G. Svenningsen, A. Palencsar, J. Kvarekval, "Investigation of Iron Sulfide Layer Growth in aqueous H₂S/CO₂ Environments", *NACE Corrosion Expo 2009 No.:*9359, Page 1
- ²¹ B. Kermani, J. Martin, K. Esaklul, " Materials Design Strategy: Effects of H₂S/CO₂ Corrosion in Materials Selection", *NACE Expo 2006- 61st Conference No.:* 6121, Pages: 3- 10
- ²² Y. Choi, S. Nestic, S. Ling, " Effect of H₂S on the CO₂ Corrosion of carbon Steel in acidic Solutions", *Electrochimica Acta* 56 1752- 1760, 2011, Page: 1760
- ²³ A. Curamings, F. Veatch, "Corrosion and Corrosion Control Methods in Amine Systems containing H₂S", *NACE Corrosion 1997 No.:* 341, Page 4
- ²⁴ M. Achour, J. Kolts, P. Humble, R. Hudgins, "Experimental Evaluation of Corrosion Inhibitor Performance in Presence of Iron Sulfide in CO₂/H₂S Content", *NACE Corrosion Expo 2008 No.:* 8344, Page: 11
- ²⁵ G. Schmitt, M. Hörstemeier, " Fundamental Aspects of CO₂ Metal Loss Corrosion – Part II: Influence of different Parameters on CO₂ Corrosion Mechanisms", *NACE Expo 2006- 61st Conference No.:* 6112, Pages: 2;3;5- 10
- ²⁶ B. Pots, I. Rippon, " Improvement on de Waard- Williams Corrosion Prediction and Applications to Corrosion Management", *NACE Corrosion 2002 No.:*2235, Pages: 5, 18
- ²⁷ U. Lotz, T. Sydberger, "CO₂ Corrosion of Carbon Steel and 13Cr Steel in particle- laden Fluid", *NACE Corrosion* 44 (1988) No.: 11, Pages: 7- 8
- ²⁸ S. Nestic, L. Lunde, "Carbon Dioxide Corrosion of Carbon Steel in two phase Flow", *NACE Corrosion* 50 (1994) No.:9, Pages: 725- 727
- ²⁹ J.K. Heuer, J.F. Stubbins, "Microstructure of Coupons exposed to Carbon Dioxide Corrosion in Multiphase Flow", *NACE Corrosion* 54 (1998) No.:7, Pages : 573- 575
- ³⁰ T. Chen, L. Xu, "Study on Factors affecting low Cr- Alloy Steels in a CO₂ Corrosion System", *NACE Expo 2011 No.:* 11074, Page: 4, 5, 13
- ³¹ A. Valdes, R. Case, M. Ramirez, A. Ruiz, "The Effect of small Amounts of H₂S on CO₂ Corrosion of Carbon Steel", *NACE Corrosion 1998 No.:* 22, Pages: 3-5; 10
- ³² J. Fink, "Oil Field Chemicals", *University of Leoben ,Gulf Professional Publishing- Elsevier Science* (Burlington MA- USA), 2003, Pages 82- 85
- ³³ M. Oberndorfer, K. Thayer, W. Havlik, "Corrosion Control in the Oil and Gas Industry- 5 succesful Case Histories", *NACE Expo 2007 No.:*7317, Page: 4-5
- ³⁴ E. Gulbrandsen, S. Nestic, A. Stangeland, T. Burchardt, "Effect of Precorrosion on the Performance of Inhibitors for CO₂ Corrosion of Carbon Steel", *NACE Corrosion 1998 No.:* 13, Page:12
- ³⁵ R. Hausler, T. Martin, D. Stegmann, M. Ward, "Development of a Corrosion Inhibition Model I: Laboratory Studies", *NACE Corrosion 1999 No.:* 2, Pages 21- 22
- ³⁶ R. Woolam, S. Merrett, "Why Water soluble Corrosion Inhibitors should be the preferred Choice for continuous Applications", *SPE No.:* 27869, Long Beach CA- USA, 1994, Pages:2- 5

- ³⁷ M. Joosten, J. Kolts, P. Humble, "Partitioning of Corrosion Inhibitor in Relation to Oil Field Applications and Laboratory testing", NACE Corrosion 2000 No.: 18, Pages: 3-4;8
- ³⁸ T. Moon, D. Horsup, "Relating Corrosion Inhibitor Surface active Properties to Field Performance Requirements", NACE Corrosion 2002 No.: 2298, Page: 8
- ³⁹ J. Kolts, M. Joosten, "Aspects of Corrosion Inhibitor Selection at elevated Temperatures", NACE Corrosion 1998 No.:37, Page: 8
- ⁴⁰ J. Palmer, "Corrosion Control by Film forming Inhibitors", NACE Corrosion Expo 2006-61st No.:6119, Pages: 2-6
- ⁴¹ E. Gulbrandsen, A. Grana, K. Nisancioglu, "How does Fluid Flow affect Performance of CO₂ Corrosion Inhibitors?", SPE No.: 95095, Aberdeen-SCO, 2005, Page: 6
- ⁴² J. Kvarekval, E. Gulbrandsen, "High Temperature and high Velocity Tests for CO₂ Corrosion Inhibitors", NACE Corrosion 2001 No.: 1025, Page 8
- ⁴³ H. Wang, H. Wang, H. Shi, C. Kang, P. Jepson, "Why Corrosion Inhibitors do not perform well in some Multiphase Conditions: A mechanistic Study", NACE Corrosion 2002 No.: 2276, Page: 6
- ⁴⁴ A. Pedersen, K. Bilkova, E. Gulbrandsen, J. Kvarekval, "CO₂ Corrosion Inhibitor Performance in Presence of Solids: Test Method Development", NACE Corrosion Expo 2008 No.: 8632, Page: 5, 10-11
- ⁴⁵ A. McCahon, J. Martin, L. Harris, "Effects of Sand and interfacial Adsorption Loss on Corrosion Inhibitor Efficiency", NACE Corrosion 2005 No.: 5274, Page: 8
- ⁴⁶ C. de Waard, U. Lotz, D. E. Williams, "Predictive Model for CO₂ Corrosion Engineering in wet natural Gas Pipelines", NACE Corrosion 47 (1991) No.: 12, Pages: 976- 985
- ⁴⁷ S. Olsen, "CO₂ Corrosion Prediction by Use of the NORSOK M- 506 Model- Guidelines and Limitations", NACE Corrosion 2003 No.:3623, Page: 7
- ⁴⁸ Discussion with Milan Dardalic on 12.4.2011, Senior Chemist OMV Austria, OMV Gänserndorf, milan.dardalic@omv.com
- ⁴⁹ C.Dong, M. O' Keefe, "New Downhole- Fluid- Analysis Tool for improved Reservoir Characterization", SPE No.: 105866, Aberdeen- SCO, 2007, Pages: 1107- 1116
- ⁵⁰ R. Boreng, T. Schmidt, "Downhole Measurement in Oil and Gas Applications by use of a Wireline Tool", SPE No.:82199, Deen Haag- NET, 2003, Pages: 1- 12
- ⁵¹ F.Schein, "Inhibition Plots", Microsoft Excel Spreadsheet based on OMV Database (GDB), 2010, Gänserndorf- Austria
- ⁵² Origin 8.5 SR0, "Kriging Correlation", Origin Help Tutorials, www. Originlab.com, 2011
- ⁵³ J. Holman, "Heat Transfer", McGraw-Hill, Singapore, 6th Edition, 1986, Page: 210
- ⁵⁴ Discussion with Milan Dardalic 5.10.2010, Senior Chemist OMV Austria, OMV Gänserndorf, milan.dardalic@omv.com, Stefan Hönig 8.10.2010, Senior Corrosion Expert OMV Austria, OMV Gänserndorf, stefan.hoenig@omv.com
- ⁵⁵ B. Brown, S. Nestic, "CO₂ Corrosion in the presence of trace amounts of H₂S", NACE Corrosion 2004 No.: 4736, Page: 7
- ⁵⁶ F. Schein, "Inhibition_Plots_21.3.11", Microsoft Excel Spreadsheed based on OMV Database (GDB), 2010, Gänserndorf - Austria
- ⁵⁷ M. Oberndorfer, W. Havlik, S. Hönig, "Feldtest von grünen Inhibitoren", OMV Laboratory E&P No.: COR20050141, 2006, Pages: 1-16
- ⁵⁸ S. Hönig, "Auswahl von grünen Inhibitoren", OMV Laboratory E&P No.: COR20050025, 2005, Page: 10- 14
- ⁵⁹ F.Schein, "Inhibitoren_FS2_FS1_WO_Vetco", Microsoft Excel Spreadsheet based on OMV Database (GDB), 2010, Gänserndorf- Austria
- ⁶⁰ 5 API Specification/5CT/ISO11966, Table C5 and Table C6
- ⁶¹ M. Handler, Chemical Analysis Number LMUL/033-2011, 9.2.2011, Breitenfeld Edelmetall
- ⁶² R. Sonnleitner, E- Mail on 24.9.2010- 10:31 AM, voestalpine tubulars GmbH, robert.sonnleitner@vatubulars.com
- ⁶³ H. Uhlig, "Corrosion and Corrosion Control- an Introduction to Corrosion Science and Engineering", John Wiley& Sons Inc., New York, 2nd Edition, 1971, Page: 113
- ⁶⁴ CD- Labor für örtliche Korrosion – Modul 2, Interim Report, 10. January 2011, Page: 10
- ⁶⁵ B. Kermani, L.Smith, "CO₂ Corrosion Control in Oil and Gas Production", European Federation of Corrosion No.: 23, The Institute of Materials, 1997, London, Chapter: 7, Page: 29
- ⁶⁶ R. Bayer, "Mechanical Wear Fundamentals and Testing", Marcel Dekker Inc. NYC- New York, 2nd Edition 2004, (3.8): Pages: 91- 93
- ⁶⁷ A. Hedayat, S. Yannacopoulos, J. Postlethwaite, "Wear and CO₂ Corrosion of Steel Couplings and Tubings in heavy Oil Screw Pump Wells", Wear 209 263- 273, 1997, Page: 272
- ⁶⁸ NACE MR0175/ISO 15156- 2, "Petroleum and Natural Gas Industries- Materials for Use in H₂S containing Environments in Oil and Gas Production- Part 2: Cracking resistant Carbon and low Alloy Steels and the Use of Cast Irons", First Edition, Houston- TX, 2003, Page: 37
- ⁶⁹ Ed Ten Berge, Imotron Instruments B.V., E-mail Offer and Specifications of Coupons to OMV, Date deleted, etenberge@imotron.com, Halsteren- The Netherlands
- ⁷⁰ Safety Data Sheets of Champion Servo and MI- Production Chemicals, 19.2.2003 and 18.4.2007, Page: 1